University of Kerbala
College of Science
Department of Chemistry

Spectrophotometric Determination of Cobalt (II) and Chromium(III) Ions using the new (Azo) Compound and their Applications.

A Thesis

Submitted   to the   College of Science Kerbala University

In partial fulfillment of the requirements for the degree of Master of Science in chemistry

By

Abd-Al-Hur Radhi Auda

Supervised by

Assist.Prof. Dr. Ihsan Mahdi Shaheed

2023 AD   1445 AH

بسم الله الرحمن الرحيم

﴿ الله نورُ السَّمواتِ والأَرضِ مَثَل نورِهِ كَمشكواةٍ فيهَا مِصباحُ المِصباحُ في زُجاجةٍ الزُّجاجَةُ كأنها كَوكبٌ دُريٌّ يُوقَدُ مِن شَجرةٍ مباركةٍ زيتونةٍ لا شرقيةٍ ولا غربيةٍ يَكادُ زيتُها يُضىءُ ولو لم تَمسَسهُ نارٌ على نورٍ يَهدي اللهُ لنورِهِ مَن يشاءُ ويَضربُ اللهُ الأمثلَ للناسِ واللهُ بكلِّ شَيءٍ عَليمٌ ﴾

صدق الله العلي العظيم

Dediction

In the name of Allah

The most compassionate and merciful praise be to Allah and pray on his prophet Muhammad and kinsfolk his home

First of all; all thanks to Allah, the almighty, for uncountable help and guidance, who enabled me the power to achieve this study.

I wish to express my profound gratitude to my supervisor ,Assist. Prof. Dr. Ihsan Mahdi Shaheed, whose encouragements, professional ideas, advice, and criticisms were unceasing from the first day this work was conceived. He has been responsible for my present scientific outlook.

Also, I wish to express my thanks to the dean of the college of science, the Head of the chemistry department, and to all chemistry staff members for all the assistance they offered. I am particularly grateful to my colleagues in the chemistry department.

Researcher :

Abd-Alhur Radhi Auda

Acknowledgements

I want to thank God almighty for His guidance and His grace which strengthens me in various ways to have successfully completed my studies.

I would like to take this opportunity to express my heartfelt gratitude to the Department of Chemistry and all its staff for their unwavering support and invaluable guidance throughout my academic journey. Their dedication to excellence and passion for teaching have played a crucial role in shaping my understanding of the subject and fostering my love for scientific inquiry.

I am deeply indebted to my family for their unending encouragement, patience, and love. Their unwavering support during the highs and lows of my academic pursuits has been the driving force behind my achievements. Their belief in me has instilled the confidence I needed to overcome challenges and reach for my goals.

I would also like to extend a special word of thanks to my supervisor, **Assist .Prof. Dr. Ihsan Mahdi Shaheed**, for being an exceptional mentor. His expertise, patience, and constructive feedback have been instrumental in guiding my research and refining my skills as a scientist. I am truly fortunate to have had the opportunity to work under his guidance, and I am grateful for the knowledge and experience I have gained under his mentorship.

Lastly, I would like to express my appreciation to all the friends and colleagues who have supported and inspired me along the way. Their camaraderie has made this academic journey an enriching and memorable experience.

Researcher :

Abd-Al-Hur Radhi Auda

Supervisors Certification

I certify this thesis conducted under my supervision at the department of chemistry, College of science, University of Kerbala, as a partial fulfillment of the requirements for the degree of M.Sc. in analytical chemistry.

Signature:

Name: Assist.Prof. Dr. Ihsan Mahdi Shaheed

Address: Karbala University – College of Science

Date: ٩ / ١١ /2023

Report of the Head of the Chemistry Department

According to the recommendation presented by the Chairman of the Postgraduate Studies Committee, I forward this thesis " **Spectrophotometric Determination of Cobalt (II) and Chromium (III) Ions using the new (Azo) Compound and their Application** " for examination.
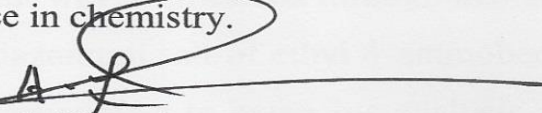
Signature:

Prof. Dr. Luma Majeed Ahmed

Head of Chemistry Department

Address: University of Kerbala, College of Science, Department of

Chemistry

Date ٩ / ١١ / 2023

Examination Committee Certification

We, the examining committee, certify that we have read this thesis and examined the student (AbdAl-Hur Radhi Auda) in its contents and that in our opinion; it is adequate as a thesis for the degree of Master of Science in chemistry.

Signature:
Name: **Dr: Alaa Frak Hussain**
Title: Professor
Address: University of Kerbala, College of Science,
Department of Chemistry
Date: ٩ ٨١ /2023
(Chairman)

Signature:
Name: **Dr.Hassan Fisal Namaa**
Title: Assist Professor
Address: University of Kerbala,
College of Science Department
Of chemistry
Date:٩/١١/ 2023
(Member)

Signature:
Name: **Dr. Hind Sadeq Jaafar**
Title: Assist. Professor
Address: University of Baghdad,
College of Science, Department
Of Chemistry
Date:٩ /١١ /2023
(Member)

Signature:
Name: **Dr: Ihsan Mahdi Shaheed**
Title: Assist Professor
Address: University of Kerbala, College of Science,
Department of Chemistry.
Date:٩/١١/ 2023
(Member & Advisor)

Approved by the council of the College of Science

Signature:
Name: **Dr.Jasem Hanoon Hashim Al-Awadi**
Title: Professor.
Address: Dean of College of Science,   University   of Kerbala.
Date ١٤ / ١١ /2023

Abstract

This study encompasses the synthesis and characterization of a novel reagent, namely Ethyl4-(5-acetyl-2,3,4-trihydroxyphenyl) diazenylbenzoate (EATDB). The reagent was synthesized through azo coupling of the imidazole derivative with the diazonium salt of ethyl 4-aminobenzoate (benzocaine). The ensuing compound was subject to extensive analysis, employing sophisticated methods such as gas chromatography-mass spectrometry (G.C. mass), UV-Vis analysis, ^{1}HNMR, ^{13}CNMR, and FT.IR spectroscopy.

Notably, the optimal conditions for the reaction between the two ions (Co(II) and Cr (III) ions) and the reagent were thoroughly explored. This entailed examining the effect of acidity function, addition sequence, stability duration of the complexes, ligand concentration, temperature influence, and ionic strength impact. The calibration curves for Cobalt (ll) and Chromium (lll) ions were constracted with concentration range from (1-100 µg.mL^{-1}) for both of ions. The Analytical parameters obtained are linearity coefficient (R^{2})0.9980 and 0.9939,molar opsorpitivity 0.212x10^{2} L.mole,cm^{-1}and 0.935x10^{3} L.mole.cm^{-1} and Sandall's sensitivity 0.278 g.cm^{-2} and 0.556 g.cm^{-2} for Cobalt (ll) and Chromium (III) ions respectively. To ascertain the equivalency of the complexes, various methods including the Mole ratio method, Job's method, and Mollard method were utilized. The stability constants (K$_{sta}$) for the cobalt (II) and chromium (III) complexes were found to be 5.967×10^{8} and 1.125×10^{14}L.mol^{-1} respectively. Moreover, the thermodynamic functions (ΔH, ΔG, and ΔS) for both complexes indicated that the reactions Co (II) and Cr (III) complexes were exothermic. Nevertheless, the study noted that there is interference from several cations and anions during the estimation of Cobalt (II) and chromium (III) ions. Consequently, the addition of appropriate masking agents was explored, taking into account the varying degrees of interaction depending on the nature and concentration of interfering ions. Impressively, the

analysis of the dissolved complexes indicated that both Cobalt (II) and chromium (III) complexes were uncharged due to the measurement at conductivity.

The precision and accuracy of the analytical method were meticulously evaluated by subjecting it to three distinct ion concentrations, and subsequently computing the relative standard deviation (RSD %) as a measure of variability. Obtained data showcased excellent precision, with RSD% ranging from(0.479% - 0.874%) for Co (II) and from (0.742% - 0.896%) for Cr (III). Moreover, the relative recovery ranged from 98.43% - 101.764% for Co (II) and from 99.41% - 101.470% for Cr (III).The Limit of Quantification L.O.Q was crucial for determining method's sensitivity alongside with Limit of Detection L.O.D. For Cobalt (II) ion, the L.O.D and L.O.Q were found to be 0.7410μg.mL^{-}, and 2.4120 μg.mL^{-1} respectively, while for Chromium (lll) ion are 0.8640 and 2.8510 μg.mL^{-1} respectively. Additionally, the reagent and the two complexes were investigated for their settling properties and physical characteristics, including melting point and molar conductivity. This analytical method proved effectively in quantifying cobalt (II) and chromium (III) ions present in a pharmaceutical sample, highlighting its utility in sensitive and accurate ion analysis.

Table of Contents

List of Figures

List of Schemes

List of Tables

List of Symbols

Symbol	Meaning
D.W	Distilled Water.
EDTA	Ethylene dianime tetra acetic acid.
DMSO	Dimethyl sulfoxide .
EATDB	Ethyl.4-((5-acetyl-2, 3, 4- trihydroxy phenyl diazonyl) benzoate.
RSD%	Relative standard deviation.
L.O.D	Limit of Detection
L.O.Q	Limit of Quantification
Rec%	Recovery%
S.D	Standard deviation
ε	Molar absorptivity
λ_{max}	Maximum wavelength
Vm	volume of the metal
VL	volume of the reagent
E%	Relative error
Abs	Absorption
R^2	Linearity Coefficient
r	Correlation Coefficient
ΔH	Enthalpy
ΔG	Free energy
ΔS	Entopy
S	Sandal sensitivity
α	Degree of dissociation
K_{sta}	Stability Constant
n	Number of mole
C	Molar cocentration
$\overline{X}$	Average

CHAPTER ONE

INTRODUCTION

1.1 Organic Reagent

Organic reagents, characterized by their high molecular weights, often exhibit limited water solubility attributed to the presence of covalent bonds. These compounds offer numerous advantages, leading to their widespread utilization across various domains such as medicine, technology, and science. Notably, their exceptional sensitivity and the vivid hues displayed by their complexes when coordinated with elements from the periodic table have rendered them invaluable in numerous applications [1].

In the field of analytical chemistry, for instance, their solubility in organic solvents enables extraction operations [2–4]. Furthermore, these reagents have been effectively employed in quantitative and qualitative assessments of trace metal ion concentrations, employing diverse models and employing a range of techniques [5-6]. An example of such organic reagents extensively employed is the extensively utilized class of azo compounds commonly referred to as azo dye

1.2 Azo Dyes.

The inception of azo compounds can be traced back to 1858 when the scientist Peter Griss made their discovery. Termed as diazo compounds, Griss postulated that these compounds resulted from the replacement of two hydrogen atoms in the benzene ring by two nitrogen atoms. Subsequently, it was observed that a significant number of aromatic amines could be converted into their respective diazo compounds. In 1883, Curtins achieved the first synthesis of diazo compounds, albeit their inherent instability and rapid dissociation into nitrogen and hydrocarbons limited their prevalence when compared to aromatic azo compounds [7].

On the other hand, the quantity of azo groups in a molecule allows for the classification of azo dyes [8]. This classification encompasses mono-azo, di-

azo, triple-azo, and higher order azo compounds. Furthermore, azo dyes can also be categorized based on the nature of the oxochrome groups incorporated within them. Acid dyes encompass acidic functional groups (-OH, -SO$_3$H, -COOH), whereas basic dyes contain basic groups such as dialkylamino, alkylamino [9], or amino groups, attached to the rings at both ends of the azo bridge [10].

The historical timeline of dyeing can be delineated into two significant periods the "pre-aniline" period, encompassing the era leading up to 1856, and the subsequent "post-aniline" era. During the pre-aniline epoch, the chromatic repertoire was relatively constrained, predominantly reliant on dyes derived from dye-producing flora and fauna. Noteworthy among the vegetal dyes were those extracted from madder roots, prevalent in both Asian and European regions, yielding a vivid crimson hue. Additionally, Indian native indigo plant leaves provided a vivid blue pigment that is being used today. Widely employed in the fabrication of denim garments .Azo compounds are characterized by the presence of the –N=N– functional group in their molecular structure, denoted as R$_1$-N=N-R$_2$. When the R groups in azo compounds are aromatic (arene) rings, the resulting structures exhibit enhanced stability compared to those with alkyl groups. This stability arises from the involvement of (-N=N-) group in a wide-ranging, scattered systems that includes the ring of aromatics. The aromatic azo compounds display intense coloration, making them valuable as dyes in various applications. The formation of aromatic azo compounds occurs through a coupling reaction involving the combination of a diazonium salt and a coupling agent [11-12].

1.3 Properties of azo compounds

Azo compounds and their derivatives are commonly employed as reagents due to their notable features, including high stability, rapid interaction with metal ions, as well as remarkable sensitivity and selectivity [13]. The stability of these compounds is influenced by the nature of the groups attached to both ends of the aliphatic or aromatic azo group, with the nitrogen within the bridge azo group (-N=N-) playing a crucial role. Furthermore, azo compounds exhibit heterocyclic properties, and many of their derivatives demonstrate insolubility in water but dissolve readily in organic solvents such as chloroform, benzene, carbon tetrachloride, and others [14].

Moreover, they exhibit exceptional stability and swift interaction with a wide array of elements from the periodic table, particularly transitional and representative ions [15-16]. These compounds offer several advantages, including their characteristic vivid colors, displaying high intensity [17]. The color range of azo compounds varies from yellow to blue, depending on the successive (π) system present within the molecule. Additionally, they possess high molecular weights and elevated melting points, making them valuable across various branches of chemistry.

1.4 Diazonium Salts

Diazonium salts can be formed by the reaction of both aliphatic and aromatic primary amines with nitric (III) acid, also known as nitrous acid (HNO_2). This reaction takes place at temperatures ranging from (0-5) $^\circ$C.

Nitric (III) acid is often produced in-situ during the reaction because of its inherent instability. This is frequently accomplished via the interaction of diluted hydrochloric acid or sulfuric (VI) acid with $NaNO_2$. [18].

$$RNH_2 + NaNO_2 + 2HCl \longrightarrow RN^+ON{:}Cl^- + 2NaCl + 2H_2O$$

$$phNH_2 + NaNO_2 + 2HCl \longrightarrow ph\text{-}N{+}ON{:}Cl\text{-} + 2NaCl + 2H2O$$
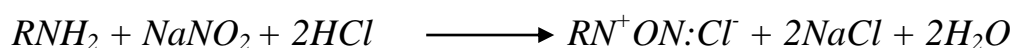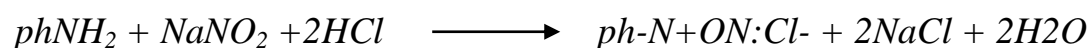
The clear, inert nitrogen gas is usually released when alkyl diazonium salts break down, which makes them extremely flammable. As compared to their aliphatic counterparts, the diazonium cations of aromatic diazonium salt are more stable. Phenylamine can be used to produce the ion of diazonium benzene.

$$C_6H_5 \text{ - } NH_2 + HNO_2 + H^+ \longrightarrow C_6H_5 \text{ - } N{+}ON{:} + 2H_2O$$
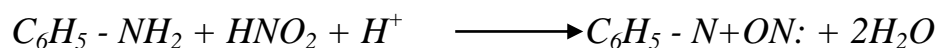
Salts of benzene diazonium, although they can be obtained in a solid state, are generally stored in a liquid form and used immediately because they have a propensity to break down, even in low temperatures, when left standing. These salts are extremely flammable when they are solid, and a small amount of pressure or temperature increase is all it takes to ignite them. The diagram below illustrates the molecular structure of benzene diazonium chloride.
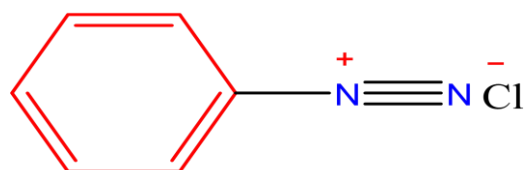
Figure (1.1): structural representation of benzene diazonium chloride

Because of the diazo group is a part of the conjugated system together with the benzene ring, the benzene diazonium cation is thought to be more stable than the alkyl diazonium cation. As a result, there is a change in how the positive charge is distributed across the ring. [19].
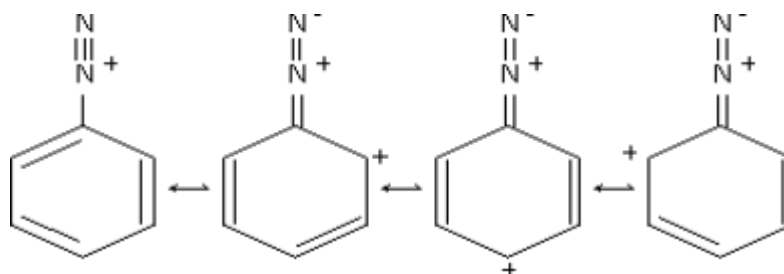
Figure (1.2): Positive charge distribution around the ring

1.5   Azo Dyes preparation

The production of azo dyes involves two steps: An aqueous solution of sodium nitrite and acid is used at low temperatures (0–5 °C) to diazotize the basic aromatic amine with sodium nitrite in an acidic mineral media (HCl, H_2SO_4, etc.). The chemical formulas below demonstrate that a temperature of degrees Celsius is required to produce the readily soluble salts in water known as diazonium salts.

$$HCl + NaNO_2 \xrightarrow{0-5°C} HONO + NaCl$$

$$R - NH_2 + HCl + NaNO_2 \xrightarrow{0-5°C} RN2Cl \longrightarrow N_2 + Mixture$$

$$Ar - NH_2 + HCl + NaNO_2 \xrightarrow{0-5°C} Ar - N = N^+Cl^- + NaCl + 2H_2O$$

$$Ar - NH_2 \xrightarrow{Diazotization} Ar - N_2 \xrightarrow[Ar-H]{Coupling\ reaction} Ar - N = N - Ar^-$$
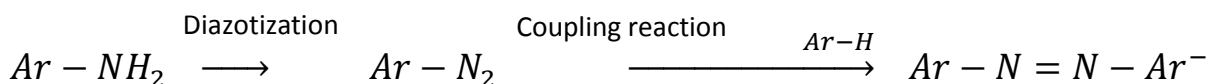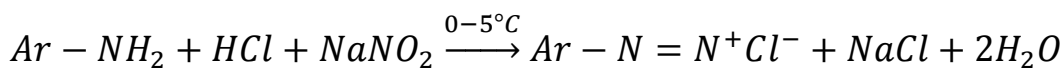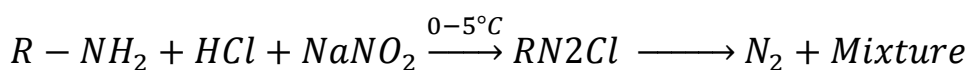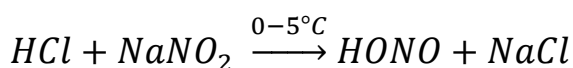
The next step was the combination stage (formation of azo dyes), where the aromatic diazonium ion was combined with reactive aromatic compounds under basic conditions to cause the dyes salt to release hydrochloric acid, which is a reactive hydrogen element in another aromatic compound (phenols and amines).[20]

1.6 Coupling reaction of azo compound

In a diazo coupling reaction, another aromatic molecule known as the coupling agent reacts with the diazonium salt. The diazonium salt reacts with the coupling agent's electron-rich benzene ring because it behaves as an electrophile. A colorful solid of an azo compound is produced when the diazonium salt is dissolved in a very cold solution and added to a solution that also contains a coupling agent. It is important to note that several of these azo compounds have vibrant hues and are widely used as colorants.

The coupling agent normally reacts at either the two or four locations of its benzene ring during the coupling process, with a functional group occupying one of the positions. The precise coupling agent utilized in the reaction with the diazonium salt determines the exact hue of the resultant product. The choice of coupling agent determines the chromophoric properties and thus the color of the azo compound formed [21].

1.7.1. Coupling with Phenols

Reaction of diazonium salt with phenol compound leads to the formation of a yellow or orange azo compound. The specific color observed may vary depending on the exact structure of the phenol used in the reaction.
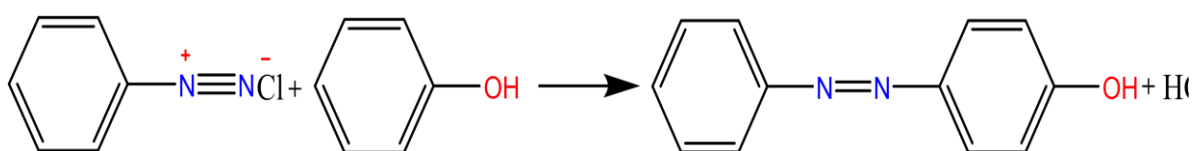
Figure 1-3 Diazonium reaction with phenols

On the other hand, when an alkaline solution of naphthalein-2-ol is employed as the coupling agent, a red azo compound is formed. The alkaline conditions facilitate the coupling reaction between the diazonium salt and naphthalein-2-ol, resulting in the formation of a distinctive red-colored azo compound.
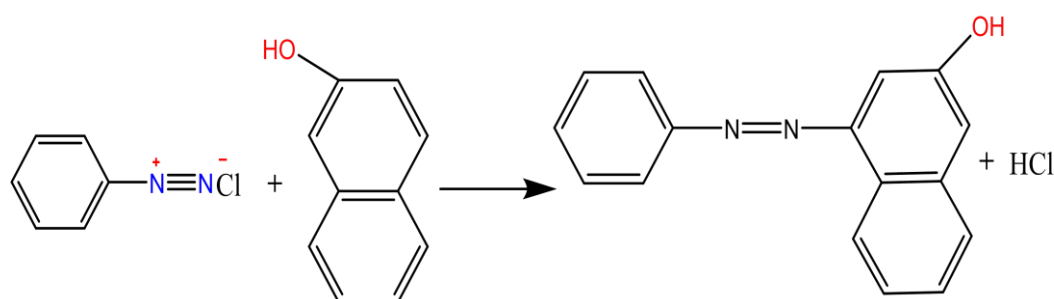
Figure (1.4): Coupling reaction of diazonium salt and naphthalein-2-ol

It is worth noting that the choice of coupling agent in diazo coupling reactions plays a crucial role in determining the color of the resulting azo compound, allowing for a wide range of colors to be obtained for various applications, including dyes and pigments.[22]

1.7.2. Coupling with Amines

When arylamines are reacted with diazonium salts, it often results in the formation of a yellow dye.
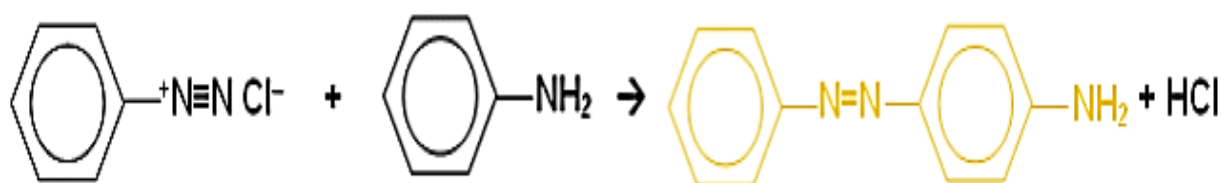
Figure (1.5): Arylamines reaction with diazonium salt

This reaction, known as coupling, involves the combination of the diazonium salt with the arylamine, leading to the formation of azo compounds. Azo compounds contain the characteristic azo group (-N=N-).

The coupling reaction can be performed with various diazonium salts, giving rise to a wide range of azo compounds with different colors. For instance, when a phenol compound is used as an electrophile, it reacts with the coupling agent to form benzene diazonium chloride.an alkaline solution, resulting in the formation of a yellow azo dye. Similarly, coupling of a diazonium salt with naphthalen-2-ol leads to the formation of a bright red precipitate.

These azo compounds exhibit vibrant colors and find applications as dyes and pigments in various industries. The specific color obtained depends on the combination of the diazonium salt and the coupling agent used in the reaction [23–25].
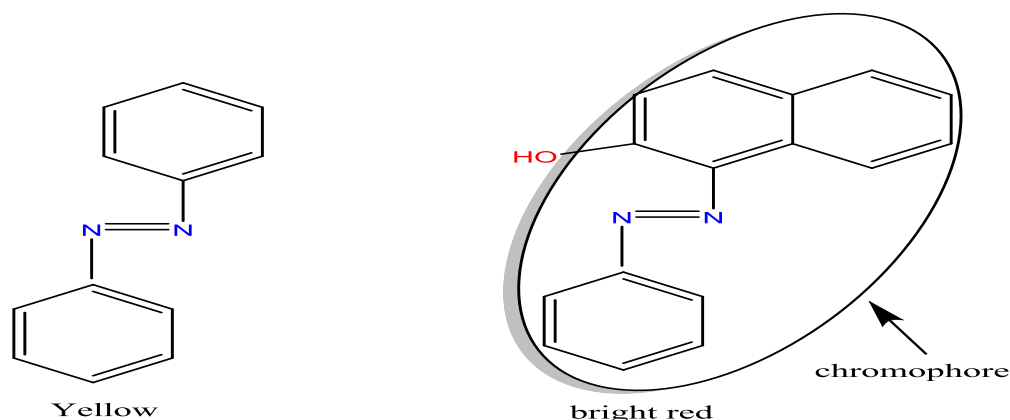
Figure (1.6):The product formed from Coupling reaction of diazonium salt.

Although the yellow and red azo dyes formed through the coupling reactions described earlier may have limited practical utility due to their low solubility in water, there is a class of azo dyes that overcomes this limitation. These dyes are modified by the introduction of one or more sulphonic acid groups, resulting in improved solubility in water. The presence of sulphonic acid groups makes these azo dyes highly soluble and significantly enhances their commercial value in the dyestuffs industry.

The introduction of sulphonic acid groups into azo dyes enhances their water solubility by increasing their polarity and promoting ionization in aqueous solutions. This increased solubility allows for easier application and incorporation of these dyes into various dyeing processes. Consequently, azo dyes with sulphonic acid groups have gained considerable importance and are extensively used in the dyestuffs industry for a wide range of applications [26–29].

Azo compounds display a unique characteristic called a chromophore, in which the (-N=N-) group is a component a long-range delocalized electron system of an extended delocalized electron system that includes aromatic ring

8

structures. In these delocalized systems, the discrete molecular electronic energy levels are closely packed, resulting in the absorption of the visible portion of the electromagnetic spectrum emits light (referred to as the energy gap or DE). When electrons go from lower to higher energy levels, there is an absorption that occurs. Consequently, azo compounds exhibit colors that correspond to the wavelengths of visible light that are not absorbed. To additionally alter the hues of azo compounds, functional groups like -OH and -NH$_2$ are frequently connected to the chromophores. These functional groups also integrate into the expanded delocalized electron system, leading to alterations in the energy gaps and subsequently impacting the colors displayed by the molecules.

When azo dyes are applied to fabrics, they exhibit various binding mechanisms depending on the type of fabric. For cotton, numerous azo pigments are insoluble and get stuck within the fibers. Others, referred to as primary pigments, attach to the fibers through interactions. Like intermolecular dipole-induced dipole bonding and hydrogen bonds. Due to the relatively weak nature of intermolecular bonding compared to covalent bonding, direct dyes must possess elongated and linear structures. This allows the dye molecules to align closely with the cellulose fibers of cotton, thereby maximizing intermolecular attractions. [30]   As an example, the structure of Direct Blue , a representative azo dye, is provided below: Fig 1-7 . [31-32].
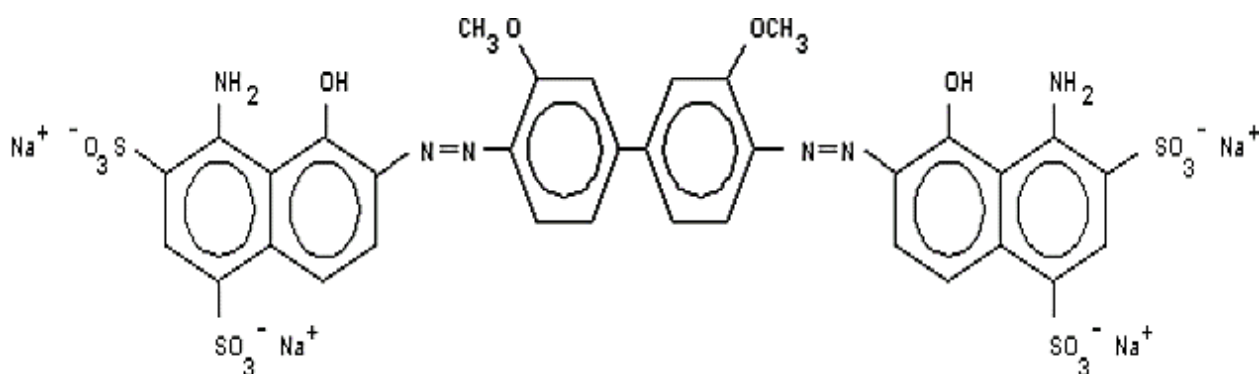
Figure (1.7): Direct blue structure

9

1.8   Classification of azo compound

Azo compounds are categorized based on the nature of the attached oxochrome groups. When the groups present are acidic in nature, such as hydroxyl (OH), sulfonic acid (SO$_3$H), or carboxyl (COOH), they are referred to as acidic azo dyes. Conversely, if the attached groups are basic, such as dialkylamino (NR$_2$) or amino (NH$_2$), they are known as basic azo dyes. Furthermore, azo compounds can also be classified depending on how many azo groups there are within the molecule, leading to designations such as monoazo, diazo, triazo, or polyazo compounds. Additionally, bridge azo compounds represent another classification within the realm of azo compounds [33].

1.8.1   Homocyclic azo compounds

This category encompasses azo compounds whose aromatic rings lack heterocyclic atoms and may or may not bear substituents, as exemplified by azobenzene. However, the effectiveness of this type is limited due to the absence of additional binding sites. In such cases, the nitrogen atom within the azo bridge group serves as the sole site available for bonding with metal ions, whether they are transitional or representative elements [34]. The rings themselves can be substituted with acidic or basic groups, such as hydroxyl (OH), sulfhydryl (SH), carboxyl (CO$_2$H), amino (NH$_2$), or dialky amino (-NR$_2$), among others. Furthermore, it is possible for a single ring to contain both acidic and basic groups [35]. The presented below are some formulas depicting homocyclic azo compounds:
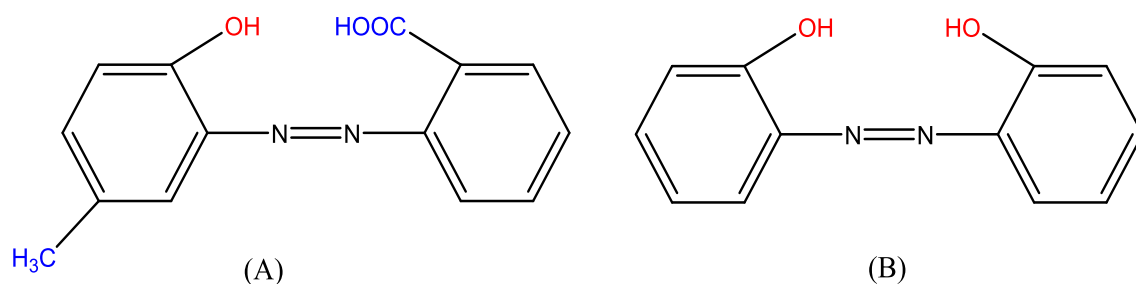
Figure (1.8): (a) 2-hydroxy-2-carboxy-5-methylazobenzene, (b) **2, 2-**dihydroxy-dibenzene azo

Homocyclic azo compounds are less common and important than heterocyclic azo compounds.

1.8.2   Heterocyclic azo compounds

These compounds represent relatively recent reagents that have found extensive utility in the realm of chemical analysis. They are characterized by the presence of heterocyclic aromatic rings situated on one or both sides of the bridge azo group. These aromatic rings may incorporate a donor atom or atoms, such as nitrogen (N), sulfur (S), or oxygen (O). Moreover, the aromatic rings themselves can be substituted with various acidic or basic groups. It is also possible for a single aromatic ring to feature one or more of the aforementioned groups,In some cases, both acidic and basic groups may coexist within the same ring [36]. Here are some examples showcasing this particular compound type.

2-((3-methoxyphenyl)diazenyl)-4,5-diphenyl-1*H*-imidazole
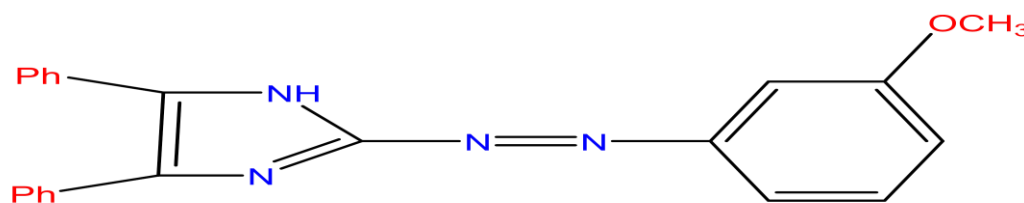
Figure (1.9): 2-(3-Methoxyphenyldiazonyl)-4, 5-diphenyl -1*H*-imidazole

This type of reagents is characterized by high stability within a wide range of pH, as well as its possession of varying solubility in different solvents, and it is insoluble in water, but dissolves in some organic solvents

1.8.3. Azo compound classification based on the amount of azo groups

Azo compounds can be categorized into different classes based on the number of azo groups present within the molecule.

1.8.3.1 Mono azo compound.

These compounds are referred to as monoazo compounds, characterized by the presence of two aryl groups connected to each other by the (-N=N-) group, as exemplified in the following compound [37]:

5-Methyl-2-(4-Chloro benzenazo) imidazole
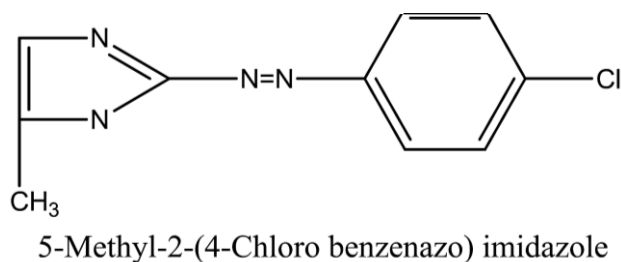
Figure (1.10): The monoazo compound

1.8.3.2 Bis azo compounds.

These compounds possess two azo groups interconnected through azo bridges (-N=N-). Substituted azo compounds are further classified into aromatic ring systems attached to both ends of the azo linkage. They can be categorized as monosubstituted or disubstituted compounds, depending on the presence of one or more substituent groups in the ortho position with respect to this linkage and the presence of additional ring systems such as naphthalene and benzene linked to the azo group. The provided below is a general formula representing these compounds [38].
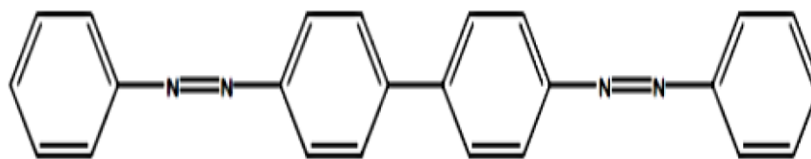
Figure (1.11): Bis azo compound.

1.9 Imidazole and its ligands, azo imidazole.

Imidazole is a soluble crystalline solid that dissolves in water and has a melting temperature of 90°C. [39]. It was initially synthesized in 1855 through the reaction of clioxal with ammonia, resulting in the isolation of a new compound known as clioxalin. However, the term clioxalin is no longer in use, and the preferred name for the compound is imidazole. The term "imidazole" refers to the five-membered heterocyclic ring containing an imino group and a secondary nitrogen atom. The structure below illustrates the numbering scheme for the imidazole ring [40].
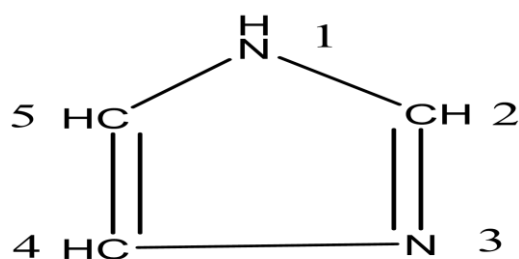
Figure (1.12): Numbering scheme for an imidazole ring

Sites 2 and 4 in the imidazole ring are the active sites where electrophilic attacks take place. Specifically, diazonium salt couples with site No. 2 in a weakly basic solution, resulting in the formation of vibrant red dyes. In a weak alkaline medium, a range of azo-imidazole ligands were synthesized by adding diazonium salt to an alcoholic solution of imidazole. Furthermore, numerous substituted azo-imidazole ligands were prepared at positions 4 and 5 [41]. The general formula for these ligands can be expressed as the following:
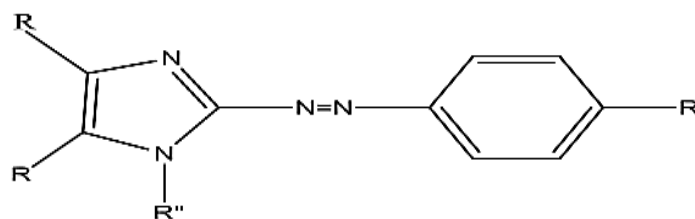
Where: R=ph, COOH, Et   R'=X'   R"=H,Me,CH$_2$C$_6$H

Figure (1.13). The general formula of ligands.

In addition to coupling diazonium salts with imidazole or its derivatives, researchers have also synthesized organic ligands containing heterocyclic rings such as pyridine and quinoline, which are linked to the imidazole ring through the azo bridge group [42]. However, compared to other types of ligands, azo-imidazole ligands and their derivatives have received relatively less research and investigation in the field of analytical chemistry. This may be due to the limited availability and exploration of this type of ligands, despite the long-standing knowledge of imidazole for over 150 years.

Furthermore, it has been discovered that the imidazole ring has significant implications in the treatment of many tumors [43] when incorporated into the composition of medical preparations and drugs. This highlights the potential therapeutic applications of imidazole and its derivatives in the field of medicine.

Some interesting studies indicate the possibility of using imidazole compounds and their complexes in different techniques in addition to their known uses as chromogenic reagents. [44]

1.9.1. Imidazole and Pyrimidyl Azo Compounds

In this type of reagents, the nitrogen atom represents the atom (A). There are two heterocyclic atoms in the heterocyclic ring, which can be either pentagonal, known as azo-imidazole compounds, or hexagonal, known as primidyl-azo compounds. An example of the azo-imidazole compound is 1-alkyl-2-(aryl azo) imidazole (RaaiR'), while an example of the primidyl-azo compound is 2-(aryl

azo)-pyrimidine (R-aa Pm). These compounds have specific formulas [45] and [43].
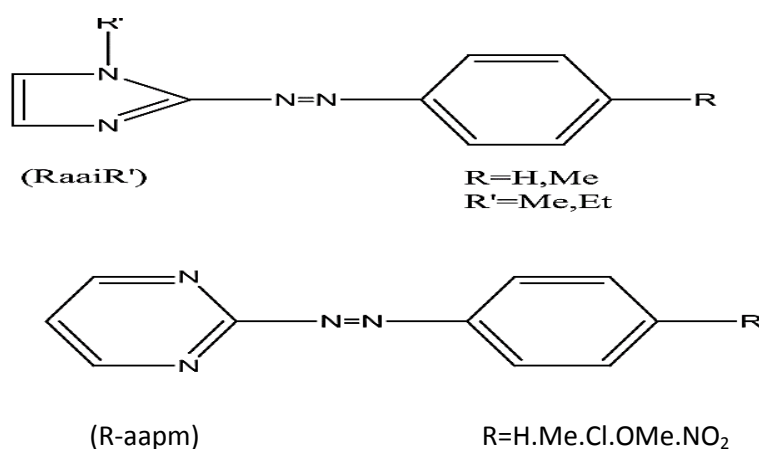
Figure (1.14): primidyl-azo compound

Primidyl azo reagents, although less commonly used compared to predyl azo and imidazole azo reagents, offer distinct advantages. while they may be expensive and require specific conditions for preparation, numerous studies have demonstrated their superiority in terms of sensitivity and selectivity towards metal ions [46] They have found multiple applications as effective indicators in various analytical techniques. A notable advantage of primidyl azo reagents is their high solubility in water, which eliminates the need for additional organic solvents during purification processes. Additionally, they exhibit sharp end points and clear color changes, indicating precise and easily detectable reactions. The stability of their metallic complexes can be attributed to the resonance structures present in their molecular formulas.

Shibata and his research team discovered that these reagents, similar to other azo dyes, are sensitive to the acidity of the solution [47]. The colors, maximum wavelengths, and molar absorption coefficients of these reagents undergo changes depending on the pH of the solution. Thus, they exhibit an acid-base equilibrium. Azo-imidazole reagents have been extensively employed in analytical chemistry, particularly in spectroscopic methods for the

determination of metal ions such as copper (II) [47], Cadmium (II) [48], Zinc (II) [44], as well as monovalent ions like silver (I) and palladium [49].

1.10. Application of azo compounds

Azo compounds have found extensive applications in various fields, including medicine, science, and technology, yielding significant outcomes in various aspects of life [46]&[50]. Numerous individual azo compounds have been utilized in the production of dyes and cosmetics, while those containing an aryl azo group have found applications in the pharmaceutical industry [51]. Furthermore, this compound type has been harnessed in diverse industrial sectors. In the domain of analytical chemistry, the characteristic color exhibited by azo compounds and their complexes with metal ions in both aqueous and organic solutions has been leveraged in spectral analyses, leading to their classification as spectral reagents [52]. Heterocyclic azo compounds have played a significant role in the field of industry. Chromogenic thiazolyl azo ligands have been widely employed as dye-generating reagents and have found application in the dyeing of fabrics, polyester, and nylon threads [53]. Azo compounds have been employed in the study of adsorption [54] and have also found applications in photography [55].In the medical field, azo compounds have been utilized for various purposes. Prontosil, the first azo dye, was employed as an antibacterial agent, marking a notable milestone in the use of azo compounds for medicinal applications. [23]
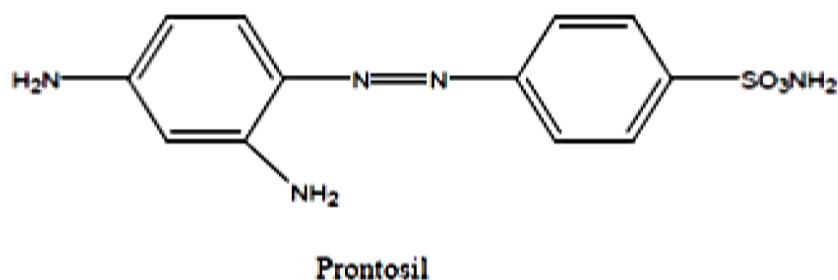
Prontosil

Figure (1.15): Prontosil the first azo dye.

1.11. Heavy Metals

Heavy metals are defined as metallic substances with a density that is high related to water, with the idea that heaviness and toxicity are associated. Heavy metals also include metalloids, like arsenic, that can induce toxicity at low doses of exposure.

The population is at risk from sub-clinical trace element deficiencies, especially the elderly, those institutionalised and patients with chronic health problems; it is particularly common in, and relevant to, critical care and maybe masked by co-existing disease.

1.11.1. Cobalt (Co)

Cobalt (Co), an element distinguished by its toughness, shiny gray color, and malleability, shows chemical properties that closely mirror those of nickel (Ni) and iron (Fe). Cobalt compounds primarily come in the cobaltic (Co^{+3}) and cobaltous (Co^{2+}) valence states, with the former being more frequently encountered in industrial and environmental settings [56].

In the natural world, cobalt metal ions are extensively spread as small amounts, which, in particular amounts, are necessary for typical physiological operations. These small amounts help in averting dietary insufficiencies, bolstering immune system operation, controlling gene manifestation, offering antioxidant protection, and helping in the avoidance of chronic diseases. [57].

One famous biological function of cobalt is its incorporation as a metallic element in vitamin B_{12}, also referred to as cyanocobalamin. Nevertheless, overexposure to different cobalt compounds has been linked to toxicity to both the ecosystem and the human organism. Considering the extensive presence of cobalt, individuals are frequently subjected to diverse cobalt compounds in their everyday existence. The overall population undergoes contact through breathing in of surrounding air, as well as consumption of food and drinking water containing cobalt substances. Work-related contact with cobalt is also relatively

frequent, particularly in industries engaged in the manufacturing of paint, granding, mining, and hard metals.[58].

Additionally, cobalt has been utilized for various medical intentions, though certain uses have been phased out over the years. [59]. Through both animal and human toxicity research, Cobalt's risk to health and potential for harm have both been thoroughly explored. Prior analyses usually focused on specific exposure scenarios, modes of consumption, toxicological mechanisms, and clinical outcomes. or the results of cobalt exposure on particular physiological systems in various exposure scenarios [60-61].

A Presented a thorough examination of cobalt origins, intake pathways, dynamics, underlying harmful mechanisms, and a crucial assessment of previously documented negative health impacts. Their research already provides a thorough numerical exposure and risk evaluation [62-63]. As a result, we want to give a more thorough and concise explanation of the following categories:

1. Examining the various exposure scenarios historic, and modern sources of Co (ll), and related intake pathways.

2. Examining the tools and techniques for measuring cobalt intake that are currently accessible and talking about recent developments in the interpretation of these measurements.

3. Examining the established as effects on overall health associated with cobalt exposure in humans. It is worth noting that the sole recognized function of cobalt is its role as the metal component of vitamin B_{12}. Consequently, cobalt deficiency manifests as vitamin B_{12} deficiency [64]

1.11.2 Cobalt Determination Studies

In the following table, different studies and reagents will be discussed.

Table (1.1): Cobalt determination studies

Method	Reagent	Result of RSD%	Results of LOD and LOQ.	Ref.
FAAS	Activated carbon modified by dithioxamide (rubeanic acid) (DTO	>2%	LOD=0.80μg/L LOQ=2.64μg/L	[65]
Spectrophotometric	5-(2-benzothiazolylazo)-8-hydroxyquinolene	1.37%	LOD=3.1ng/ml LOQ=9.1 ng/ml	[66]
C.P.E	1-(2-Pyridylazo)-2-naphthol (PAN)	>5%	LOD=0.03ng/ml LOQ=0.99ng/ml	[67]
Electro thermal atomic absorption spectrometry (ETAAS) Co 17	1-nitroso-2-naphtol (1N2N)	3.4%	LOD=3.8ng/L LOQ=12.54ng/L	[68]
Spectrophotometric	Amberlyst A-26	2.9%	LOD=2.0μg/L LOQ=6.6μg/L	[69]
Spectrophotometric	2-[(2-mercaptophenylimino) methyl]phenol	1.2 %	LOD=.21μg/L LOQ=0.693μg/L	[70]
Spectrophotometric	2-(2-thiazolylazo)-p-cresol	5%	LOD=3.2μg/L LOQ=9.6μg/L	[71]
Spectrophotometric	3,3′-(1E,1E′)-(propane-1,2-diylbis(azan-1-yl-1-ylidene)bis(methan-1-yl-1-ylidene)bis(4-bromophenol)	1.8%	LOD=0.06ng/ml LOQ=1.98ng/ml	[62]

Spectrophotometric	Ion-exchange with microwave plasmatorch-atomic emission spectrometry	3.73%	LOD=1.28µg/L LOQ=4.22µg/L	[63]
Spectrophotometric	Solid Phase Extraction with Fibrous 2 - C 3 N 4 Nanocomposites Coupled with ICP.	3.9%	LOD=0.12 pg/ml LOQ= 0.39pg/ml	[72]
Spectrophotometric	4-(2pyridy azo) resorcinol (napar)	0.98 %	LOD=3.09ng/ml LOQ=10.19ng/ml	[73]
Spectrophotometric	1-hexylpyridinium hexafluorophosphate	2.36%	LOD=0.70µg/L LOQ=2.31µg/L	[74]
Spectrophotometric	Simultaneous	1.2%	LOD=0.20mg/L LOQ=0.66mg/L	[75]
Spectrophotometric	Hydroxy naphthol blue	2.2%	LOD=0.56 µg/L LOQ=1.84 µg/L	[76]
Spectrophotometric	Adopting schiff base complexes	0.00184%	LOD=0.52 µg/L LOQ=1.74 µg/L	[77]
Spectrophotometric	1-nitroso-2-naphthol	7.1%	LOD=1.10µg L^{-1}, LOQ=3.60µg L^{-1}	[78]
Spectrophotometric	2-(5-bromo-2-pyridylazo)-5-diethylaminophenol	2.4%	LOD=0.97µg /L LOQ=3.2µg/L	[79]
Spectrophotometric	Ethyl4-(5-acetyl-2,3,4-trihydroxyphenyl) diazenylbenzoate (EATDB	0.479% - 0.874%	LOD=0.74µg/mL LOQ=2.46µg/mL	Present Work

1.11.3 Chromium (III)

Chromium, a heavy metal present in the environment, occurs naturally in two predominant forms: trivalent chromium Cr^{+3} and hexavalent chromium Cr^{+6} the reduction of Cr^{+6} to Cr^{+3} generates reactive intermediaries involved in the cytotoxic, genotoxic, and carcinogenic properties of compounds containing $Cr^{+6.}$ Human exposure to chromium primarily occurs through non-occupational sources, including cigarette smoking, smog from cities, meat, vegetables, and meat products [80].

Chromium (VI) finds extensive use in various industrial chemicals, particularly in paints, steel production, wood treatment, alloy cast iron production (including the production of stainless steel). Contrarily, Cr (lll) salts including the functions of chromium polynicotinate, chromium chloride, and chromium picolinate (Cr P), which are used as dietary supplements, have been demonstrated to offer significant benefits. Health advantages in both people and animals [81]. Inhalation, ingestion, and skin contact are the three main ways that chromium enters the body. The main method of occupational exposure is inhalation, whereas non-occupational exposure happens when people consume food and drink that contain chromium.

Notably, regardless of the exposure route, Cr (III) is poorly absorbed while Cr (VI) is more easily absorbed. Oral absorption of Cr (VI) is relatively low, making it less toxic when introduced orally. However, chromium poses considerable toxicity risks when absorbed both cutaneous and inhalation pathways, causing lung cancer, rhinitis, nasal ulcers, hypersensitivity responses, both contact dermatitis and every eaten Cr (VI) is converted to Cr (III) before it enters the bloodstream...

The kidneys/urine and the bile/feces are the two main ways that chromium is excreted. In contrast to Cr (VI), Cr (III) is not transported into cells via

membrane anionic transporters. Within the cells, Cr(VI) undergoes metabolic reduction to Cr (III). With macromolecules, both Cr (lll) and the reductional intermediate Cr (VI) can coordinate and form covalent bonds. although Cr (VI) does not directly react with them. These macromolecules consist of lipids, proteins, DNA, and RNA. The body need chromium, a vital vitamin, in order to optimize the way insulin uses sugars, proteins, and fats. As a dietary supplement, Cr P has been used to help diabetics manage their blood sugar levels. It may also lower cholesterol and blood pressure. Chromium promotes improved insulin sensitivity by improving insulin's ability to attach to cells, increasing the number of insulin receptors, and activating insulin receptor kinase. [81].

In the metabolism of glucose and the function of insulin, chromium plays a part. Similar to type II diabetes, chromium deficiency causes reduced glucose tolerance, neuropathy, increased plasma fatty acids, and atherosclerosis as symptoms. Only patients receiving long-term parenteral nourishment have been known to have chromium deficiencies. Chromium is primarily eliminated through the kidneys, thus people with kidney disease shouldn't take supplements of the metal. Chromium toxicity is common in working environments, especially among welders, and it causes contact dermatitis. Chromium vapors can cause lung cancer and other lung illnesses when inhaled. [64].

1.11.4. Chromium Determination Studies

Table (1.2): Chromium Determination Studies

Method	Reagent	Result of RSD%	Results of LOD& LOQ	Ref
C. P. E	2-[BenzeneThiazolylAzo]-4-Benzene Naphthol)BTABN.	0.31%	LOD=0.017μg/ ml LOQ=0.0568 μg/ml	[82]
C.P.E	4-(2-thiazolylazo) resorcinol (TAR)	3.7%	LOD =3.2μg/L LOQ=10.5 μg L	[83]
Dispersive liquid-liquid microextraction (DLLME)	Rhodamine 6G hydrochloride dye (RG+)	2.16%	LOD=7.48μg/L LOQ=24.68μg/L	[84]
Spectrophotometric	indigo carmine dye	(0.70 - 1.86)%	DOL=0.0012μg/ml LOQ=0.00396μg/ml	[85]
Spectrophotometric	2-((E)-(1H-benzo[d]imidazol2-yl)diazenyl)-5-((E)-benzyl ideneimino) phenol (BIADPI	(0.9-0.467) %	LOD=0.27μg/ml LOQ=0.891μg/ml	[86]
Spectrophotometric	4-(nitro phenyl azo imidazole)	0.29%	LOD=0.13μg/ml LOQ=0.435μg/ml	[87]
Spectrophotometric	4-(2-benzothiazolylazo) 2,2′-biphenyldiol complex	<1.85%	LOD=0.13 ng. L^{-1} LOQ=4.4 ng. L^{-1}	[88]
Spectrophotometric	N-hydroxy-N, N'-diphenylbenzamidine	± 2.0%	LOD=0.3μg/L LOQ=0.99μg/L	[89]
Spectrophotometric	polymethine dye Astra *P[Phloxine FF	3.59%.	LOD=1.87μg/L LOQ=6.17μg/L	[90]
Spectrophotometric	Ethyl4-(5-acetyl-2,3,4-trihydroxyphenyl) diazenylbenzoate (EATDB	0.742%-0.896%	LOD=0.864 μg/mL LOQ=2.851 μg/mL	Present Work

1.12 Aims of the Research

1-Prepration of novel compound from an Azo derivative, isolate and purify in the solid phase, followed by analysis using FT-IR, UV-is,^{1}HNMR,^{13}C,NMR,and GC/mass spectrometry techniques .

2-Examining the characteristics of the link between new both ions (cobalt and chromium ions) by determining the proportion between ion and ligand through techniques such as the method of mole ratios , Job's method ,and Molllared method. .

3- The research also involved recognition of solid compound and recognition of certain physical properties Determination of ligand and synthsis compound through UV-Vis and FT-IR method subsequently suggesting a synthetic formulation for compounds.

4-Applying the new proposed method to determine Co(II) and Cr(III) in various samples.

CHAPTER TWO

EXPERIMENTAL WORK

2.1 Apparatus.

In the table below are list of the apparatus used in this thesis.

Table 2.1 Apparatus used.

No.	Instrument name	Type & origin	Place
1.	Digital balance	SartoriusBS-210 (Germany)	Kerbala University college of Science
2.	Double beam UV-visible spectro-photometer	Cecil 7200,(England).	Kerbala University College of Science
3.	FT-IR. Spectro - photometer	8400, Shamadzu,(Japan)	Kerbala University College of Science
4.	GC/MS spectrophotometer	5975CLMSDwith Tripe-AxisDetector/agilent technologies	University of Basrah college of education
5.	Molar conductivity meter	WTW.270.inolab GERMANY	Kerbala University College of Science
6.	PH/meter	HANNA, ITALY	Kerbala University College of Science
7.	Shaker	GEMMYORBIT VRN480 England	Kerbala University College of Science
8.	Single- beam visible-spectrophotometer	Made in Japan- Sp -300	Kerbala University College of Science
9.	Temperature control circulator	BS-11, (Korea)	Kerbala University College of Science

2.2 Materials of Chemical

In the table below are list of chemical materials that are used in this research.

Table (2.2): List of Chemical Materials.

Seq	The name of subject	Chemical formula and M.Wt	The company	purity
1	Sulfuric acid	H_2SO_4 98.08g/mol	G.C.C	99,0%
2	Nitrite of sodium	$NaNO_2$ 69.00g/mol	E.M.darmstad	99,0%
3	Hydroxide of sodium	NaOH 39.99 g/mol	B.D.H	99,0%
4	Hydrochloric acid	HCl37w/v%36.5g/mol	Himedia	Analar
5	Nitric acid	HNO_3 65w/v% 63.018g/mol	Merckdarmstadt	Analar
6	Sodium nitrate	$NaNO_3$ 84.99g/mol	fulka	98.00%
7	ethanol	C_2H_5OH 46.068g/mol	fulka	99,00%
8	Cd (II) nitrate-hydrate	$Cd(NO_3)_2.4H_2O$ 308g/mol	fulka	99.0%
9	Nickel(II)nitrate-hydrate	$Ni(NO_3)_2$ $6H_2O$ 290.7g/mol	B.D.H	98.0%
10	Cobalt(II)nitrate -6hydrate	$Co(NO_3)_2.6H_2O$ 291g/mol	B.D.H	99.0%
11	Iron(III)nitrate-hydrate	$Fe(NO_3)_3.9H_2O$ 404g/mol	(B.D.H)	99.0%
12	Mercury(II)nitrate-hydrate	$Hg(NO_3)_2.H_2O$ 342g/mol	MERCK	98.5%
13	Lead (II)nitrate	$Pb(NO_3)_2$ 331.2g/mol	(B.D.H)	99.0%

14	Magnesium (II) nitrate-hydrate	$Mg(NO_3)_2.6H_2O$	(B.D.H)	99.5%
15	Silver nitrate	$AgNO_3$	(B.D.H)	99.0%
16	Copper (II)nitrate -hydrate	$Cu(NO_3)_2.3H_2O$	(B.D.H)	99.0%
17	Potassium Sulfate	K_2SO_4	MERCK	99.0%
18	Potassium bromide	KBr	NANIWA	99.0%
19	Potassium thiocyanate	KSCN	(B.D.H)	99.0%
20	Potassium Iodate	KIO_3	GCC	99.0%
21	Potassium dichromate	$K_2Cr_2O_7$	Riedel	99.0%
22	Potassium carbonate	K_2CO_3	(B.D.H)	99.0%
23	Potassium cyanate	KCN	(B.D.H)	99.0%
24	Thiourea	CH_4N_2S	AAG	99.0%
25	Ascorbic acid	$C_6H_8O_6$	(B.D.H)	99.0%
26	Ethylene diamine tetra acetic acid disodium salt	Na_2EDTA	Fluka	98.0%
27	Citric Acid	$C_6H_8O_7$	Scharlou	99.0%
28	Potassium chloride	KCl	GCC	98.0%
29	Dimethyl sulfoxide	DMSO	Fluka	98.0%
30	Sodium Dodecyl Sulfate(SDS)	$NaCl .H_2SO_4$	Thermo	99.0%
31	Zinc(II)nitrate -hydrate	$Zn(NO_3)_2.6H2O$	HIAMEDIA	99.0%
32	Chromium(III)nitrate hydrate	$Cr(NO_3)_3.9H2O$	(B.D.H)	99.0%
33	Benzocaine	$C_9H_{11}O_2N$	HIAMEDIA	98%
34	2,3,4-trihydroxy phenyl acetophenone	$C_8H_8O_4$	HIAMEDIA	98.00%

35	Formaldehyde	CHO	HIAMEDIA	99.00%
36	Disodium phosphate	$Na_2HPO_4.12H_2O$	HIAMEDIA	99.00%
37	Chloroform	$CHCl_3$	HIAMEDIA	99.4%

2.3 Synthesis Ligand Ethyl.4-((5-acetyl-2, 3, 4-trihydroxyphenyl) diazonyl) benzoate (EATDB).

Ethyl 4-aminobenzoat (Benzocaine) (1.651 g, 10 mmole) is dissolved in a mixture produced by adding distilled water (25 mL) to 5 mL of concentrated HCl acid. The nitrogenation process is completed by let the solution to remaining in the mixture for 15 minutes after cooling it to between (0 -5) degrees Celsius and the solution of sodium nitrite (0.69 g, 10 mmole) was added ,diluted in 10 mL of distilled water. After dissolving (1.681 g.) of the 2,3,4-tri hydroxyacetophenone in 10 mL of ethanol and 25 mL of NaOH (10%), the solution should be cooled to between (0 -5) ^{0}C and allowed to sit for 30 minutes. The salt solution was chilled to between (0-5) ^{0}C and then progressively infused with this imidazole derivative solution. After being given a heavy red stain, the solution was kept at (0 -5)^{0}C for an hour. Then, diluted HCl acid (5 mL, 1 M) was gradually added to it in order to produce a reddish-orange precipitate and acquire the acidity function (pH = 5–6). In order. Upon precipitation, the resulting solid was subjected to filtration, followed by thorough washing with distilled water to eliminate any traces of sodium sulfate, which might have formed in the process of pairing and neutralization reactions. To create the pure form, it was then dried and recrystallized with ethanol, and the yield was 67% [91].

2.4 Preparing the Standerd solution.

2.4.1 Preparation of Co (ll) Standard solution (1000 μg.mL^{-1}):

The Co (II) ion standard solution (1000 μg.ml^{-1}) equal to 1.696×10^{-2}M prepared by dissolving 0.4936g of Cobalt nitrate Co $(NO_3)_2.6H_2O$ was dissolved in 100ml of deionized water. This standard solution was repeatedly diluted with deionized water to yield additional standard solutions as a starting point.

2.4.2 Preparation of Cr (lll) Standard solution 1000 μg . mL^{-1}.

Cr (lll) ion standard solution was created by dissolving 0.770 g of chrome nitrate (Cr $(NO_3)_3).9H_2O$ in distilled water to achieve a concentration of 1000 μg.ml^{-1} equal to $(2.493 \times 10^{-3}$M). In other standerd solution with different concentrations were prepared.

2.4.3 Preparation of Reagent Solution (1000μg.mL^{-1})

A reagent was made by dissolving 0.100 g of EATDB, M.Wt. is 344 g. mol^{-1} in ethanol, then complete the volume with 100mL ethanol to the mark of volumetric flask.

2.4.4 Preparation of Sodium hydroxide solution (0.1M)

A 0.400g of sodium hydroxide was dissolved in 100ml distilled water to prepare.0.1M of NaOH.

2.4.5 Preparation of hydrochloric acid solution (0.1M).

A 0.833mL of concentrated hydrochloric acid 37% was dissolved in 100mL deionized water to prepare 0.1 M of HCl.

 2.4.6 Preparation of cations solution.

Cation solutions with concentration of 100μg.mL^{-1}were prepared by dissolving the necessary amounts of elemental nitrate salts in (100 ml) deionized water .

Table (2.3): list of the weights utilized in the creation of cation solutions.

No	Structure of cation	Wt.g
1.	$[Cd(NO_3)_2].4H_2O$	0.273
2.	$Ni(NO_3)_2.6H_2O$	0.495
3.	$Fe(NO_3)_3 .9H_2O$	0.723
4.	$Hg(NO_3)_2.H_2O$	0.170
5.	$Pb(NO_3)_2$	0.159
6.	$Mg(NO_3)_2.6H_2O$	1.055
7.	$AgNO_3$	0.157
8.	$Cu(NO_3)_2.3H_2O$	0.380

2.4.7 Anions solution preparation:

From elemental potassium salts, A 100 µg.ml^{-1} concentration of anions was created in solution, by dissolve the necessary amounts in 100ml of deionized water as stated.

Table (2.4): list of the weights utilized in the creation of anions solutions.

No	Anions formula structure	Wt.gm
1	K_2SO_4	0.045
2	KBr	0.037
3	KSCN	0.041
4	KIO_3	0.030
5	$K_2Cr_2O_7$	0.030
6	K_2CO_3	0.055
7	KCN	0.061

2.4.8 Preparation solution to study the Ionic strength.

2.4.8.1 Preparation of 0.5 M sodium sulfate solution. (Na$_2$SO$_4$).

A 0.5 M sodium sulfate solution can be made by weighting 1.780 g of sodium sulfate (Na$_2$SO$_4$) and dissolving it in distilled water with volume of 5 mL, Fill the volumetric flask to the mark with 25 mL of distilled water. Small volumes of the stock solution were diluted to create a concentration (0.5, 0.05, 0.005,and 0.0005) M.

2.4.8.2 Preparation of 0.5M of (NaNO$_3$) solution.

For studying the impact of Ionic Strength, A 1.063 g of NaNO$_3$ was dissolved in 25 ml deionized water to prepare 0.5M of NaNO$_3$ from this stock solution series of solution with different concentration (0.5, 0.05, 0.005, and 0.0005) were prepared.

2.4.9 Masking agent solution preparation.

To make masking agent solutions with a 25 mL volume, calculated amount for each element was first dissolved in 5 mL of distilled water. The resulting solution was then transferred to the volumetric flask with 25 mL complet to the mark with deionized water.

Table (2.5): lists the masking agent parameters used.

No.	masking agent 0.1M	Wt. g
1.	Thiourea	0.190
2.	ascorbic acid	0.440
3.	Na$_2$EDTA	0.890
4.	Citric Acid	0.020
5.	K Cl	0.180
6.	Na$_2$HPO$_4$.12H$_2$O	0.890
7.	CH$_2$O	0.075

2.5 Preliminary analysis of the reagent's interaction and several ions of metal.

In a test tube, a 1 mL solution containing cobalt (II) and Chromium (lll) ions at a concentration of 1000 µg. mL^{-1} was carefully placed. Subsequently, drop by drop, 2 mL of a prepared solution containing the reagent (EATDB) at a concentration of 1000 µg. mL^{-1} was added to the test tube while shaking, resulting in the formation of a colored precipitate.

To observe the effect of the acid function, drops of hydrochloric acid (0.1M) were added to a portion of this mixture, while drops of sodium hydroxide (0.1M) were added to another portion. The purpose was to assess the impact of the acid and base on the color formation.

It was observed that the color formed prominently under basic conditions, indicating a positive response. However, there was no change in color under acidic conditions, indicating a lack of reactivity or color formation. This observation suggests that the cobalt (II) and Chromium (lll) complexes with the reagent (EATDB) exhibits a strong color response in basic environments, while acidic conditions do not elicit a visible color change.

2.6 UV-Visible study.

2. 6 .1 UV-Visible study of ligand (EATDB).

For the spectral scanning of the reagent EATDB at a concentration of 1.45x10^{-3} M within the specified range of 190-1100 nm, a dual-beam UV-visible spectrophotometer was employed. The measurements were carried out using quartz cells with a light path thickness of 1 cm. Subsequently, the peak absorbance of the reagent was identified at a wavelength of λ_{max}=289 nm.

2.6.2 UV-Visble study for Co(ll) and Cr (lll) ions.

To study the UV-Vis spectrum 2ml 0f reagent solution with concentration 2.450×10^{-4} M equivalent to 100 µg.mL^{-1} was added to two volumetric flasks .First one contain 1 ml Co (ll) ion solution with concentration 3.440×10^{-4}M equivelant to 100 µg.mL^{-1} and the second contain 1 mL Cr (lll) ion with concentration 2.500×10^{-4} equivalent to 100 µg.mL^{-1} and complet the volum to the mark for each volumetric flask .Blank solution was prepared in same conditions except the addition of Co (ll) and Cr (lll) ions

A spectrophotometric device was used to scan the complex solutions produced in the previous sentence the maximum absorbance values were computed over the wavelength range of 190-1100 nm . When compared to the comparable reagent solution (Blank), the complexes in this region exhibit the highest absorption value.

2.7 Optimum condition for the development of Cobalt (ll) and Chromium (lll) complexes.

After determining the $\boldsymbol{\lambda}_{max}$ absorption of each complex, which were found to be at $\boldsymbol{\lambda}_{max}$ = 437 nm and 573 nm for Co(II) and Cr(III) respectively, further investigations were conducted to identify the optimal conditions for generating these two complexes. These examinations were carried out with meticulous attention to detail to ensure the accuracy and reliability of the results. The aim was to establish the most favorable reaction conditions that would yield the Co (II) and Cr (III) complexes with maximum efficiency and precision

2.7.1 Effect of pH value.

2.7.1.1 Study effect pH on the Co (ll) complex.

A 1mL of Co (ll) ion solution with concentration at 1.6962×10^{-2}M equivalent to 100µg.mL^{-1} was added to set of 10 ml volumetric flask followed by addition of 2mL of reagent solution with concentration at (1.453×10^{-3} M) equivalent

to 500 µg.ml^{-1} for each volumetric flask than adjusting the pH (2-10) by using HCl 0.1M and NaOH 0.1 M and the absorption has been taken at λmax of Co (ll) ion.

2.7.1.2 Study the effect of acidic function on Cr (lll) complex

A 1ml of Cr (lll) ion solution with concentration at 1.923×10^{-3}M equivalent to 100µg.mL^{-1} was added to set of 10 ml volumetric flask followed by addition of 2ml of reagent solution with concentrationat (1.453×10^{-3} M) equivalent to 500 µg.ml^{-1} for each volumetric flask than adjusting the pH (2-10) by using HCl 0.1M and NaOH 0.1 M and the absoption has been taken at λmax of Cr (III) ion.

2.7.2 The stability and effect of time on complex.

Absorbance of Co (ll) and Cr (lll) complexes with the reagent at λmax for two ions were investigated at different time to study the stability of the two complexes.

2.7.2.1 Analyze the impact of Time on the assimilation for cobalt (ll) complexes.

A Cobalt (ll) complex was made by mixing a solution of Cobalt (II) ions which have concentrations (3.42×10^{-4}) M, or 100 µg .ml^{-1} , with a solution of reagents at concentrations (1.45×10^{-3}) M, or 500 µg.mL^{-1}. The optimal acidic function PH= 9 then completthe volume to the 10 ml .followed by measuring the absorbance at 437 nm compared to the Blank solution at various time ,starty from the beginning of reaction until 48 hrs

2.7.2.2 Analyze the time impact on the assimilation of chromium (III) complexes.

A Cr (lll) complex made by mixing a solution of Cr (lll) ions at $(1.923 \times 10^{-3}$ M), equivalent to 100µg.mL^{-1}, with a solution of reagents at concentrations

(1.45×10^{-3}) M, or 500 μg.mL^{-1}. The optimal acidic function pH= 8 then complet the volume to the 10 ml .followed by measuring the absorbance at 573 nm compared to the Blank solution at various time ,startly from the beginning of reaction until 48 hrs

2.7.3 Effect of sequential addition.

A series of successive addition for reagent solution $(2ml, 1.45 \times 10^{-3}M)$ and metals $(1ml, 3.34 \times 10^{-4}$ M for Co^{+2}, and $2.49 \times 10^{-4}M$ for $Cr^{+3})$) and adjusted the pH=9,8 at optimum conditions were made to obtained the best intensity

Table (3.8): the effect of sequential addition on Co (ll) and chromium (lll)

No.of Sequence	Seq of addition
1	M+PH+L
2	L+PH+M
3	L+M+PH
4	M+L+PH

M=Metal ,   L=Ligand

2.7.4 Effect of Temperature.

2.7.4.1 The effect of temperature on Co (ll) ion complex.

A (1mL) of Cobalt (II) ion at a concentration of $(3.4 \times 10^{-4}M)$ equivalent to (100 μg.ml^{-1}) to a set of 10 ml of volumetric flasks followed by 2mLof ligand at $(1.45 \times 10^{-3}$ M) equal to(500μg.ml^{-1}) concentration, the effect of temperature on the Cobalt complex was examined .After adjusting the ideal pH = 9 . Transferring to the Volumetric flask, 10ml, filling to the mark with deionization putting these flasks in water bath that has a temperature range of $(10 - 60\ ^{0}C)$, and comparing with blank but without cobalt,

2.7.4.2 The effect of temperature on Cr (lll) ion complex.

A (1mL) of Chromium (III) ion at a concentration of $(2.51 \times 10^{-4}M)$ equivalent to (100 μg.ml^{-1}) to a set 10 ml of volumetric flasks followed by 2mLof ligand

at (1.45 x10^{-3} M) equal to(500µg.ml^{-1}) concentration, the effect of temperature on the Chromium complex was examined .After adjusting the ideal pH = 8 . Transferring to the Volumetric flask, 10ml, filling to the mark with deionized water putting these flasks in a water bath that has a temperature range of (10 – 60 ^{0}C), and comparing with blank but without Chromium (lll).

2.7.5   Effect of ionic strength,

2.7.5.1 Impact of ionic strength on Co (ll) ion complex.

The amount of the reactants' solubility, the rate at which they react, the effects of the ions and the sensitivity of the estimation various Ionic Forces. Investigating this impacting aspect . This was demonstrated using the below: 1ml of a Cobalt(II) ion solution, with a concentration of (3.4x10^{-4}M), equal to (100 µg.ml^{-1}), was introduced to a set of volumetric flasks, and then 1ml each of sodium nitrate and sodium sulfate solutions, with varying concentrations were added. Separately, after which 2ml of each ligand at concentration of (1.45 x 10^{-3}M) was added. The flasks then filled up to the mark, and ideal acidity function set at (pH=9) for creating of Co (II) complex, the complex's maximum (λ_{max} = 437 nm) was measured in contrast to a solution created with the same chemicals as a solution that is comparable to it (Blank), and for all the solutions that were examined. , (0.5,. 0.05, 0.005,and 0.0005 M) were added.

2.7.5.2 Impact of ionic strength on Cr (lll) ion complex.

The amount of the reactants' solubility, the rate at which they react, the effects of the ions and the sensitivity of the estimation various Ionic Forces. Investigating this impacting aspect . This was demonstrated using the below: 1ml of a Chromium (III) ion solution, with a concentration of (2.51x10^{-4}M), equal to (100 µg.ml^{-1}), was introduced to a set of volumetric flasks, and then 1ml each of sodium nitrate and sodium sulfate solutions, with varying concentrations. Separately, after which 2ml of each ligand at concentration of (1.45 x 10^{-3}M) was added. The flasks then filled up to the mark, and ideal

acidity function set at (pH=8) for creating of Cr (lll) complex, the complex's maximum (λ_{max} = 573 nm) was measured in contrast to a solution created with the same chemicals as a solution that is comparable to it (Blank), but with the ion added, and for all the solutions That were examined. , (0.5, 0.05, 0.005, and 0.0005 M) were added.

2.8   Calibration Curves.

2.8.1   Calibration Curve of Co (II) complexes.

Different concentrations of Cobalt (ll) ion solution (1 mL), 1.72×10^{-3}-2.4×10^{-4}M corresponding to (0.5-100 µg.mL^{-1}), were added to a series of volumetric flasks (10 mL). Then 2 ml of the ligand solution with concentration at 1.45×10^{-4} M was added to each volumetric flask followed by adjusting the pH =9 and complet the volume to the mark with deionozation.

By Absorbance measurement of all solutions at the complex's maximum wavelength of (λ_{max}= 437 nm), it is possible to conduct a calibration curve between absorption and concentration.

2.8.2 Calibration Curve for the Cr^{+3} complexes

Different concentrations of chromium (III) ion solution (1 mL), 1.24×10^{-5}-2.4×10^{-4}M corresponding to (1.00 -100 µg.mL^{-1}), were added to a series of volumetric flasks (10 mL). Then 2 ml of the ligand solution with concentration at 1.45x10-4 M was added to each volumetric flask followed by adjusting the pH =8 and complet the volume to the mark with deionization.

. By measuring the absorbance of all solutions at the complex's maximum wavelength of 573 nm, it is possible to conduct a calibration curve between absorption and concentration**.**

2.9   The stoichiometry study

Under ideal conditions, it is possible to investigate the Metal to Ligand ratio (M: L) by use, Mole Ratio method, Continuous Variations (Job's method), and Mollard method.

2.9.1 Job's method (continuous variation).

2.9.1.1 Cobalt (II) ion complex.

The following step is to make two solutions for the Cobalt (II) complex at concentrations of (3.00 x10^{-4} M) and the same concentration of metal ion and Ligand, after   adjusting the pH =9 the volume completed to the mark .and measure the absorbance for each volumetric flask at λ_{max} of Co (II) ion against blank solution which prepared in the same procedure except adding the solution of Co (II) ion [92].

2.9.1.2 **Chromium (III) ion complex.**

The following step is to make two solutions for the Chromium(lll))Complex at concentrations of (3 x10^{-4} M) and the same Concentration of metal ion and Ligand, after   adjusting the PH =8 the volume completed to the mark .and measure the absorbance for each volumetric flask at λmax of Cr (lll) ion against blank solution wich prepared in the same procedure except adding the solution of Cr (lll) ion [92].

2.9.2 Method of the mole ratio.

2.9.2.1 Complex of Cobalt (ll) ion.

A series of 10 ml volumetric flasks were employed for the experiment. Each flask was filled with a precise and constant concentration of cobalt (II) ions, precisely 3.43x10^{-4} M. Additionally, varying concentrations of the ligand were introduced into the flasks, ranging from 2.5x10^{-4} M to 7.0x10^{-4} M, in a proportional manner. Throughout the experiment, the acidity function was modified accordingly. The optimal conditions for complex formation were carefully maintained at a pH of 9. To achieve the desired maximum concentration, ethanol was gradually added to each flask until the target concentration was reached. During the complex preparation, instead of using the Cobalt (II) ion solution, a volume of deionized water, was utilized as a substitute. This allowed for the creation of comparison solutions, which were

prepared in a manner similar to that of the complex solutions. After completing the preparations, measurements of the complex's absorption were taken for all the solutions at a specific wavelength, which was determined at λmax=437 nm. These absorbance measurements were crucial in assessing and comparing the complex formations at different ligand concentrations and under varying acidity conditions. The data obtained from these measurements provided valuable insights into the behavior and properties of the formed complexes in the specified experimental conditions [93].

2.9.2.2   Complex of Chromium (III) ion.

In this experiment, a set of 10 mL volumetric flasks was utilized. Each flask was filled with a known and constant concentration of chromium (III) ions at 2.5×10^{-4} M. The reagent was then added to each flask in increasing amounts, ranging from 2.5×10^{-4} M - 7×10^{-3} M, proportionate to the concentration of the chromium (III) ions. The acidity function was set at pH 8.

For the comparison solutions, the volume of the chromium (III) ion solution was replaced with an equivalent volume of distilled water. These comparison solutions were prepared using the same steps as the complex preparations.

The absorbance of the complexes was measured for all solutions at a wavelength of λmax=573 nm. This allowed for the assessment and comparison of the complex formations at different ligand concentrations and under the specified acidity conditions. The measurements provided valuable data regarding the behavior and properties of the formed complexes at the designated experimental conditions [93].

2.9.3 Mollard's Method

2.9.3.1 Cobalt (ll) ion complexes

In a volumetric flask 1ml of Co (ll) with a concentration at solution of, $(3 \times 10^{-3}$M) was mixed with a reagent solution with a concentration of $(1 \times 10^{-4}$M). By adding ethanol, the volume was completed to 10ml and the acidity function was

be to (pH = 9). absorbance was measured at (λmax = 437 nm) in comparison to the comparator solution.In a volumetric flask, Cobalt (II) ion solution and reagent solution were combined at low concentrations (3.00×10^{-4} M for the reagent solution and (1.0×10^{-4} M for the cobalt (II) ion solution), and the pH value was changed to pH= 9 before the volume was finished to (10ml) with Ethanol . The greatest absorption in relation to the comparator solution was calculated at,λ_{max}=437nm [94].

2.9.3.2 Chromium (III) ion complexes

   In one experimental setup, a ligand solution with a concentration of 3.0×10^{-3} M was mixed with 5 ml of a chromium (III) ion solution at a concentration of 1.0×10^{-4} M in a volumetric flask. The pH of the solution was adjusted to 8 and the volume was completed to 10 mL by adding ethanol. The maximum absorption of this complex was recorded at 573 nm, and it was compared to a control comparator solution. In another experiment, a chromium (III) ion solution with a concentration of 3.0×10^{-4} M was combined with a low concentration of the reagent solution, specifically 1.0×10^{-4} M, in a volumetric flask. The pH of this solution was set to 8 using an acidic function, and the volume was completed to 10 ml using ethanol. The absorption of this complex was measured at λmax = 573 nm, and it was compared to the comparator solution. Both experiments involved creating complexes with chromium (III) ions and the reagent at different concentrations and under the same pH conditions. The absorbance measurements at 573 nm were used to assess and compare the complex formations to the control comparator solution[94].

2.10 Determination of the thermodynamic functions, stability constant, and degree of dissociation of the two generated complexes.

2.10.1 Complex of Cobalt (II).

The first volumetric flask, which contained (1 mL) of the Co (ll) concentration of ion 3.4×10^{-4} M and 2ml of the ligand with concentration 1.46×10^{-3} M, was utilized. The volumetric flask was then filled with distilled water until the mark was reached, and the ideal acidic function was changed to (pH = 9). Last but not least, the second volumetric flask was filled with 1 mL of Co (ll) at a Concentration 3.4×10^{-4} M and 2mL of the ligand a concentration of 3×10^{-3} M. The two volumetric flasks were then placed in a water bath at 10 to 30 °C, and the solutions' absorption was assessed at the wavelength where their maximum absorbance compared to the comparator solution at each temperature. The dissociation constant determined from absorption data from the first volumetric flask (As) and second volumetric flask (Am).

2.10.2 Complex of Chromium (lll) ion

A two volumetric flasks (10 mL each) were utilized, and the ideal acidic function was modified to be at pH = 8.1M 1ml of Chromium (III) ion was present in the first flask with concentration (2.5×10^{-4} M), and in the second, 2mL with concentration of (3.3×10^{-4} M) , with the ideal acidic function set to (pH = 8). Followed by transferring the solution to a volumetric flask (10 mL),and complet the volume to the mark .The absorption of the solutions were measured at the wavelength corresponding to their respective maximum absorption at each temperature within a water bath. The water bath was set to maintain a temperature range of 10 - 30°C. For each temperature point, the absorption of the solutions was compared to the absorption of the comparator solution . The dissociation constant determined from absorption data from the first volumetric flask (As) and second volumetric flask (Am).

2.11 Impact of the masking agent Anions and Cations interference.

2.11.1 Interference of Cations.

2.11.1.1 Determination of Cobalt (ll) and certain interference Cations ion.

   This study was conducted that might interact with the Cobalt (ll) ion under research in a set of 10mL volumetric flask 1 mL of the Cobalt (II) ion was discovered in this work. First, 1 mL of a Cobalt (II) ion solution (100 µg.mL $^{-1}$) was added. Next In each flask ,(1ml) of metallic ion solutions (100 µg. ml^{-1}) of(Ag^{+1}, pb^{+2}, Fe^{+3}, Mn^{+2}, Zn^{+2}, Cu^{+2}, and Cd^{+2}), which can interfere with the Cobalt (ll) ion separately, were added Finally, 2 mL of reagent solution at concentration (1.45×10^{-3}M),equal to(500 µg.ml^{-1})was added The volume was completed to the appropriate level with D.W and the absorbance was measured (λ_{max}=437nm) after the acidic function was set to (pH = 9) of Cobalt (ll) complex.

2.11.1. 2 Determination of Chromium (lll)) ions using various interference cations.

In this study, the identification of chromium (III) ions involved the introduction of various metal ion solutions that might potentially interact with chromium (III) ions. For this purpose, a set of 10 ml volumetric flasks was used. Each flask received 1 mL of metallic ion solutions (Zn^{+2}, Mn^{+2}, Ag^{+1}, Pb^{+2}, Fe^{+3}, Cu^{+2}, Cd^{+2}) at a concentration of 100 µg.mL^{-1}. Subsequently a 2 mL portion of the chromium (III) ion solution, with a concentration of 100 µg.ml^{-1} , was added to each flask individually, to investigate its interaction with the respective metallic ions. Before the addition of the chromium (III) ion solution, 1.45×10^{-3} M (or 500 µg.ml^{-1}) of the reagent solution was added to each flask. The acidic function was adjusted to pH 8 to promote the formation of chromium (III) complexes. To complete the volume in each flask, distilled water was added up to the mark, and then the absorbance was measured at λ_{max} = 573 nm against a blank. This experimental setup allowed the assessment of how the presence of

different metal ions might interfere with the formation of chromium (III) complexes. The absorbance measurements at λ_{max} = 573 nm provided crucial data to evaluate the complex formations and their interactions with the reagent and metallic ions under investigation.

2.11.2 Anions Interference Interaction

2.11.2.1 Investigating Cobalt (ll) ion with certain Interferences anions ions

In this study, the identification of cobalt (II) ions involved the addition of a solution of anions that might potentially interfere with cobalt (II) ions. A group of 10 ml volumetric flasks was utilized for this purpose. Each flask received 1 mL of anion solutions (SO_4^{-2}, Br^{-1}, SCN^{-1}, IO^{-3}, CrO_7^{-2}, CO_3^{-2}, CN^{-1}) at concentrations of 100 µg.mL^{-1} and 200 µg.mL^{-1}. Following the addition of the anion solutions, 1 mL of cobalt (II) ion solution at a concentration of 100 µg.mL^{-1} was added to each flask individually. This allowed the examination of its interaction with the respective anions. Subsequently, 2 mL of reagent solution at a concentration of 500 µg.mL^{-1} (or $1.7x10^{-3}$M) was added to each flask. To complete the volume in each flask, distilled water was added up to the mark. The acidic function was adjusted to pH 9 to facilitate the formation of the cobalt (II) complex. The absorbance of the resulting complex was then measured at λ_{max} = 437 nm against a comparison solution (blank). The blank is a control solution containing all components except the cobalt (II) ion, used for baseline correction. The absorbance measurements at λ_{max} = 437 nm provided crucial data to identify and analyze the cobalt (II) complexes and their interactions with the reagent and anions under investigation.

2.11.2.2. Investigating of Chromium (lll) ion and some anions ions.

In this experiment, the identification of chromium (III) ions involved the addition of solutions of anions that might interact with the chromium (III) ion under investigation. A group of 10 mL volumetric flasks was used for this purpose. Each flask received 1 mL of anion solutions at concentrations of 100 µg.mL^{-1} and 200 µg.mL^{-1}. After adding the anion solutions, 1 mL of chromium (III) ion solution at a concentration of 100 µg.mL^{-1} was added to each flask. This allowed the investigation of the potential inhibitory effect of the anions on the chromium (III) ion individually. Subsequently, 2 mL of the reagent liquid at a concentration of 1.5×10^{-3} M (or 500 µg.mL^{-1}) was added to each flask. The acidic pH was adjusted to 8 to facilitate the formation of the chromium (III) complex. The volume in each flask was completed to the mark with distilled water. Finally, the absorbance of the resulting chromium (III) complexes was measured at **λ**max = 573 nm against (blank). The blank is a control solution containing all components except the chromium (III) ion, used for baseline correction. This experimental setup allowed researchers to assess how the presence of different anions might interact with and potentially inhibit the formation of chromium (III) complexes. The absorbance measurements at **λ**$_{max}$ = 573 nm provided crucial data for identifying and analyzing the chromium (III) complexes and their interactions with the reagent and anions under investigation.

2.11.3 Study of using masking agent to determine Co (ll) and Cr (lll) ions in presence of other ions.

 2.11.3.1 Cobalt ion complex

A 1.00 ml of various masking agent solution with concentration (100 µg.ml^{-1}) were added to (1ml) of Cobalt (ll) ion solution separately with concentration (100µg.ml^{-1}) then 2ml of reagent solution concentration of 500µg . mL^{-1} were added . Using distilled water to fill the acidic function after it had been adjusted

to pH=9 . Measurements were taken of both the absorbance and volume to the mark After learning that the agents for masking had no impact on the Cobalt (II) ability to absorb light at (λ_{max}=437)nm, compared to the (Blank), For each of the ions interfering with the process, a research was conducted to determine the appropriate masking agent and its volume. Cobalt (II) ion.

2.11.3.2 Chromium (lll)) ion complex .

A 1.00 ml of various masking agent solution with concentration (100 $\mu g.ml^{-1}$) were added to (1ml) of Chromium(lll) ion solution separately with concentration (100$\mu g.ml^{-1}$) then 2ml of reagent solution concentration of 500$\mu g . mL^{-1}$ were added . Using distilled water to fill the acidic function after it had been adjusted to PH=8 . Measurements were taken of both the absorbance and volume to the mark After learning that the agents for masking had no impact on the Cobalt (II) ability to absorb light at (λ_{max}=573)nm, compared to the comparator solution (Blank), For each of the ions interfering with the process, a research was conducted to determine the appropriate masking agent and its volume Chromium (III) ion.

 2.11.4 Using more effective masking agent

 2.11.4.1 Cobalt (ll) ions Complex

   Take a collection of 10 mL volumes flasks .filled with Cobalt (II) ion solution with a concentration of (100 $\mu g.ml^{-1}$),selected cations (Zn^{+2}, Mn^{+2},Ag^{+1}, $pb^{+2,}$ Fe^{+3}, Cu^{+2}, Cd^{+2})with a concentration of   (100 $\mu g.mL^{-1}$),appropired masking agent with a concentration of (0.1 M), reagent at a concentration of (500 $\mu g.ml^{-1}$),The PH of solution were adjusted at (pH = 9), and then fill the volume to the mark with deionized water. Absorbance was measured at (λ_{max}= 437nm) in comparison to the compartor solution

2.11.4.2 Chromium (lll) ion complex

Using a set of volumetric flasks 10ml added 1ml of Cr (lll) ion at a concentration of 100 µg.mL^{-1}, 1ml of the concentration of the cations ion is 100 µg.ml^{-1} , 1 mL of masking agent 0.1M, 2ml of the reagent at a concentration of 500 µg.ml^{-1}, and finally (1ml) of the solution. Finally, the pH value of the acidity function was adjusted to 8 and complet the volume to the mark Absorption was evaluated in relation to at comparison approach ($\boldsymbol{\lambda}_{max}$ = 573nm)

2.12 Statistically Results Treatment.

Precision. . [95]

The accuracy of the analytical techniques was assessed five replicates and from each metal ion, different concentration were utilized, exactly three concentrations for the purpose of calculation of the Standard Deviation (SD) and relative standard deviation percentage R.S.D%. As well as by establishing the ideal circumstances for each ion. Then, the maximal absorption for each complex was assessed in contrast to the identical conditions-produced comparator solution

$$S.D = \sqrt{\frac{\sum (Xi - \bar{X})}{n-1}} \qquad\qquad 2.1$$

$$R.S.D\% = \frac{S.D}{\bar{X}} * 100 \qquad\qquad 2.2$$

S. D = standard deviation.

RSD% = relative standard deviation.

X$^{'}$= The sample mean

Xi = Value   in the data absorption

n=No. of Values.

Accuracy. [96]

Under optimum for the calibration curves produced from earlier investigations, the produced reagent employed to regulate. The approach taken to calculate these metal ions the error relative (Ere %) was calculated

$$Er\% = \frac{E}{Xt} X\ 100 \hspace{6cm} 2.3$$

$$E = Xi - Xt \hspace{6.5cm} 2.4$$

$$Re\% = 100 \mp Ere\ X\ 100 \hspace{4.7cm} 2.5$$

E = the differentiation between analytical reading and the truth.

Xt = The real values.

2.13 Solid Complexes Preparations of Co (ll) and Cr (lll) ions.

2.13.1 The solid Complex of Co (ll).

A (0.250 mmole 0.1g) of the ligand (EATDB) dissolved in 10ml ethanol was mixed with (0.125mmole, 0.01g) of Cobalt (ll) ion dissolved in 10ml deionized water in a ratio of (1:2), the solid Cobalt (ll) complex was produced. The Cobalt (ll) a circular flask is continuously stirred while ion solution is added to it. Ligand solution is then gradually added while the acidic function is set to (pH = 9), stirring continuously for two hours. A dark brown precipitate was seen 24 hours later, once the ethanol solvent had dried at room temperature.

2.13.2 The Complex of Cr(lll) .

A (0.250mmole 0.1g) of the ligand (EATDB) dissolved in 10ml ethanol was mixed with (0.125mmole, 0.1g) of Chromium(III) ion dissolved in 10ml deionized water in a ratio of (1:2), the solid Cobalt (ll) complex was produced. The Chromium(III) a circular flask is continuously stirred while ion solution is added to it. Ligand solution is then gradually added while the acidic function is set to (pH = 8), stirring continuously for two hours. A dark brown precipitate was seen 24 hours later, once the ethanol solvent had dried at room temperature.

2.14 The (Melting points) of the ligand, Co (ll) complex, and Cr (lll) complexes.

A Melting points of Cr (lll) and Co (ll) complexes, were measured in order to compare them with those of the reagent. The goal of figuring out the melting points is to make sure that the reagent and the melting points of the Co (ll)   and

Cr (lll) complexes are different enough to allow for the creation of the 2 complexes [97].

 2.15 The Molar Conductivity of the Chromium (lll)   and cobalt (ll) complexes. [97]**.**

In order to measure the conductivity 0.01gm of complex was dissolved in 10mL ethanol then measuring the molar conductivity at room temperature, A Co (II) complex solution with a concentration of ($3x10^{-4}$ M) was created using the same procedure as earlier studies. By dissolving (0.01gm) of the complex's Cr (lll) in 10ml of ethanol, the Cr (lll) complex at concentration of $1x10^{-3}$M was created in a similar way

2.16   Estimation spectroscopy.

UV-Vis Spectrophotometer.

A double beam and a single beam UV-visible spectrophotometer were used to detect the UV-Vis spectra of the ligand and its dispersed complexes**.**

Forrier Transfer InfraRed spectra (FTIR).

The Ligand (EATDB), Cobalt (ll) complex, the Chromium (lll) complex all have been characterized by using FT-IR analysis .

Nuclear magnetic resonance spectroscopy ^{1}HNMR, ^{13}CNMR.

To count the amount of carbon and hydrogen atoms in the solvent (DMSO), an NMR spectrum was used.

Gas Chromatography Mass spectrometry. (GC/MS)

Measure the reagent's molecular weight based on the ablation process using GC/MS spectrometry.

2.17 Application.

 The spectroscopic technique used to identify Chromium (III) ions and the Cobalt (II) ion in pharmaceuticals samples.

2.17.1 Determination of Cobalt (II) ion in drug:) [98]

Vitamin B_{12} drug ampule (250 µg.mL^{-1}) contains the Cobalt (II) ion (cyanocobalamin 43.37µg/mL was taken, shaking well, then take a 4ml from the vitamin B_{12} solution to a dry beaker, add 8ml nitric acid(1:1) and heat until dry, add 8ml hydrochloric acid (1:1) and heat again nearly dried, cool the sample, add distilled water, and transfer the sample to a 10ml volumetric flask. From there, take 5ml to extract cobalt (II) by 5ml from the reagent (EATDB.

2.17.2 Determination of Cr (lll) ions in drugs. [98].

Ten tablets each of chromium (III) niacin (200 µg Cr^{+3}) and chromium picolinate (1000 µg Cr^{+3}) were taken separately, ground, and heated for 2 hours at approximately 300°C in a furnace. The resulting liquid was transferred from the furnace to a volumetric flask and then filled to the mark with 0.1 M HCl. The mixture was then filtered. Next, 10 mL of the chromium niacin solution and 5 mL of the chromium picolinate solution were separately filtered, and to each of them, 2.5 mL of 1 M KCl solution was added. After that, distilled water was used to dilute each solution to a final volume of 100 mL. Subsequently, 5 mL of each prepared drug solution (chromium niacin and chromium picolinate) were added to each of 10 mL volumetric flasks. Then 3 mL of the ligand solution at a concentration of 2.032×10^{-3} M was added. The pH was then adjusted to 8, following the optimal conditions found in this study. Finally, the volume in each flask was filled to the appropriate mark with distilled water. The same dilution technique was applied to prepare comparison solutions, but instead of using the medication solution, an equivalent volume of distilled water was used. This experimental procedure allowed for the preparation of solutions containing the drug samples and the ligand solution, under specific conditions, to investigate their complex formations. The comparison solutions, prepared similarly, served as a control to evaluate the interactions and complex formations between the drugs and the ligand.

CHAPTER THREE

RESULT & DISCUSSION

3.1 Azo Ligand Synthesis: Ethyl 4-((5-Acetyl-2,3,4-trihydroxyphenal) Diazonyl) Benzoate (EATDB)

The reagent (EATDB) is produced by dissolving ethyl 4-amino benzoate diazonium salt pairs (Benzocaine) in a solution made by combining sodium nitrite mixed in distilled water with strong HCL acid. The solution was allowed to remain in the container while being stirred and the temperature was kept below (0-5) °C in order to finish the azotization process and create a diazonium salt (solution1).

In this experiment, a solution containing 2,3,4-trihydroxyacetophenone was dissolved in ethanol and sodium hydroxide. The resulting solution was then gradually added to solution 1, with continuous stirring. The primary objective was to synthesize the reagent (EATDB), which exhibits a distinct reddish-orange color. The preparation mechanism is outlined in scheme (3.1) [91].
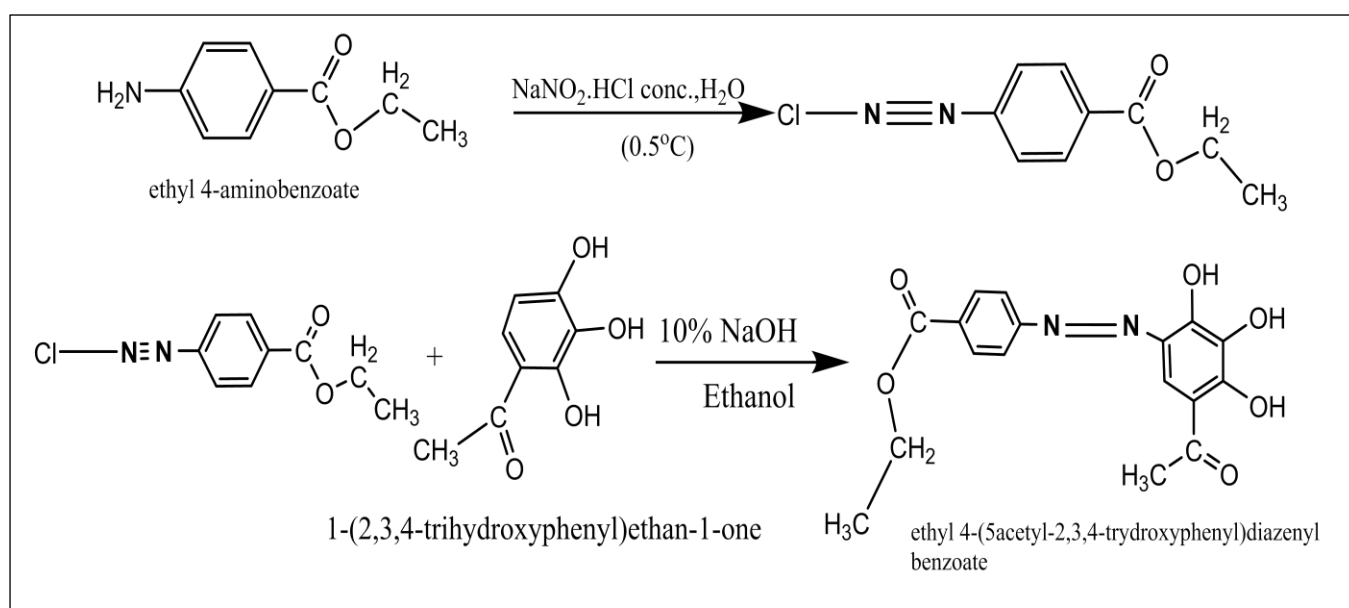
Scheme 3.1 Preparation of Ethyl4-((5-Acetyl-2,3,4-trihydroxyphenyl)Diazonyl)Benzoate (EATDB).

3.2 The Physical Properties of (EATDB).

Some of physical properties of (EATDB) Reagent were investigated as showed in table (3.1).

Table (3.1): Physical characteristics of the (EATDB).

Compounds	Formula	M.Wt (g/mole)	M.P($^{\circ}$C)	Color
EATDB	$C_{17}H_{16}N_2O_6$	344.12	218-222	Reddish-Orange

3.3 Spectroscopic Studies of (EATDB).

3.3.1 UV-visible.

The UV-vis study conducted on the ligand (EATDB) revealed the presence of a peak in the visible region. These transitions are attributed to atoms with the capacity to donate electrons, such as the bridge azo group, leading to an absorption peak at a maximum wavelength of 289 nm. This peak corresponds to the electronic transition from n-electron donor orbitals to π*-electron acceptor orbitals (n→π*).
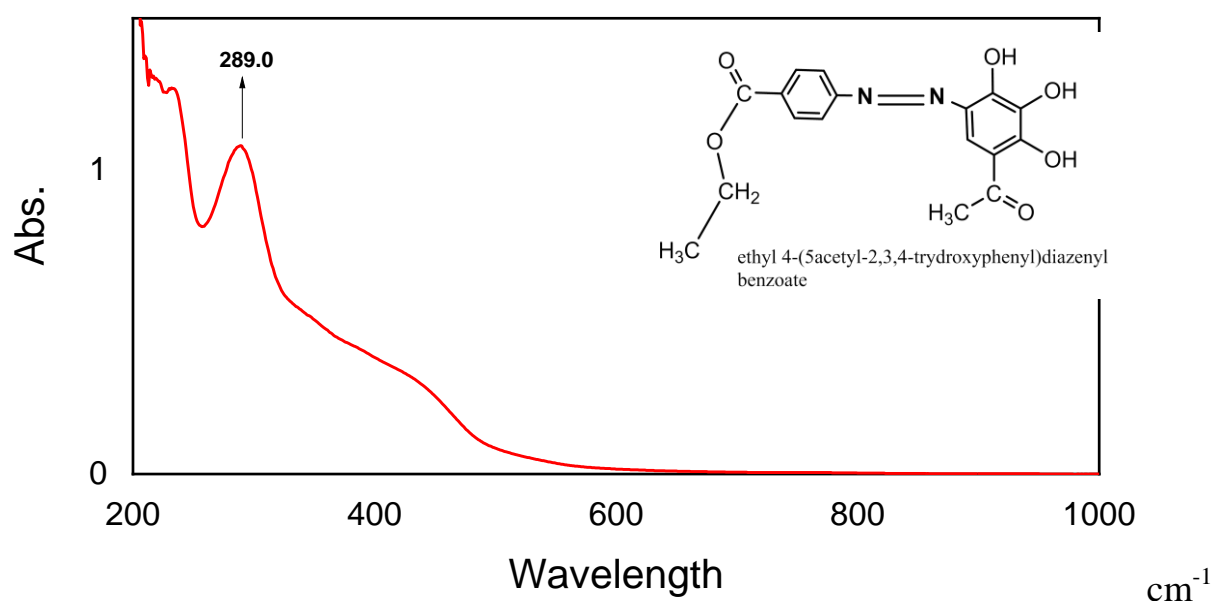
Figure (3.1): UV-Visible of [EATDB].

53

3.3.2 FT-IR of ligand (EATDB) and its raw materials.

To confirm the reagent was successfully prepared, the product was characterized utilizing various characterization tools including FT-IR spectrometry, (^{1}H and ^{13}C) NMR spectroscopy, and mass spectrometry. The FT-IR spectrum of reagent exhibits a broad significant peak at 3372 cm^{-1} which belongs to the presence of hydroxyl groups (OH) and a strong peakat1712cm^{-1} corresponding to an ester carbonyl (ester C=O) as illustrated in fig (3.4). The other interruption peaks were listed in the table (3.2).

3.3.2.1 FT-IR Spectrum of 2, 3, 4-Trihydroxyacetophenone.
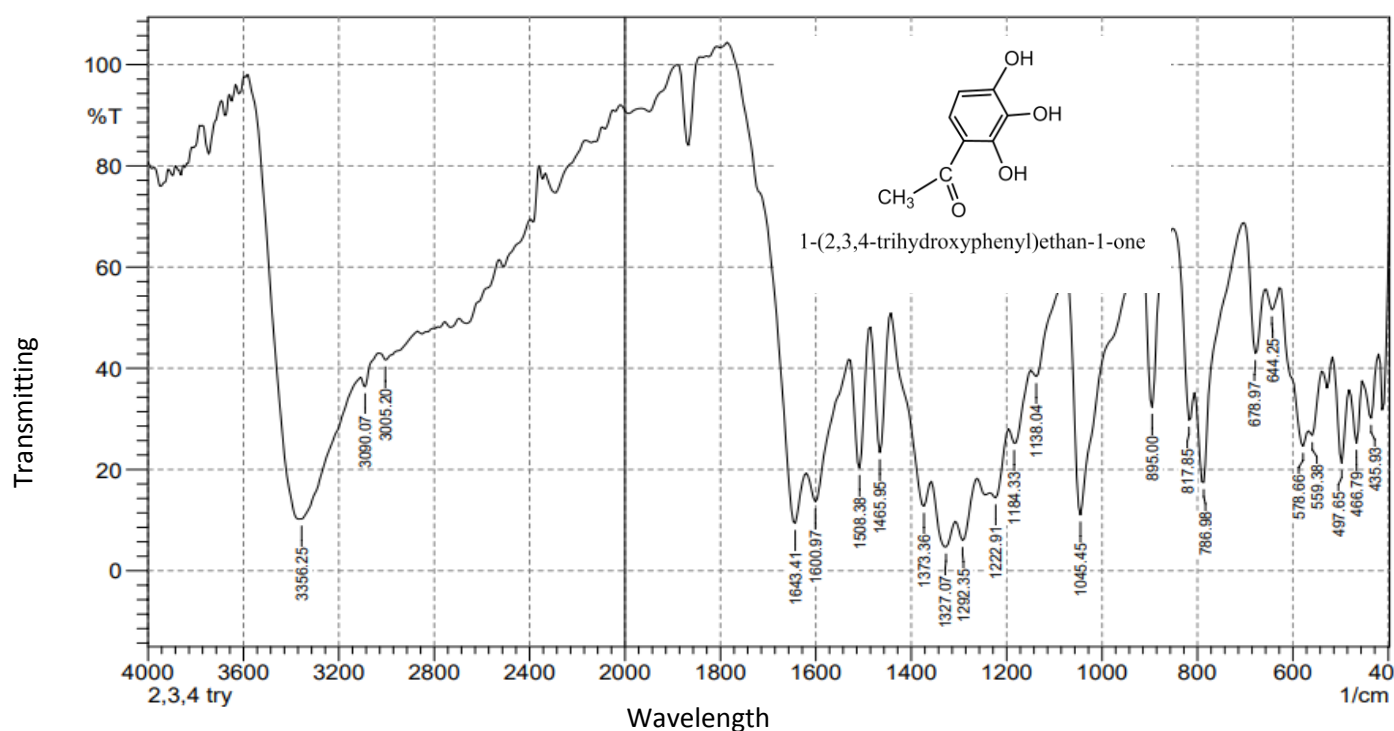
Figure (3.2): FT-IR spectrum of 2,3,4-trihydroxyacetophenone

3.3.2.2-FT-IR   Spectrum   of   1-(2,3,4-trihydroxyphenyl)ethan-1-one) Benzocaine .
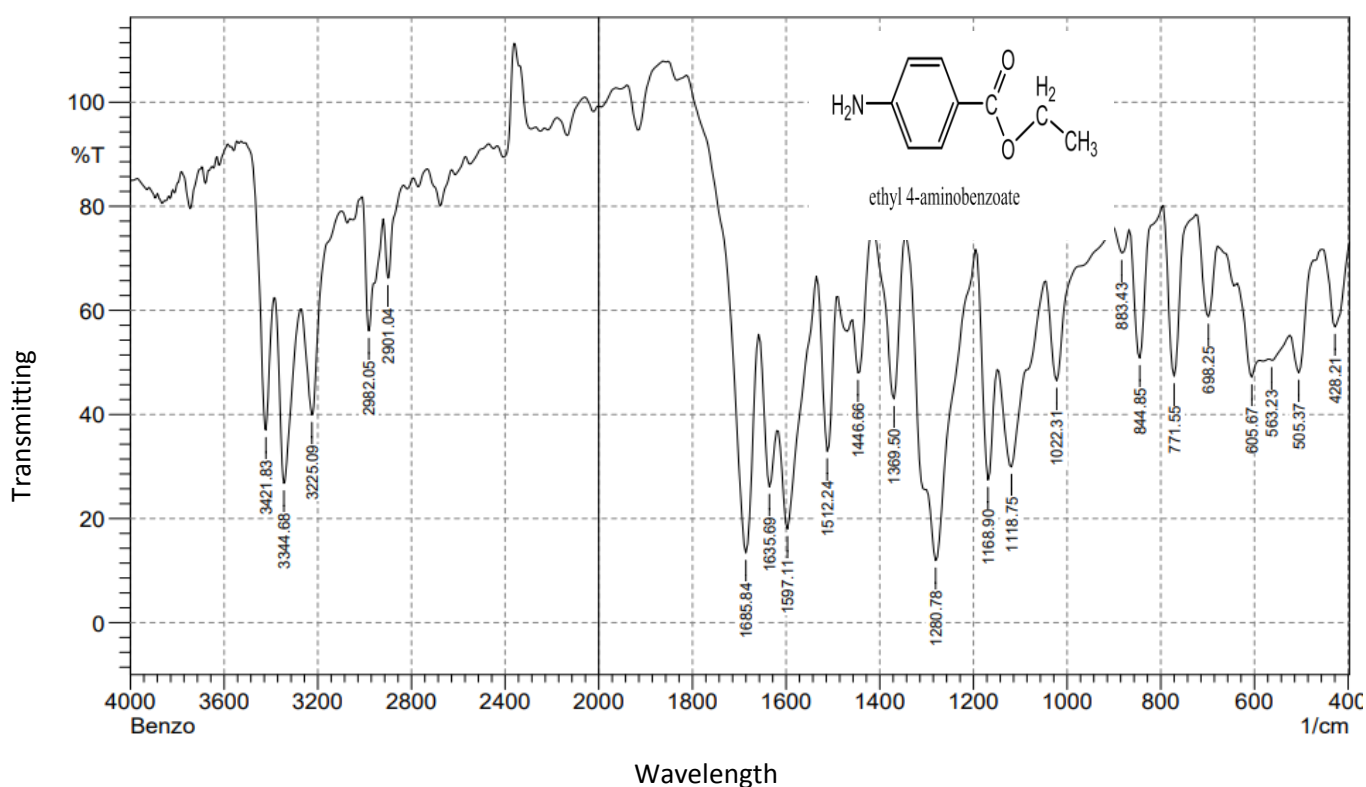
Figure (3.3) FT-IR test result for the benzocaine showing its spectrum.

3.3.2.3 FT-IR spectrum of the reagent (EATDB).
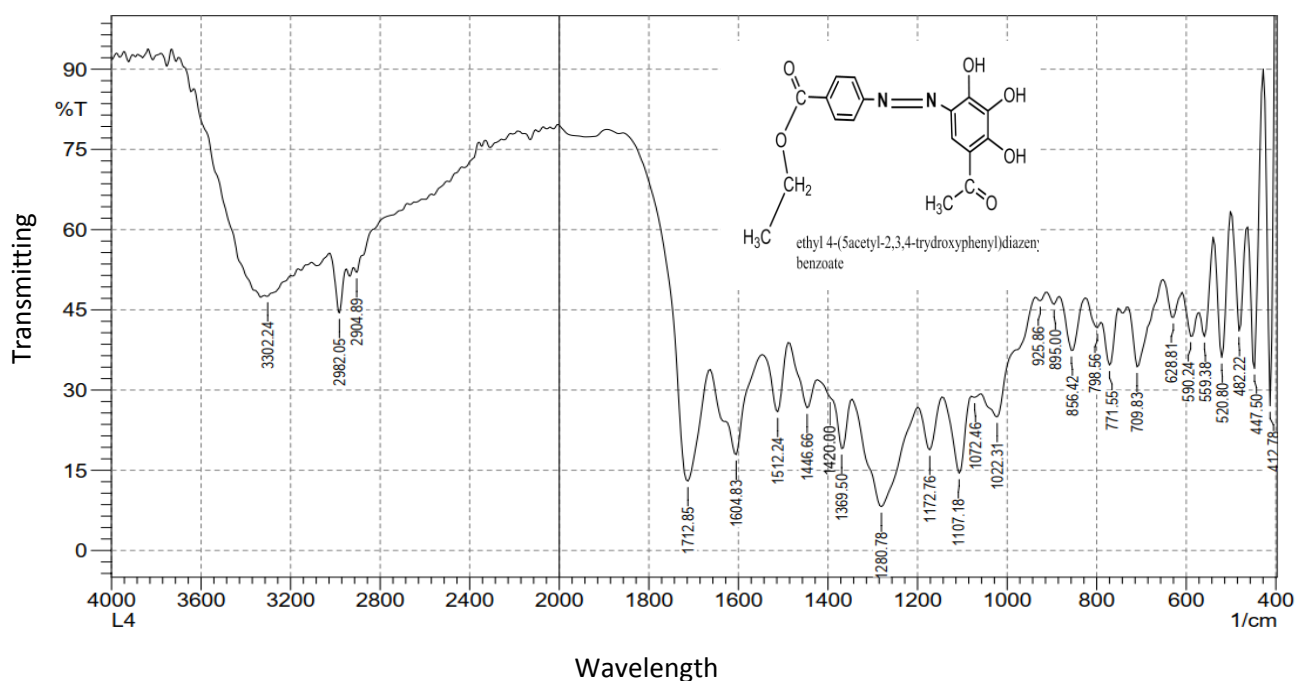
Figure (3-4) FT-IR test result for (EATDB) showing its spectrum.

55

Table (3.2) the main data of FT-IR spectrums of ligand with its raw material.

Type of Bond	Ethyl 4-aminobenzote	2,3,4-trihydroxyacetophenone	(EATDB) reagent
St.(N-H)	3225.05	-------------------------	------
(C --H) Aromatic	2982.,2901	3005,3090	2982
(C -- H) Aliphatic	2901	3005	2982
(C = C) Aromatic	1512, 1446,	1508, 1465	1604,1512, 1450
(N = N)	----------	----------	1420
(C = O)	1685	-----------------	1712
(C -- N)	1280	1292	1276
(O—H)			3302

3.3.3 ^{1}HNMR spectrums for the reagent.

One of the best techniques for determining the chemical structure of organic molecules is proton nuclear magnetic resonance spectrometry. By using 1D NMR spectroscopy, the reagent's structure (EATDB) was further established. Using DMSO-d6 as a solvent, the ^{1}HNMR spectrum of the Reagent were examined. Figures (3-5) show the reagent (EATDB). $^{.1}$H NMR spectrum.^{1}H NMR is a valuable equipment for support hydrogen abundance. The ^{1}HNMR spectrum of (EATDB) Figure 3.5 displayed three slight broadening signals for OH groups; the first signal was at 11.08 ppm corresponds to OH, the second signal at 8.54 ppm contributed OH, proton of the third signal at 8.25 ppm belongs to OH. The spectrum exhibits a triplet signal at 1.36ppm, representing the CH_3 proton in C**H**$_3$-CH_2 which is adjacent to the CH_2 group. Furthermore, there were also two signals displayed in the spectrum; the first signal was a quartet at 4.32 ppm corresponding to (C**H**$_2$-CH_3), and the second signal was a singlet at 3.65 ppm, corresponding to the methyl protons adjacent to the carbonyl group -C**H**$_3$-C=O, also the spectrum showed the signals of five aromatic protons in the range of 7.79-7.25 ppm..
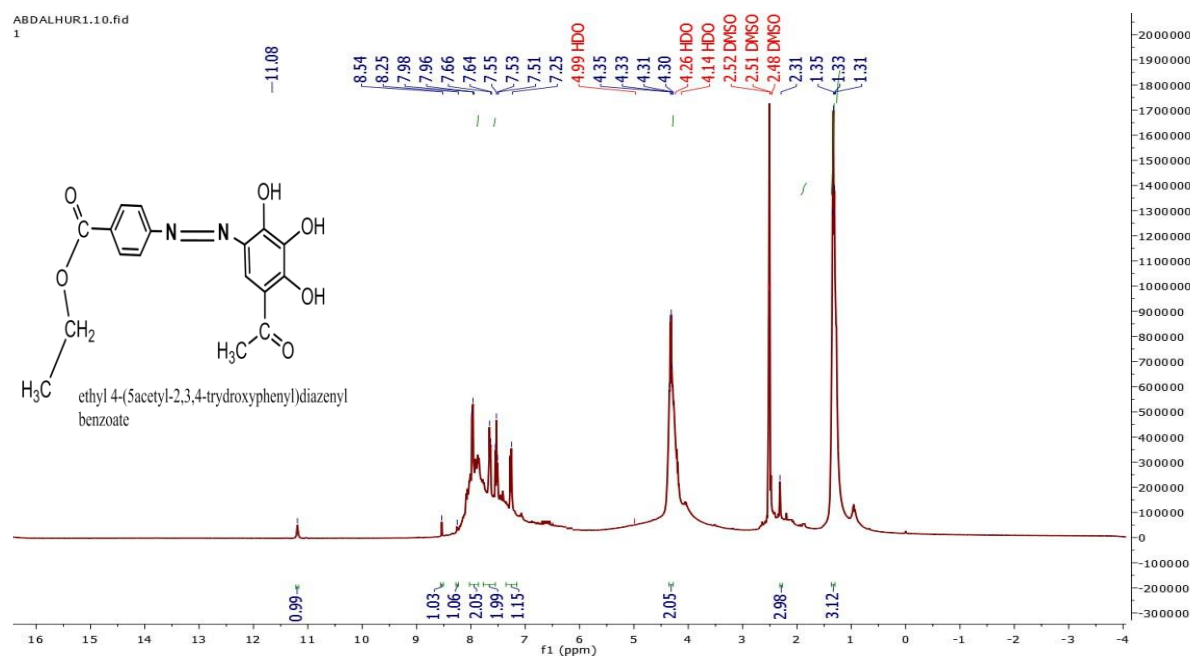
Figures (3.5) the ^{1}HNMR spectroscopic spectrum of reagent.

Figure (3.5) display 16 peaks that represent information coming from sixteen different kinds of protons. Proton 16 (s, 1H, O-H) was given a singlet with an integration of one proton at 11.08 ppm. (s, 1H, Ar-O-H),8.54(S,1H,OH),8.25(S,1H,OH),and two proton at7.79(d,j=8.0Hz,2H,Ar-H), 7.65(d,j=8.1Hz,2H,Ar-H), 7.25(s,1H,Ar-1H) 4.32,(q.j=6.4Hz,2H,CH2), 2.31(S,3H,CH3), 1.36(t,3H,CH3), 1.36(t,j=7.0Hz,3H).

3.3.4 ^{13}CNMR spectrum for the reagent

^{13}CNMR was utilized to confirm the reagent structure which demonstrated a characteristic peak one peak for ester carbonyl at 166.4 ppm and the second peak at 203.2 ppm for the carbonyl group in ketone in addition to that there are peaks between 61.1 - 14.2 ppm, confirming for CH_2- and -CH_3 proton environments for the reagent and seven aromatic carbons in the range of 152.4 to 108.5 ppm. ^{13}CNMR is a particularly useful tool for examining reagent. The results indicate that the molecular ion peak closely matched the expected molecular weight, as determined from the ideal structure, as depicted in figure 3.6.
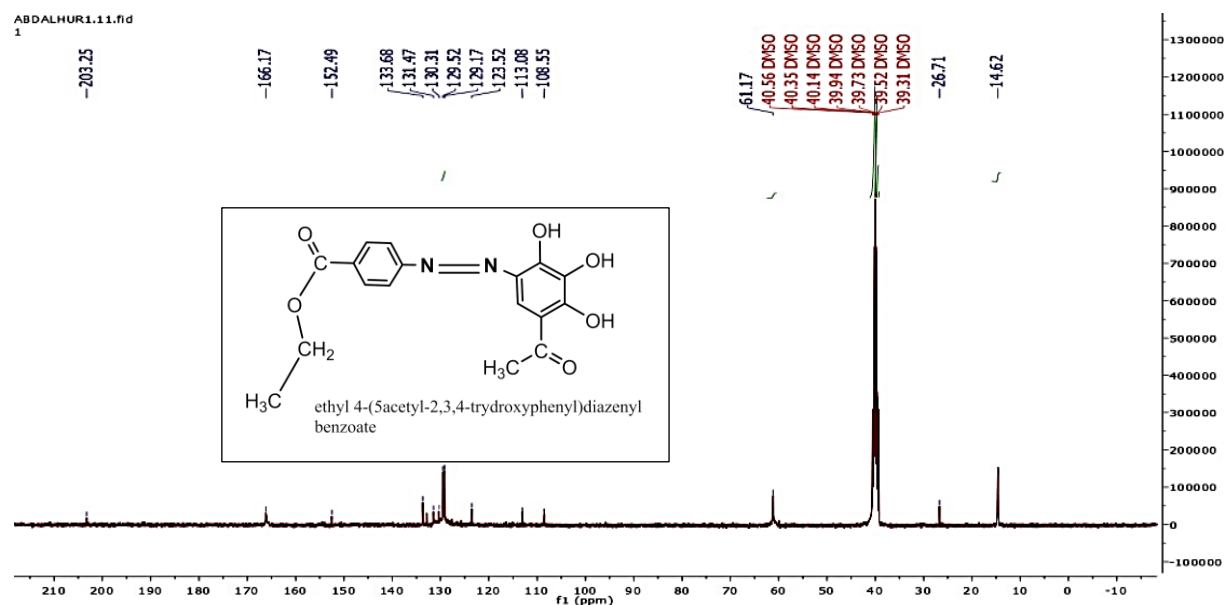
Figures (3.6). ^{13}CNMR spectroscopic spectrum of reagent

3.3.5 Gas Chromatography (Mass) for the (EATDB).

Figure (3-7) presents the Gas Chromatography/Mass Spectrometry (GC/MS) spectrum of the ligand (EATDB). Notably, the figure demonstrates a close match between the theoretically calculated molecular weight (M.Wt) and the experimentally obtained value, both being equal to 344 g.mole^{-1}. This correspondence validates the accuracy and consistency of the ligand's molecular weight determination through GC/MS analysis.
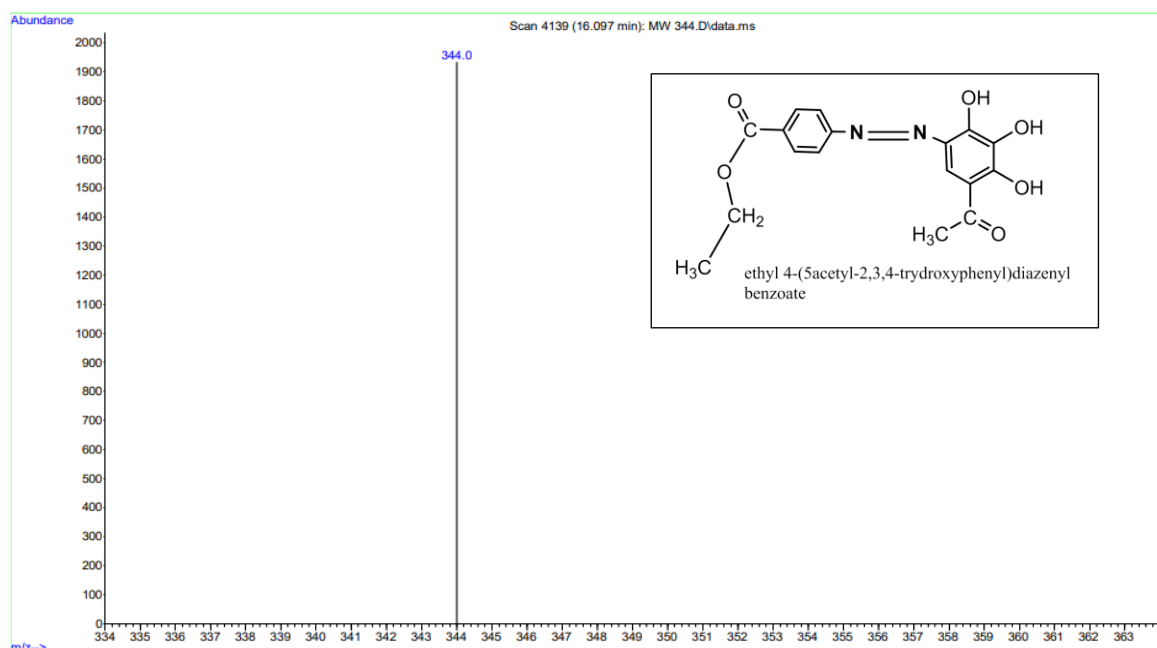
Figure 3.7 Gas. Chromatography/MS of reagent (EATDB).

3.4 Preliminary testing

Initial experiment was done to investigate the reaction between a newly prepared reagent and 12 different metal ions. These ions (Hg^{2+}, Ni^{2+}, Mg^{2+}, Ag^{2+}, Pb^{2+}, Fe^{3+}, Co^{2+}, Cu^{2+}, Sr^{2+}, Cd^{2+}, Zn^{2+} and Cr^{3+}) Colored solutions that showed a reaction occurred were used to demonstrate how these ions and the reagent interact. The findings of the early analyses for reaction reagent with Co^{+2} and Cr^{+3}ions are shown in table 3-3. These ions were picked out of the remaining ones for research and spectrophotometric examination.

Table (3.3). The results from an initial test show reagent reactivity with Co(ll) and Cr(lll) ions.

Ions	color of Complex	Acid Medium	Base medium
Cobalt (ll)	Light orange	Light orange	Brown
Chromium(lll)	Purple	Purple	Light green

59

3.5 Study of UV-Visible spectrum of Co(ll) ion and (EATDB) complex.

As it can be seen in figure (3.8), Co (II) complex's absorption associated with newly prepared reagent are presented. The spectrum of absorption is detected within the wavelength (190-1100) nm. Co (II) complex exhibits a distinct peak of absorption at (λ max = 437 nm). Interestingly, the formation of the complex is accompanied by a bathochromic shift, indicating a displacement towards longer wavelengths, along with a substantial increase in light absorption. These observations strongly suggest significant alterations in the electronic transitions, implying the successful creation of a compound between Cobalt (II) and the reagent.
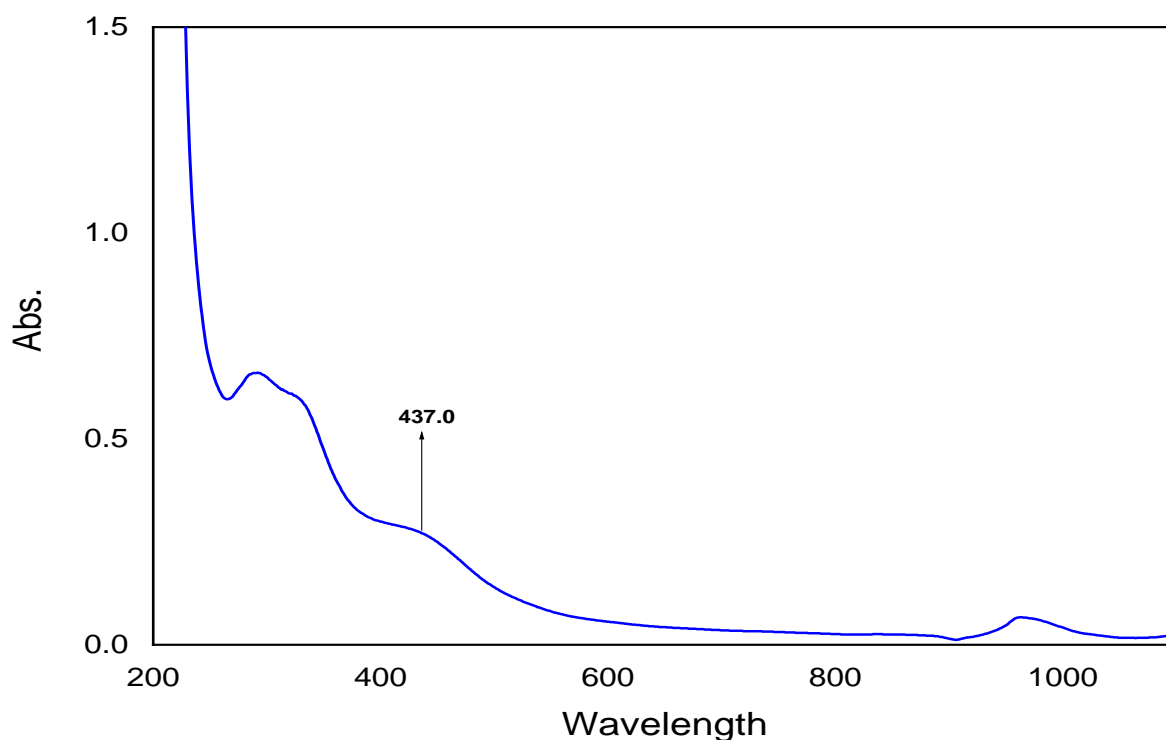
Figure (3.8): UV-Visible Cobalt (II) - [EATDB] complex.

3.6 Effect of pH value on Cobalt (ll) Ion.

Figure (3-9) demonstrates the impact of acidic conditions on the Cobalt (II) complex solutions absorption. The gradual increase in color intensity of the complex solutions was noticed, distinct intensity was observed at pH=9

Nevertheless, upon surpassing this level of acidity, a decline in the absorbance value of the complex was observed. This decrease can be attributed to the possible precipitation of ions or the formation of unstable complex ions due to the excessive

acidity. These observations underscore the sensitivity of the complex to changes in pH and highlight the importance of maintaining an optimal acidic environment for stable complex formation.
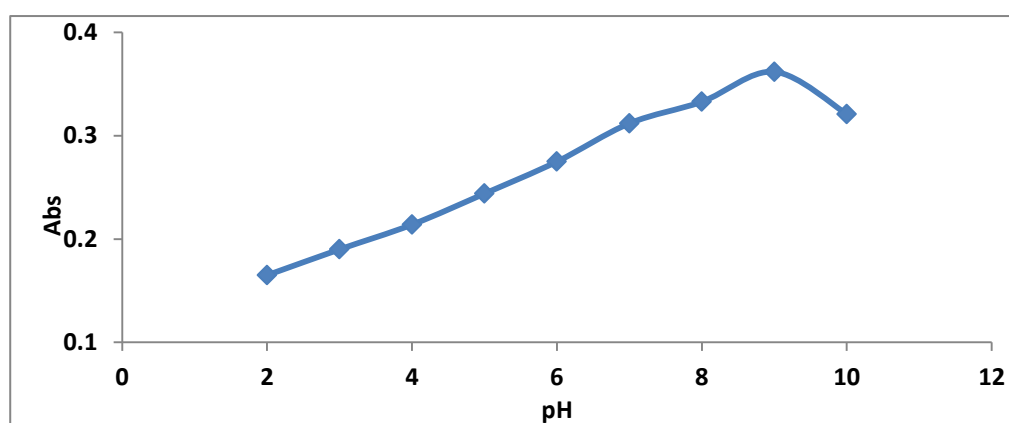
Figure (3-9) effect of pH for Cobalt (ll) complex,

3.7 Time Influence on Co (II) complex stability.

The absorption characteristics of the Cobalt (II) complex with the ligand (EATDB) were thoroughly examined under the optimized conditions. The obtained results are presented in table (3.4). The stability of the generated complexes was carefully examined, as it represented a crucial aspect in determining the optimal time frame during which the complex could remain stable.

Our findings from investigation reveal that the Cobalt (II) complex exhibits remarkable stability, remaining stable for up to 24 hours after its formation. This stability ensures that the complex can be reliably utilized in practical applications without undergoing significant changes over a considerable period. The study out comes of the underscore the suitability and robustness of the Cobalt (II) complex for various analytical and scientific purposes.

Table (3.4) Time influence on Co (ll)-(EATDB)

Time	1 min	10 min	20 min	30 min	60 min	120 min	240 min	24 h
Absorbance.	0.360	0.362	0.359	0.357	0.360	0.357	0.360	0.359

3.8 Effect of Temperature on Co (II) Ion

Temperature has an effect on the complex formation for that different temperature were tested. The results are presented in table (3.5), it can be observed that the cobalt (II) complex has the highest absorption values and produce the best results. The Cobalt (II) complex exhibits vivid color intensity within the temperature range of (10 – 40)°C. Increasing in temperature leads to a noticeable reduction in the complex's absorption levels, possibly stemming from diminished substance stability or increased dissolution at elevated temperatures. Thus, maintaining the temperature within the optimal (10- 40) °C range becomes critical to preserve the complex's stability and desirable color properties, ensuring reliable and accurate results in various applications.

Table 3-5. Temperature influence on Co (ll)-EATDB

Temp ^{o}C	10	20	30	40	50	60
Absorbance.	0.361	0.360	0.358	0.358	0.334	0.326

3.9 Effect of Sequence addition on Co (II) Ion.

Using four different addition arrangements, a complex absorbance's reaction content was examined in terms of its order. According to the information in table 3.6 below, the cobalt (ll) complex had an equal impact on rate of absorbance.

Table (3.6) the influence of sequence addition on Co (ll)-EATDB

Sequence.	Sequence of addition	Absorbance
1	M+L+PH	0.360
2	M+ PH +L	0.354
3	L+PH +M	0.349
4	L+M+PH	0.355

M=Metal ,L=Ligand

According to the data presented in Table (3.6), the cobalt (II) complex was identified through the implementation of the first sequence, resulting in favorable outcomes. Conversely, using the alternative sequence resulted in a reduction of the complex's absorbance, potentially due to the interaction of ions (Both base & acid) with the metal.

3.10 Effect of Ionic Strength on Co (II) Ion.

In the investigation of the cobalt (II) complex's absorption behavior, the study utilized sodium nitrate ($NaNO_2$) and sodium sulfate (Na_2SO_4) salts to examine the influence of ionic strength. By introducing solutions containing these salts (1 mL each) to the cobalt (II) complex, a diverse set of concentrations (0.0005-0.5 M), for every salt was investigated. This method allowed for a thorough examination of the impact of ionic strength on the Co (II) complex in terms of absorption behavior.

Table (3.7) Ionic strength Influence on Co (ll)-(EATDB)

Adding salt	Concentration of added salt (M)	Absorbance.	Added the salt	Concentration of added salt (M)	Added salt
	0.0005	0.359		0.0005	0.360
	0.005	0.350		0.005	0.349
Na_2SO_4	0.05	0.352	$NaNO_3$	0.05	0.355
	0.5	0.348		0.5	0.352
Absorption value of Co(II)-(EATDB) without adding = 0.360					

According to the findings presented in table (3.7), it is evident that none of the listed concentrations have a notable impact on the absorption value. From this observation, it can be refereed that the ions investigated do not exert any significant influence on the solubility or sensitivity of cobalt ion detection. The results strongly suggest that the presence of these ions does not interfere with the absorption behavior of the cobalt (II) complex, confirming its reliability and selectivity as a dependable method for detecting cobalt ions.

3.11 Calibration curve of Co (II) complex.

The optimal condition was found and used to generate the calibration curve for the ions of cobalt (II). The results of the investigation are depicted in fig. (3.10), for the cobalt (II) ion.
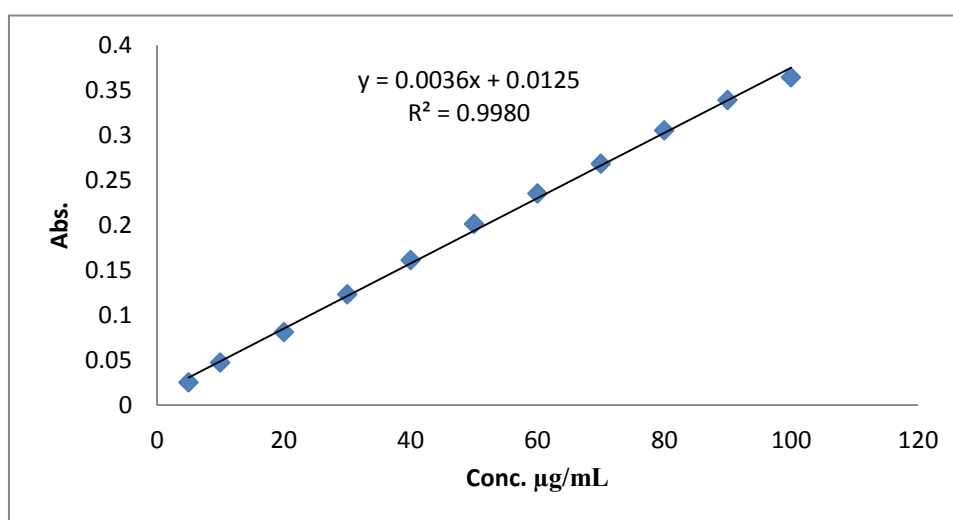
Figure (3.10): Calibration curve of Co (ll).

Figure (3-10) illustrates that the cobalt (II) ion adheres to the Lambert-Beer rule within the concentration range of (1 - 100 $\mu g.mL^{-1}$). The cobalt complex exhibits a molar absorptivity of (0.212×10^2 $L.mole^{-1}. Cm^{-1}$), demonstrating its sensitivity to changes in concentration. The absorbance of the complex displays a linear relationship with the metal concentration, further supporting the validity and applicability of the Lambert-Beer law in this analytical context. This characteristic

ensures reliable and accurate determination of cobalt (II) ion concentrations within the specified range[94] & [96–98].

$$A = \varepsilon b C \qquad\qquad (3.1)$$

$$slope = \frac{\varepsilon}{At.Wt x 1000} \qquad\qquad (3.2)$$

ε = molar absorptivity

$$S = \frac{10^{-3}}{a} \qquad\qquad (3.3)$$

S = Sandal sensitivity

Table 3-8 Analytical parameters data for quantifying cobalt ion using ligand (EATDB).Table (3.8): Analytical parameter for Co (II) analysis.

Analytical parameters	value
Molar absorptivity (L.mol^{-1} .cm $^{-1}$)	0.212×10^2
Range conc.(μg.mL^{-1})	(1-100)
Linear equation	Y=0.0036X+0.0125
Slope	0.0036
Limit of Quantification (μg.mL^{-1})	2.4120
Limit of Detection (μg.mL^{-1})	0.7410
Sandal sensitivity(μg.cm^{-2})	0.2780
Linearity coefficient	R^2=0.9980
λ_{max}	437nm

3.12 Stoichiometry of the Co (II) complex.

Under optimal conditions, the composition of the cobalt (II) complex was investigated using three different methods. Firstly, the mole ratio approach was employed, followed by Job's method (continuous variations), and finally Mallard's method. These techniques were utilized to determine the composition of the

formed cobalt (II) complex with precision and accuracy. These analytical techniques allowed for a comprehensive exploration of the stoichiometry and composition of the complex, providing valuable insights into the interaction between cobalt (II) ion and the ligand (EATDB). The utilization of multiple methods ensured the accuracy and robustness of the findings, enabling a thorough understanding of the complex formation process.

3.12.1 Mole Ratio Method for complex of Co (II).

In this method, a series of 10 mL volumetric flasks was employed, each containing a constant and predetermined concentration of cobalt (II) ion (3.00×10^{-4} M). Gradually increasing and proportionate concentrations for reagent were inserted into each flask, ranging from (2.5×10^{-4} - 7.00×10^{-4} M). Furthermore, the pH of both components was adjusted to 9, representing the optimized conditions for complex formation. Ethanol was added to each flask to the mark to complete the volume. Same procedure was utilized for preparing the complex solution was employed for preparing the comparison solutions, ensuring consistency and reliability in estimating the complex [92].
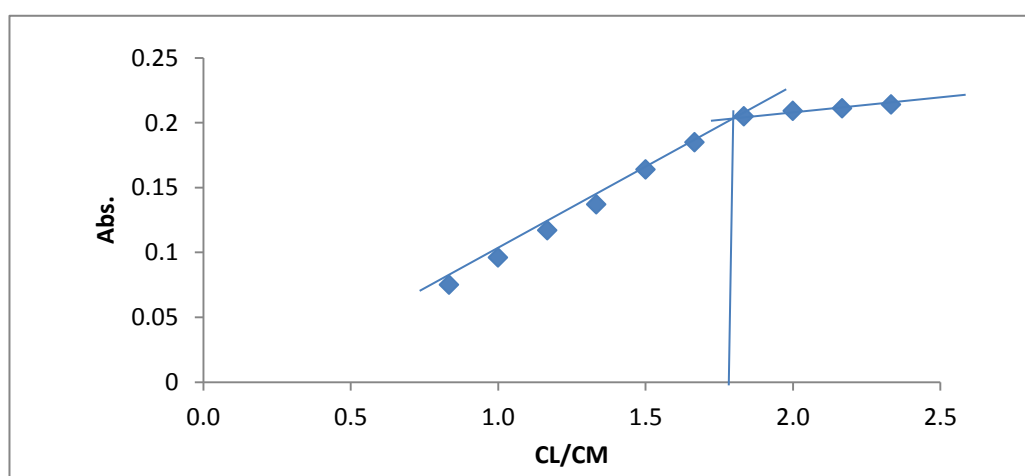
Figure (3-11) Mole ratio for the complex of Cobalt (ll).

Figure 3-11 illustrates the bonding of the cobalt (II) complex with a stoichiometric ratio of two to one for the reagent and the Co ion respectively, denoted as (M: L) (1:2).

3.12.2 Job's method for Co (II) Complex.

In this approach, different volumes of solutions, all containing Co (II) ion at the same concentration $(3.43 \times 10^{-4}$ M), were mixed with (EATDB) with a concentration of $(1.45 \times 10^{-3}$ M) for obtaining a final volume of 10 mL. The measurements were conducted under optimized conditions, and at $(\lambda_{max} = 437$ nm) the Co (II) complex's absorbance was measured. figure (3-12) illustrates the outcomes of this method, offering valuable insights into the formation of the complex and its distinctive absorption properties at the specified wavelength [93].
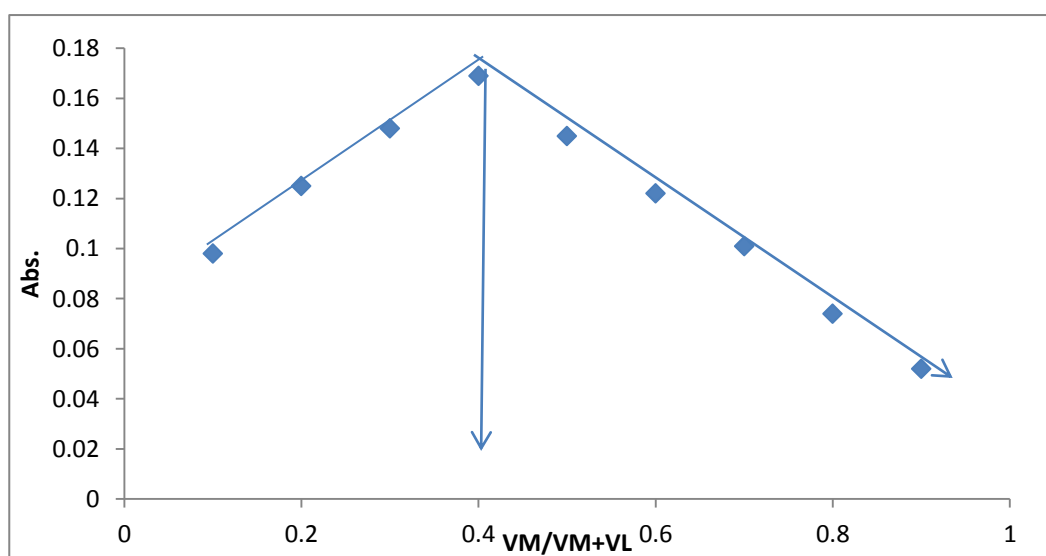
Figure (3-12) Job's method result for the Cobalt (ll).

As shown in figure 3-12, the cobalt (II) complex exhibits a bonding ratio of (M: L) (1:2), where one mole of the cobalt ion coordinates with two moles of the reagent (ligand - EATDB). This stoichiometric arrangement holds valuable significance as it sheds light on the coordination and interaction between the cobalt (II) ion and the ligand, EATDB, thereby offering deeper insights into the molecular structure and stability of the complex.

3.12.3 Mollard's Method Cobalt (II) ion complex

The experiment involved the mixing Cobalt (ll) ion solution having (1.00×10^{-4}) M concentration and a reagent solution with a concentration of 3.00×10^{-4} M. The pH of the mixture was precisely adjusted to 9. Afterward, ethanol was carefully added to achieve a final volume of 10 mL. The resulting solution's absorbance was measured at $\lambda_{max} = 437$ nm, yielding a value of 0.179. This particular value signifies called as (As) and it express the complex's absorptivity at equivalence point.

In an alternative experiment, reagent solution at a lower concentration (1.00×10^{-4} M) combined with higher concentration cobalt (II) ions solution (3.00×10^{-4} M). pH adjusted to 9, and volume precisely adjusted to 10 mL using ethanol. Subsequently, absorbance at $\lambda_{max} = 437$ nm recorded meticulously, revealing a value of 0.348. This specific absorbance value signifies absorption of complex at equivalence point (Am) [94].

$$\frac{m}{s} = \frac{Am}{As} = \frac{0.348}{0.179} = 1.944 \qquad (3.4)$$

3.13 Calculating the complex Co (II) stability constant.

The absorption values obtained from the mole ratio technique of the cobalt (II) complex can provide valuable insights into its stability constants. By utilizing the concentrations of cobalt (II) ions in the solutions and their corresponding absorption data, the stability constants of the colored complexes can be calculated, particularly when they are combined. The stability constants were determined using the following equations: [100]&[94].

$$M^{+n} + nl \leftrightarrow Mln \qquad (3.5)$$
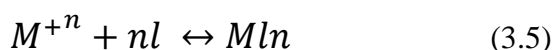
$$a + nca \leftrightarrow (1 - a)c \qquad (3.6)$$

$$K = \frac{[MLn]}{[M^{+n}][L]} \qquad (3.7)$$

L = Reagent, α = the degree of dissociation following formulae are used to compute:

$$K = \frac{(1-a)c}{ac(nac)^n} \qquad (3.8)$$

$$K = \frac{1a}{n^n a^{n+1} c^n} \qquad (3.9)$$

$$a = \frac{Am - As}{Am} \qquad (3.10)$$

As = the complex's absorption at the equivalence point.

Am = a complex's highest rate of absorption.

n= number of mole,   C=molar concentration,   L=Reagent M^n=ion

Table 3-9 the value of K_{sta} for cobalt (ll) complex

Complex	Highest rate of absorption (Am)	Absorption at the equivalence point (As)	(α)	(K)mol^{-1}.dm^{-3}
[Co (EATDB)$_2$]	0.360	0.290	0.194	5.967×10^8

The stability constant (K) values presented in table (3.9) illustrate the high stability of the generated complex. This remarkable stability enhances the efficiency of the process and allows for the reliable use of the reagent (EATDB) in estimating the spectrum of cobalt (II) ion. The determined stability constants provide crucial evidence for the robustness of the complex formation and its potential as a valuable tool for spectroscopic analysis and determination of cobalt (II) ions.

3.14   Calculation of dissociation degree, K_{sta}, and the Co (ll) complex's Thermodynamic functions.

3.14.1 Temperature influence on the Co (ll) Complex's level of dissociation and stability constant.

An extensive research has been conducted to examine the influence of temperature on a compound, encompassing both the stability constant and the degree of dissociation of the Cobalt (II) complex. The outcomes of this investigation are meticulously presented in table 3.10, offering significant and valuable insights into the complex's behavior, which is contingent on changes in temperature.Table (3.10) Temperature variation impact on the Co (II) complex's stability constant and degree of stability.

Temp. ^{0} C	Temp. (K)	Value of α	Value of $K\times10^8$
10	283.15	0.168	3.795
15	288.15	0.180	3.040
20	293.15	0.187	3.028
25	298.15	0.194	2.380
30	303.15	0.198	2.234
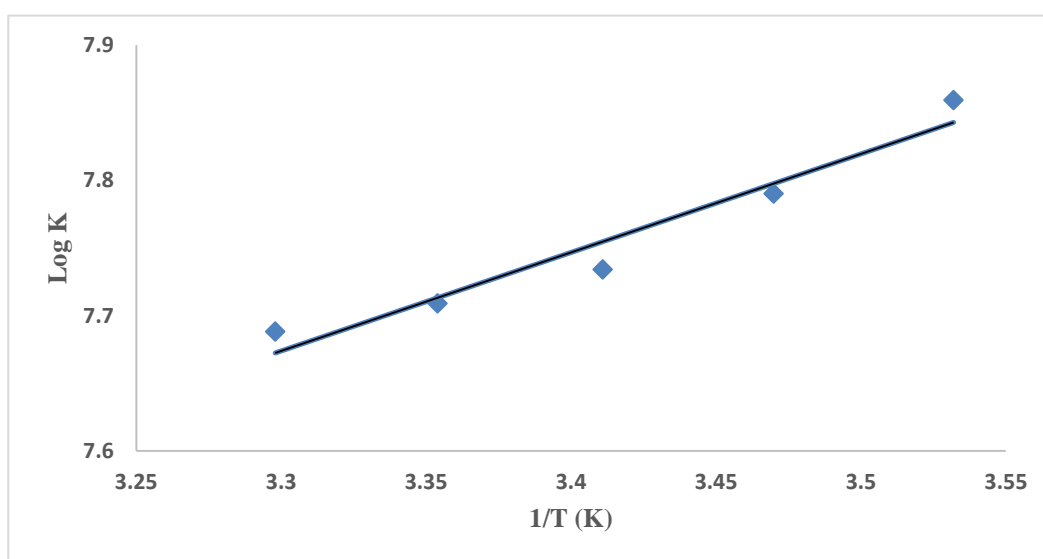
Figure (3-13) Relation between temperature and Log K for Co (ll) ion.

The thermodynamic behavior of the Cobalt (II) complex, including its stability constant and degree of dissociation, was extensively investigated, and the pertinent data is illustrated in table (3-10) and figure (3-13). The negative value of ΔG indicates that the reaction of the ion is spontaneous, while the negative value of ΔH suggests an exothermic reaction. These findings align with the data presented in the aforementioned table and figure.

Additionally, temperature plays a critical role in influencing hydrolysis shells that cobalt ion is surrounded with. Cobalt ion's inherent properties, such as its concentrated charge, contribute to its limited solubility. However, as observed, temperature exerts a beneficial impact on the hydrolysis shells, leading to alterations in the cobalt complex's charge and other characteristics. These insights significantly contribute to understanding the thermodynamic behavior and stability of the Cobalt (II) complex, shedding light on its reactivity across varying temperature conditions.

3.14.2 The calculation of the thermodynamic properties of Co (II) Complex

The thermodynamic characteristics of the Cobalt (II) complex were thoroughly investigated in this study to explore its influence on temperature. Employing data derived from the previous section, the enthalpy (ΔH), Gibbs free energy (ΔG), and entropy (ΔS) were meticulously computed. The results pertaining to the Cobalt (II) complex are methodically displayed in table (3.11) and graphically depicted in figure (3-14).These computed thermodynamic parameters offer crucial insights into the complex's stability, spontaneity, and reactivity under various temperature conditions. The investigation significantly enhances our comprehension of the complex's behavior across diverse thermodynamic scenarios, enriching our knowledge of its attributes and potential implications.

Table (3.11): Temperature impact on Co (ll) complex Thermodynamic function.

T(K)	1/Tx10⁻³(K)	LogK	Δ H	Δ G (KJ/mole)	Δ S (KJ/mole K)
283.15	3.532	8.579		-46.655	0.11
288.15	3.470	8.485		-46.71	0.09
293.15	3.411	8.480		-47.515	0.01
298.15	3.354	8.376	-18.15	-47.730	0.20
303.15	3.298	8.334		-48.371	0.09

As shown in table 3.11 the results indicated that temperature showed no significant influence on the complexes' stability. The Cobalt (II) complex exhibited remarkable stability, which further highlights the potential of utilizing the reagent (EATDB) in spectrophotometric analysis. Its consistent stability under varying temperature conditions enhances the reliability and applicability of this method for determining and analyzing Cobalt (II) ions in various samples.

3.15 Anions and Cations ions interference impact on Cobalt (ll) complex.

3.15.1 Cobalt (II) ion determination with interference cations ions.

Concisely outlined in table (3.12) are the investigation results of a methodical selection of diverse cations. This exploration was carried out to assess their potential interference with the absorption of the Cobalt (II) complex. These findings offer valuable insights into the influence of various cations on the stability and sensitivity of the Cobalt (II) complex. Consequently, these in devising effective strategies to minimize or mitigate any potential interferences encountered during the analysis of Cobalt (II) ions in complex samples. Such knowledge is crucial for enhancing the accuracy and reliability of the analytical process when dealing with real-world samples containing multiple cations.

Table (3.12) cations interference impact on Co (II) complex.

foreign /ions	Cations structure	(100µg/mL) Absorption after addition of cations	Error%
Cd^{2+}	$Cd(NO_3)_2.4H_2O$	0.321	11.30
Mn^{2+}	$Mn(NO_3)_2.6H_2O$	0.313	13.4
Fe^{3+}	$Fe(NO_3)_3.9H_2O$	0.298	17.60
Zn^{2+}	$Zn(NO_3)_2$	0.320	11.3
Pb^{2+}	$Pb(NO_3)_2$	0.302	16.50
Ag^+	$AgNO_3$	0.313	13.4
Cu^{2+}	$Cu(NO_3)_2.3H_2O$	0.305	15.6
Absorbance without interferences = 0.360			

The finding obtained in tables (11) and (12) explained that specific ions resulted in increasing the absorbance on the other hand, others led to decreasing the absorbance. This impact can be attributed to the competition between these ions and Co(II) ion for complex formation with the reagent.

3.15.2 Cobalt (II) ion determination with some interference anions ions.

To examine the interference of selected anions with Cobalt (II) ions, their presence was thoroughly investigated. The results obtained from these experiments are clearly presented in table (3-13). The data obtained showed light on the impact of these specific anions on the absorption behavior of the Cobalt (II) complex. By discerning the potential interferences, this study contributes to the refinement of analytical methods and ensures the accurate determination of Cobalt (II) ions in the presence of these selected anions.

Table (3-13) Anions interference impact on complex of Co (ll).

The ions	Anions Formula	(100µg/mL) Absorption after Anion addition	E%	(200µg/mL) Absorption after Anion addition	E%
$SO4^{-2}$	K_2SO_4	0.231	34.3	0.304	27.61
Br^{1-}	KBr	0.219	39.4	0.310	26.15
SCN^{1-}	KSCN	0.237	31.28	0.306	27.18
IO_3^{1-}	KIO_3	0.249	43.54	0.321	21.29
CrO_7^{-2}	K_2CrO_7	0.246	31.8	0.330	21.14
CO_3^{-2}	K_2CO_3	0.234	38.60	0.317	25.58
CN^{1-}	KCN	0.222	36.17	0.319	25.0
	Absorbance without interferences = 0.360				

When combining the reagent with the cobalt (II) ion complex, it was observed that there is noticeable impact of various ions on the absorption values. That influence is contingent upon the type and concentration of the introduced ions. Such interferences can lead to either a decrease or an increase in the absorption of cobalt. A notable observation is that both Anions ions and the reagent form a complex, resulting in reduced competition and enhanced sensitivity of the method for detecting cobalt (II) ions. This phenomenon could be attributed to the role of anions as masking agents, which helps mitigate interference effects.

By comprehending these intricate interactions, we gain valuable insights into the behavior of the cobalt (II) complex and can optimize the analytical process to achieve accurate determination of cobalt ions, even in the presence of various interfering species.

3.16 Effect of masking agent

3.16.1 Co (II) Complex

Masking agents were utilized to overcome the interference caused by cations overlapping with the Cobalt (II) complex. Seven masking agents were selected to assess their impact on the interaction between the reagent and interfering ions. By introducing these agents, the specificity of the Cobalt (II) complex formation was enhanced, leading to more accurate and reliable results. This approach allows for customized analysis based on the sample's specific interfering ions, ensuring a selective determination of the Cobalt (II) complex. Further optimization and validation are necessary for complex sample matrices with multiple interfering ions.

Table (3.14): Co (II) complex absorption impacted by masking agent

Masking agent 0.1M	Absorption of Co (ll) complex
Ascorbic acid	0.358
Citric acid	0.340
formaldehyde	0.313
KCl	0.335
Na_2EDTA	0.345
$Na_2HPO_4.12H_2O$	0.327
Thiourea	0.311
Without masking agent	0.362

Results in table (3.14) demonstrate the formed complex's absorption is minimally affected by Ascorbic acid. This observation suggests that Ascorbic acid could be used successfully as a masking agent against interference. However, it is crucial to note that in scenarios where other ions dissociate with cobalt (II) ion, Ascorbic acid may not be suitable as a masking agent. Therefore, careful

consideration of the specific interfering ions and their interactions is of utmost importance when selecting an appropriate masking agent for ensuring accurate determination of the Cobalt (II) complex. A tailored approach to masking agent selection is crucial to optimize the analytical process and mitigate potential interference effects effectively.

3.16.2 Using a more effective masking agent to detect Cobalt (ll) ions when cations are interfering.

Ascorbic acid was chosen as the best masking agent to overcome the interference obtained from the cations. table (3.15) shows the data obtained.

Table (3-15) masking agent effect on the absorption of a cobalt (II) complex when cations are present.

foreign ions	Abs after addition cations (100µg/ml) with addition of the masking agent(0.1M)	Relative Error (E %)
Cd^{2+}	0.344	4.444
Ni^{2+}	0.340	5.551
$Fe^{3}+$	0.339	5.870
$Hg^{2}+$	0.341	5.270
$Pb^{2}+$	0.345	4.187
$Mg^{2}+$	0.349	3.040
Ag+	0.338	6.160
$Cu^{2}+$	0.346	3.816

In table (3.15), complex of Cobalt (II) absorbance values in the presence of interfering cations are presented, alongside the introduction of a more effective masking agent. Additionally, the table includes absorbance values that can be compared to those observed prior to the interference. The results clearly demonstrate that the new masking agent effectively eliminat the influence of interfering cations, thereby enabling accurate determination of the Cobalt (II)

complex absorbance levels. The successful implementation of this improved masking agent ensures enhanced precision and reliability in the analysis, making it a valuable addition to the analytical process when dealing with complex sample matrices containing interfering species.

3.17 Accuracy and Precision for the proposed method for Co (II).

The precision and accuracy of the method were thoroughly evaluated by employing two crucial parameters: the relative standard deviation (R.S.D %) and the percentage recovery for Cobalt (II) ions. These assessments offer essential insights into the consistency and reliability of the analytical results obtained from the method. By analyzing these parameters, the study was able to ascertain the robustness and effectiveness of the analytical approach in accurately determining Cobalt (II) ions, even in the presence of interfering species or complex sample matrices. Such evaluations are vital for establishing the method's practical applicability and ensuring the generation of reliable and precise analytical data [95][96].

Table (3-16) Precision and Accuracy for the complex of Co (ll).

Concentration of Co^{+2} present(M)	S D	Concentration of Co^{+2} found (M).	Percentage R.S.D %	Percentage Recovery %	Percentage Error %
1.738×10^{-4}	$1.732 \times 10^{-}$	1.740×10^{-4}	0.479	100.115	-0.115
3.400×10^{-4}	$3.674 \times 10^{-}$	3.460×10^{-4}	0.874	101.764	-1.764
5.100×10^{-4}	$1.870 \times 10^{-}$	5.020×10^{-4}	0.437	98.430	1.571

The value of RSD% (< 0.9) and recovery ranged from $98.43 - 101.764$ indicate that the optimized method was accurate and precise to determine Co (ll) ion.

3.18 Limit of Detection and limit of Quantification Calculation cobalt (II) ions.

The sensitivity of the spectroscopic technique employed for quantifying cobalt (II) ions is described by the term Limit of Detection LOD and quantification LOQ It represents the lowest concentration of cobalt (II) ions, which is (8.62×10^{-6} M) or (0.5 µg.mL^{-1}), that can be reliably measured using this spectroscopic method. The fact that the method can accurately detect such low concentrations indicates its excellent sensitivity and efficacy in determining cobalt (II) ions. The calculation for the Limit of Detection (D.L) and Quantification can be illustrated by the following relationship:

$$LOD = \frac{SD}{Slope} \text{ X } 3.3$$

$$LOQ = \frac{SD}{Slope} \text{ X } 10$$

S.D = standard diviation.

3.19 Synthesis of the solid complex.

Employing the reagent (EATDB) under optimal conditions, determined through extensive investigations into factors such as, the reagent's temperature, volume of the reagent, molar ratio, in addition to acidity function, the ion complex formed. For this, individual metal ions (Co^{+2}) with the reagent (EATDB) dissolved in ethanol, creating aqueous solutions. Thorough mixing and subsequent cooling led to the formation of precipitates. These precipitates were filtered and underwent a recrystallization process. Meticulous examination and analysis of the physical characteristics of the two solid complexes followed.

3.20 The Co (ll) complex Melting temperature and reagent measurements.

Cobalt (II)complex melting temperature was determined to be greater than 390°C, while the ligand (EATDB) exhibited a melting point range between 218°C to 222°C. Notably, a substantial difference in melting points was observed between the reagent and the two formed complexes in determining the melting temperature for cobalt (II) ion complex with the investigated reagent. These findings serve as compelling evidence for the formation of new complexes during the reaction process. Maintaining a consistent passive voice and formal tone in scientific writing ensures clear communication of research findings and conclusions.

3.21 Measurements of molar conductivity of cobalt (II).

The electrical conductivity of a substance is inherently linked to the abundance of charged ions present in its solution, often diminishing significantly, and occasionally approaching a near-zero state, when the complex lacks distinct ionic characteristics. In the context of this investigation, the molar conductivity of the cobalt (II) complex with (EATDB) is meticulously scrutinized at concentration of $(3x10^{-4}$ M), under ambient conditions, with ethanol serving as the solvent. The ensuing results, thoughtfully presented in table 3-17, unequivocally affirm that the cobalt (II) complex in conjunction with the reagent exhibits no discernible ionic character or charge. The rigorous and objective language employed in this scientific presentation establishes a clear and unambiguous conclusion, rendering these findings an invaluable addition to the broader research landscape on cobalt (II) complexes and their electrical properties.

Table (3-17) the molar conductivity value of solution for Co (ll) complex.

No	Complex	Λ_m(µS/cm)
1	[Co(EATDB)$_2$]	8.500

3.22 The Stoichiometry of Co (II) complex.

It was discovered through the study of paragraphs (3.22) that the cobalt (II) complex is not charged and the stric structure of the cobalt (II) complex has a tetrahedral shape and sp^3 hybridization because the cobalt (II) ions tend to form tetrahydral complexes more frequently than four-coordinated complexes.
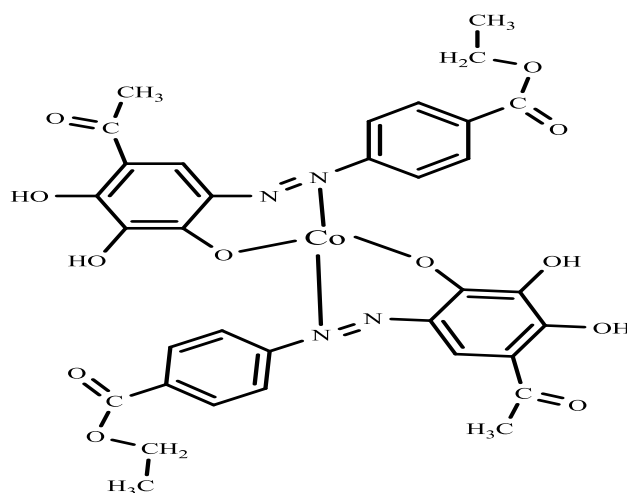
Figure 3-14 the suggested stucture of Cobalt (ll) complex.

3.23 Application of Cobalt (II) ion.

The optimized method proved highly effective in accurately determining the levels of cobalt (II) ions in drug samples. The comprehensive results of this experiment are succinctly summarized in Table 3-18, signifying the method's proficiency in providing precise and reliable measurements of cobalt (II) ions in pharmaceutical formulations. This successful application underscores the method's practical utility for quality control and assurance in the pharmaceutical industry, bolstering confidence in the accuracy and validity of the analytical approach [98].

Table (3.18): the results of application for Cobalt (ll) determination

Ampoules	Manufacturer	Conc. present $(\mu g.mL^{-1})$	Absorption	Conc. Found $(\mu g/mL)$	Recovery Percentage	E%
Vit.B$_{12}$	GERDA	43.370	0.180	42.910	98.939	1.061

When the statistical and actual amount of sample compared it was noticed that the spectrophotometric approach were in good agreement for that The technique can be used to check the quality of cobalt (II)-containing medicinal dosage forms.

3.24   UV-Visible test of Cr (III) - (EATDB).

Figure 3.16 explained the absorption spectrum for Cobalt (II) complex when paired with EATDB, within the range (200-1000) nm. An absorption maximum at (λ max = 573 nm) is observed for the Cr (III) complex, The intriguing observation of a bathochromic shift and a remarkable increase in absorbance provide compelling evidence of complex formation. These spectral changes suggest a distinct alteration in the electronic transitions, corroborating the successful formation of the Cobalt (II) complex in conjunction with the reagent. Such analytical insights significantly contribute to a deeper understanding of the complexation process and validate the suitability of the reagent for cobalt (II) ion determination in spectral studies.
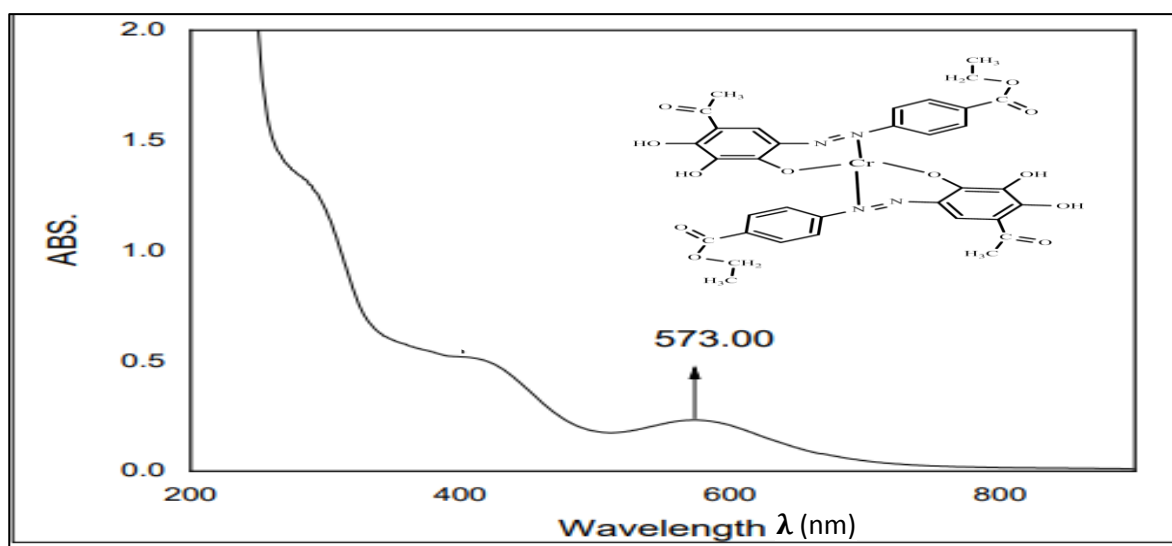
Figure (3-15): UV-visible test showing Cr (III)-[EATDB] spectrum.

81

3.25 Influence of pH on Chromium (III) Ion.

In Figure 3-17, the impact of the acidic function over Cr (III) complex's solution absorption, is visually depicted. Notably, the color intensity of the complex solutions exhibits a gradual increment, culminating in its maximum at an acidic function of 8. However, as the acidic function surpasses this level, a discernible reduction in the absorbance value of the complex is observed. This intriguing phenomenon could be attributed to several factors, including potential ion precipitation or the formation of unstable complex ions under higher acidic conditions. These observations highlight the significance of controlling the acidic function within a specific range to ensure optimal stability and reliability when studying the behavior of the Chromium (III) complex in solution. The analytical insights provided by this investigation contribute to a more comprehensive understanding of the intricate behavior of the complex and pave the way for further exploration of its chemical properties and applications.
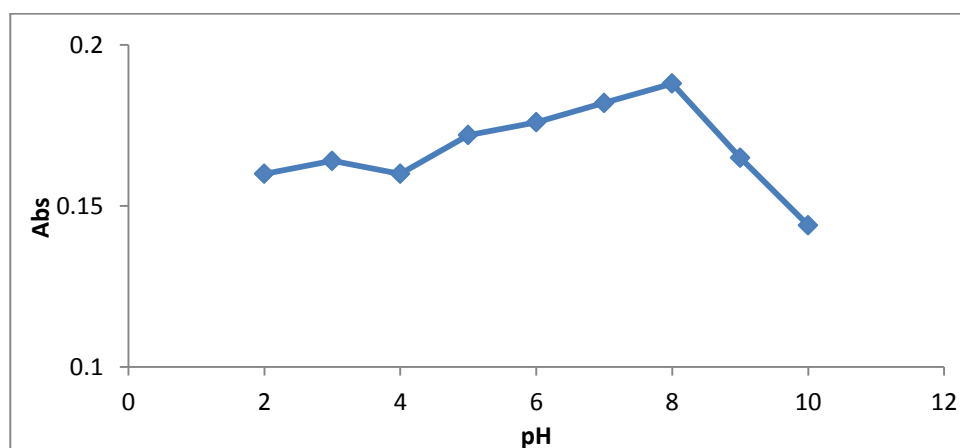
Figure (3.16): The absorption of Cr (III) complex effected by pH**.**

3.26 Cr (lll) Complexes Stability influenced by time:-

Cr (III) with (EATDB) absorption under optimized conditions are shown in table (3.19). The investigation aimed to assess the stability of the formed complexes and determine the ideal time frame for maintaining their stability. The

findings reveal that the Chromium (III) complex remains highly stable for 24 hours after its formation.

Table 3-19 Time influence on Cr (lll)-(EATDB).

Time (min.)	1	10	20	30	60	120	240	1440
Absorbance.	0.188	0.188	0.186	0.190	0.192	0.189	0.184	0.185

3.27 Effect of Temperature on Cr (III) Ion

Cr (III) complex formation that was affected by temperature is investigated through series tests, and the results are presented in Table (3.20). Notably, the Chromium (III) complex exhibited the highest absorption values and color intensity within the temperature range of (10- 40 °C). However, as the temperature increased beyond this range, the absorption levels decreased, possibly due to reduced stability or solubility at higher temperatures. These findings offer valuable insights into the temperature-dependent behavior for Cr (III) complex, aiding the selection for optimal temperature conditions for analytical applications and enhancing the understanding of its spectral properties and overall stability.

Table (3-20) influence of the Temperature on Cr (lll)-(EATDB)

Temp. ^{0}C	10	15	20	30	40	50	60
Absorbance.	0.190	0.189	0.188	0.189	0.185	0.154	0.139

3.28 Effect of Sequence addition on Cr (III) Ion.

Investigation in complex absorbance's order of the reaction content, was conducted through examination of four different addition arrangements. The result

presented in Table 3.21 demonstrates that the Cr (III) complex displayed an equal impact on the rate of absorption across all tested arrangements. These findings suggest a consistent and uniform behavior of the complex regarding its absorption rate, irrespective of the specific addition sequence employed. This insight further contributes to the understanding of the complexation kinetics and the overall stability of the Chromium (III) complex, serving as a valuable reference for future studies and analytical applications.

Table 3-21 Addition sequence impact on Cr (lll)-EATDB

Seq.	Addition Seq.	Absorption of complex
1st	M+L+PH	0.189
2nd	M+PH +L	0.186
3rd	L+PH +M	0.180
4th	L+M+PH	0.185

L=Ligand, M=Metal The first sequence was selected for determining the Cr (lll) complex using this method, as the results in table (3.21) indicate that it yields the best outcomes. The other sequences lead to a decrease in complex absorbance, possibly because of the influence of ions that have acid and base nature on the metal.

3.29 Ionic strength influence on Cr (lll) ion.

The effect of ionic strength on the absorption behavior of the Cr (III) complex was explored using sodium nitrate and sodium sulfate salts. Incremental additions of 1 mL were made to the Cr (III) complex, with concentrations of both salts ranging from 0.0005 M to 0.5 M. for both salts This experimental approach enabled a comprehensive assessment of how ionic strength influences absorption characteristics for Cr $^{+3}$ complex. Careful investigation for the ionic strength's impact offers valuable insights into the stability and behavior of the complex in the presence of different ionic environments, contributing to a deeper understanding of its chemical properties and potential applications.

Table 3-22 Ionic strength impact on Cr (lll)-(EATDB**).**

Salt Added	Concentration of added salt (M)	Absorption	Added salt	Concentration of added salt (M)	Salt Added
	0.5	0.186		0.5	0.183
	0.05	0.182		0.05	0.181
Na_2SO_4	0.005	0.179	$NaNO_3$	0.005	0.186
	0.0005	0.189		0.0005	0.188
Absorption of Cr(II)-(EATDB) without adding = 0.189					

The results are shown in table (3.22), indicating that the different concentrations of sodium nitrate and sodium sulfate salts used did not significantly affect the absorption value of the Cr (lll) complex. From these findings, it can be inferred that these ions do not have any influence on the solubility and sensitivity of the detection of Chromium (III) ion.

3.30 Calibration curve of Cr (III) complex.

The optimal condition was connected to generate the calibration curves for the ions of Chromium (III). The results of the investigation are depicted in fig. (3.17), for the chromium (III) ion.
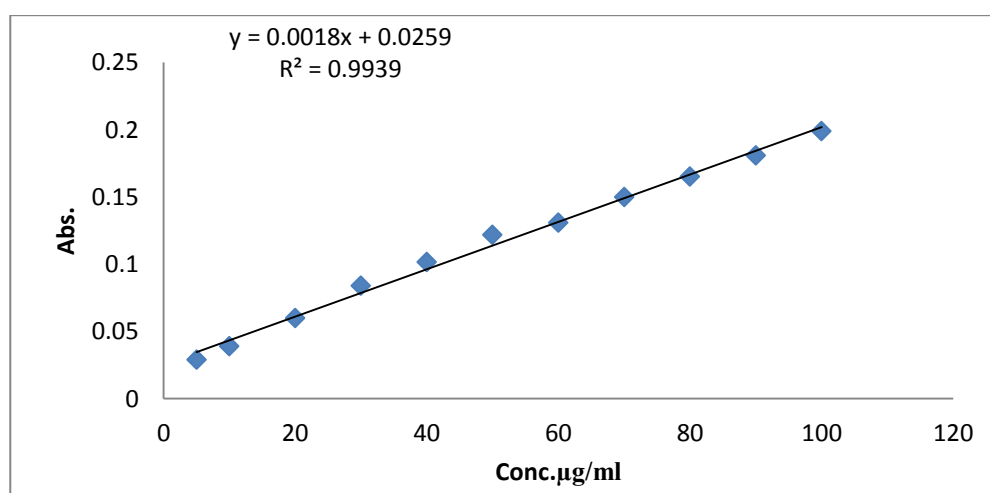
Figure (3-17) Cr (lll) ion calibration Curve.

Calibration curve of Chromium (III) ions obey Lambert-Beer law, which is fall into (1- 100 µg.mL^{-1}) in terms of concentration range, as shown in figure (3-17).Based on the metal concentration, It was discovered that the absorbance of chromium complex is linear and has a molar absorptivity of 0.935x10^2 L mol^{-1} cm^{-1}.

$$A = \varepsilon bC \qquad (3.1)$$

$$slope = \frac{\varepsilon}{At.Wtx1000} \qquad (3.2)$$

ε = molar absorptivity

$$S = \frac{10^{-3}}{a} \qquad (3.3)$$

S = Sandal sensitivity

Table (3.23): Analytical parameter for the analysis of Cr (lll)

Analytical Data	Value
Linear equation	Y=0.0018X+0.0259
Linear range(µg.mL^{-1})	(1-100)
Linearity coefficient (R^2)	0.9939
Molar absorptivity(L.mol cm)	0.935x10^2
sandall sensitivity (µg.cm-^{2})	0.5560
Limit of Detection (µg.mL^{-1})	0.8640
Limit of Quantification (µg.mL^{-1})	2.8510
Slope	0.0018
λ_{max}	573 nm

3.31 Stoichiometry of Cr (III) complex.

The composition of the Cr (III) complex is subjected to rigorous investigation through the application of three distinct methods: mole ratio, Job's, and Mallard's methods. These analytical approaches collectively provided a comprehensive analysis of the complex's composition and stoichiometry. By employing these techniques, valuable insights were gained into the molecular ratios and interactions

between the Chromium (III) ion and the ligand, Such thorough examinations contribute significantly to the understanding of the coordination chemistry of the Chromium (III) complex and its potential applications in various scientific domains.

3.31.1 Mole Ratio Method for Cr (lll) complex.

In the study, the composition of Cr (III) complex is determined through series of carefully prepared volumetric container. Each flask contained a fixed concentration of Cr (III) ion (3.00×10^{-4} M) combined with varying concentrations of the reagent ranging from(2.5×10^{-4} M- 7.00×10^{-4} M). The pH was adjusted to 9 for optimal complex formation. Comparison solutions were also prepared under the same conditions. These experiments provided valuable insights into the molecular ratios and interactions between the Chromium (III) ion and the reagent, allowing for a comprehensive determination of the complex's composition. The findings contribute to a deeper understanding of the chemical behavior and potential applications of the Chromium (III) complex [92].
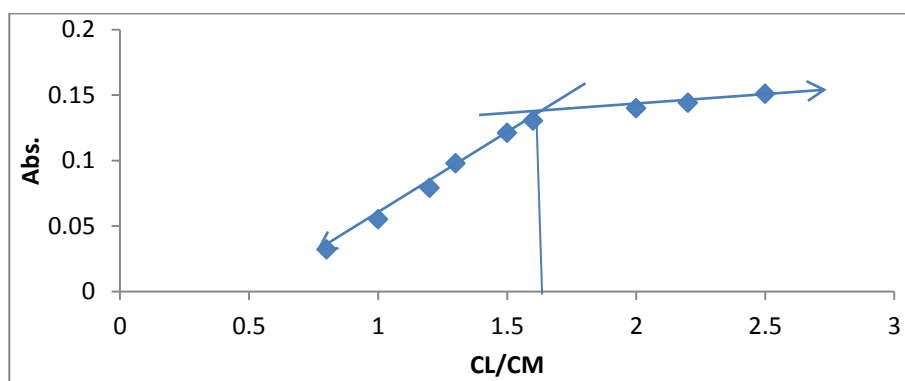
Figure (3.18) the mole ratio associated to the complex of Chromium Ion.

The bonding in the Cr (lll) indicates a stoichiometric ratio of (M: L) as 1:2, this means that there are two and one of moles for both the reagent and ion respectively, as illustrated in figure (3-18).

3.31.2 Job's method for Cr (lll) complex.

The experimental procedure involved combining different volumes of solutions, each with equal concentrations of 2.5×10^{-4} M of Cr (III) ion and 1.45×10^{-3} M of reagent (EATDB), to achieve a final volume of 10 ml. Under the optimized conditions, at (λmax = 573 nm) Cr (III) complex absorption was obtained [93].
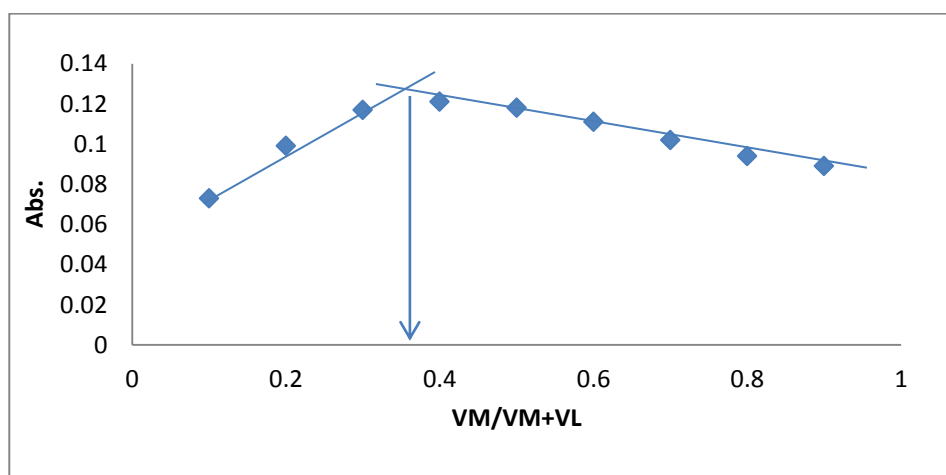
Figure (3-19) Cr (III) complex showed with Job's method

In figure (3.19), the bonding within the Cr (III) complex follows a (M: L) ratio of 1:2, signifying the presence of two and one mole for both of the reagent and the ion in the complex respectively.

3.31.3 Mallard's Method for Chrome (III) Ion Complex.

Valuable spectral data for further analysis was obtained from the resulting complex when Cr (III) ions (3.00×10^{-4}) M were mixed with the reagent solution (1.00×10^{-4}) M. The pH was adjusted to 9, and ethanol was utilized to achieve a total volume of 10 mL. The complex exhibited an absorbance of 0.179 at λmax = 573 nm [94].

In comparison to the comparator solution, which had an absorbance of 0.119, the complex showed a higher absorption value (0.062), represented as (As).

$$\frac{m}{s} = \frac{Am}{As} = \frac{0.119}{0.062} = 1.91 \text{------------} 3.4$$

From the obtained results, it becomes apparent that the stoichiometric ratio (M-L) in both the cobalt (II) and chromium (III) complexes is 1:2. This implies that each complex is consisting of two and one mole for the reagent and the complex respectively.

3.32 Calculated K_{sta} for Cr (lll) complex.

Stability constants of the Cr (lll) complex might be able to be calculated using the absorption values obtained from the mole ratio technique of the complex. The concentrations of Cr (III) ions in their solutions can be utilized for calculation of colored complex in terms of stability constant, particularly when they are combined with the reagent (EATDB). Calculated have been made using the following equation [101] :
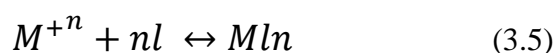
$$M^{+n} + nl \leftrightarrow Mln \qquad (3.5)$$

$$a + nca \leftrightarrow (1-a)c \qquad (3.6)$$

$$K = \frac{[MLn]}{[M^{+n}][L]} \qquad (3.7)$$

L = Reagent, α = the degree of dissociasion.

$$K = \frac{(1-a)c}{ac(nac)^n} \qquad (3.8)$$

$$K = \frac{1a}{n^n a^{n+1} c^n} \qquad (3.9)$$

$$a = \frac{Am-As}{Am} \qquad (3.10)$$

Am = the max absorption of complex

As = the absorption at equivalence point.

n=no.of mole,   C=molar of concentration,   L=Reagent M^n=io

Table 3-24 stability constant value for Cr (lll) complex

Complex	Value of (Am)	Value of (As)	(α)	(K)
[Cr (EATDB)₃]	0.191	0.122	0.361	1.125×10^8

Table (3.24) shows that the remarkable stability of the newly prepared complex can increases the process of the complex leading to estimate the Cr (lll) complex accurately

3.33 Calculation of dissociation degree, Ksta, and Cr (lll) complex Thermodynamic functions.

3.33.1 The effects of temperature on the Cr (lll) Complex's level of dissociation and the stability constant.

Table (3.25) presents the influence of temperature on a compound of Cr (lll) with taking into consideration the stability constant and degree of dissociation.

Table 3-25 Temperature variation impact on the Cr (lll) complex's stability constant and degree of stability.

T ⁰ C	T K	α	$K \times 10^{10}$
10	283.15	0.333	7.233
15	288.15	0.347	6.250
20	293.15	0.362	5.433
25	298.15	0.367	5.122
30	303.15	0.372	4.879
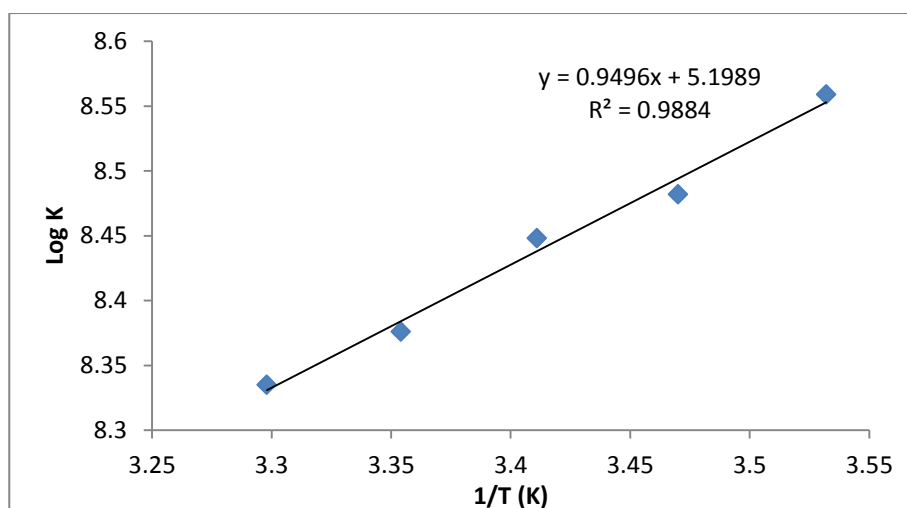
Figure 3-20 relationship between Temperature & Log K for Cr (lll).

The negative value of ΔG indicates that the ion's reaction was spontaneous. Furthermore, the negative value of ΔH suggests that the reaction was exothermic, as can be seen in table (3-26) and Figure (3-20). Temperature positively influences the hydrolysis shells surrounding the chromium ion, which possesses a concentrated charge and distinctive properties that hinder easy dissolution. The elevated temperature enhances the favorable effects on the hydrolysis shells, resulting in improved solubility. These observations shed light on the temperature-dependent behavior of the chromium ion, providing valuable insights into its stability and reactivity under different thermal conditions. Finding obtained was sorted in Table 3-26 and explained in Fig 3-21.

Table 3.26: Temperature impact on Cr (lll) complex Thermodynamic function.

T(K)	1/Tx10^{-3}K)	logK	Δ H	Δ G (KJ/mole)	Δ S (KJ/mole) .K)
283.15	3.532	7.859		-47.94	0.109
288.15	3.470	7.790		-48.43	0110
293.15	3.411	7.734		-48.93	0.108
298.15	3.354	7.709	-17.12	-49.62	0.109
303.15	3.298	7.688		-50.337	0.109

The data in tables 3.26 reveal that temperature had minimal influence on Cr (III) complexes stability. Considerable stability for Cr (III) complex underscores the promising utility of the reagent (EATDB) in spectrophotometric analyzing, offering consistent and dependable results.

3.34   The impact of interferences in terms of Anions and Cations for Cr (III) Complex.

3.34.1   Calculation of Cr (lll) ion with some interference cations ions.

Table 3.27 displays the results obtained from the investigation of the effect of various cations on the Cr (III) complex's absorption. The main objective of the study was to evaluate the possible interferences caused by the combination of these cations with the reagent.

Table (3-27) cations interference impact on Cr (lll) complex.

foreign ions	Cations formula	Absorbance after addition cations ($100\mu g.ml^{-1}$)	Error %
Cd^{2+}	$Cd(NO_3)_2.4H_2O$	0.202	-3.60
Ni^{2+}	$Ni(NO_3)_2.6H_2O$	0.177	7.80
Fe^{3+}	$Fe(NO_3)_3.9H_2O$	0.207	-7.80
Hg^{2+}	$Hg(NO_3)_2.H_2O$	0.211	-9.89
Pb^{2+}	$Pb(NO_3)_2$	0.189	1.50
M^{n2+}	$Mn(NO_3)_2.6\,H_2O$	0.206	-4.07
Ag^+	$AgNO_3$	0.198	-3.78
Cu^{2+}	$Cu(NO_3)_2.3H_2O$	0.178	7.29
Absorbance without interferences = 0.190			

The finding obtained in table (3-27) explained that specific ions resulted in increasing the absorbance m on the other hand, others led to decreasing the absorbance. This impact can be attributed to the competition between these ions and Cr(lII) ion for complex formation with the reagent.

3.34.2 Determination Cr (lll) ion with some interference anion ions

The effect of the presence of some selected an ions were studied to find out the interference of these ions with Chromium (III) ion. Result were sorted in table (3.28).

Table 3-28 Anions interference impact on Cr (lll) complex

Foreign ions	Formula ions	Absorption (100μg/mL)	E%	Absorption (200μg/mL)	E%
SO_4^{-2}	K_2SO_4	0.185	3.6	0.195	-1.40
Br^{-1}	KBr	0.180	6.2	0.168	12.50
SCN^{-1}	KSCN	0.181	5.7	0.192	0.00
IO_3^{-1}	KIO_3	0.185	3.6	0.195	-1.40
CrO_7^{-2}	K_2CrO_7	0.194	-1.4	0.210	-9.30
CO_3^{-2}	K_2CO_3	0.176	6.7	0.183	3.60
CN^{-1}	KCN	0177	6.9	0.179	6.70
Absorbance without interferences = 0.190					

The finding obtained in table (3-28) explained that specific ions resulted in increasing the absorbance on the other hand, others led to decreasing the absorbance. This impact can be attributed to the competition between these ions and Cr(lII) ion for complex formation with the reagent

3.35 Effect of masking agent on Cr (lll) complex.

3.35.1 Identifying the best Masking Agent for Accurate identification of the Cr (III) Complex

In response to the interference caused by various cations overlapping with the Cr (III) complex, a strategic plan was devised to mitigate this influence. To assess the impact of these interfering ions on the reagent's interaction with the complex, seven masking agents were selected. As a solution to this problem, 1 mL of each masking agent was added, as depicted in table (3.29).

Table (3-29) masking agent impact on Cr (lll) abs.

Masking agent (0.1M)	Absorbance of Chromium (lll)
Ascorbic acid	0.179
Citric acid	0.186
formaldehyde	0.189
KCl	0.191
$Na_2 HPO_4.12H_2O$	0.177
Na_2EDTA	0.184
Thiourea	0.169
Without masking agent	0.190

3.35.2 Using a more effective masking agent to detect Chromium (lll) ions when cations are interfering.

Ascorbic acid was chosen as the best masking agent to overcome the interference obtained from the cations .Data obtained were sorted in table (3.30).

Table 3-30   masking agent influence on Cr (lll) complex absorption when cations are present.

foreign ions	Abs. after addition cations (100µg/ml) and adding masking agent 0.1M	Relative error percentage E %
Cd^{2+}	0.179	5.26
Fe^{3+}	0.184	2.64
Zn^{2+}	0.186	1.5
Pb^{2+}	0.186	1.5
Mn^{2+}	0.195	-8.4
Ag^+	0.191	-0.526
Cu^{2+}	0.189	0.00

Table (3.30) displays the absorbance values of the Cr (III) complex when there are interfering cations in a condition of more effective masking agent is applied. It is evident from the table that the absorbance values closely resemble those

observed prior to the interference, indicating successful mitigation of the interference using the selected masking agent.

3.36 Accuracy and precision for suggested method for Cr (lll).

Evaluation of method's precision and accuracy involved the utilization of essential parameters such as relative standard deviation (R.S.D %) and percentage recovery for Chromium (III) ions respectively [95][96], Table 3.31 showed obtained results .

Table (3-31) precision & accuracy for Chromium (lll) complex

Concentration of Cr(III) present M	SD	Concentration of Cr(III) found M	R.S.D%	REC%	Error%
1.739×10^{-4}	1.22×10^{-3}	1.690×10^{-4}	0.742	99.41	0.590
3.400×10^{-4}	1.65×10^{-3}	3.450×10^{-4}	0.896	101.470	-1.470
5.100×10^{-4}	1.65×10^{-3}	5.120×10^{-4}	0.833	100.392	-0.392

The RSD% value < 0.9 and percentage recovery between 99.41 - 101.470 demonstrated that the analytical method (EATDB) utilized to measure the reagent exhibits a high degree of precision and accuracy. This indicates that the method is reliable and capable of providing precise measurements of the reagent's concentration in samples.

3.37 Limit of Detection (L.O.D) and limit of Quantification (L.O.Q) Calculation Chromium (III) ions.

The concept of Detection Limit encompasses the spectral technique's sensitivity utilized in quantifying cobalt (II) ions. Nevertheless, within the present investigation, the focus shifts to the detection limit concerning the determination of chromium (III) ions. The profound capability of this method is revealed by the identification of the minimum detectable concentration for Chromium (III) ions,

which stands at an impressively low value of (1.34 x 10^{-5} M), which in terms is equal (0.7µg.mL^{-1}). This observation highlights the method's remarkable sensitivity, rendering it a powerful tool for precisely determining ionic chromium in analytical applications. The exemplary relationship elucidated in the equation for the computation of (D.L) further exemplifies the method's efficacy in achieving accurate and reliable results in the determination of Chromium (III) ions, signifying its potential significance in diverse scientific endeavors and analytical investigations.

$$D.L = \frac{SD}{Slope} X\ 3.3$$

SD = standard deviation

3.38 Preparation of solid complex for Chromium (III) ion.

Under the optimized conditions obtained from extensive research on parameters such as acidity function, volume of the reagent, molar ratios and temperature, the reagent (EATDB) utilized to form ion complexes. This involved combining the metal ion (Cr^{+3}) with the reagent (EATDB) dissolved in ethanol. Upon mixing and cooling, a precipitate was observed to form during and after the process. Subsequently, the solutions were allowed to precipitate completed before undergoing filtration and recrystallization. Intensive investigation was conducted on the two solid complex to determine their physical properties.

3.39 Melting point measurements for Cr (III) complex and the reagent.

Chromium (III) ions complex exhibited a melting point above 390°C, while the ligand displayed a melting point ranging between 218°C to 222°C. A notable contrast in melting point values was evident while determining the melting points of the Cr^{+3} ion complex with reagent. The significant difference indicates formation of a new complex.

3.40   Measurements of molar conductivity of Chromium (III)

Table 3-32 presents the molar conductivity values of the chrome (III) complex-reagent, with concentration $(1.00 \times 10^{-3}M)$ in ethanol at room temperature. The research findings demonstrate that the complex lacks any ionic character or charge, resulting in very low levels of electrical conductivity approaching zero. This characteristic is attributed to absence of ions that are charged in the solution, as complex lacks the necessary properties to conduct electric current. The investigation sheds light on the complex's non-conductive behavior in solution, offering valuable insights into its molecular characteristics and enhancing our understanding of its distinct properties for potential applications in various scientific endeavors.

Table 3-32 the value of molar conductivity of the solution of the Cr (lll) complex

Seq.	complex	$\Lambda_m(\ \mu s.cm^{-1})$
1	[Cr(EATDB)₃]	14.8

3.41 The Stoichiometry of Cr (lll) complex.

It was discovered through the study of paragraphs 3–22 that the chromium (III) complex's steric structure has a tetrahedral shape and sp^3 hybridization because the chromium (III) tend to form hexagonal complexes more frequently than four-coordinated complexes.
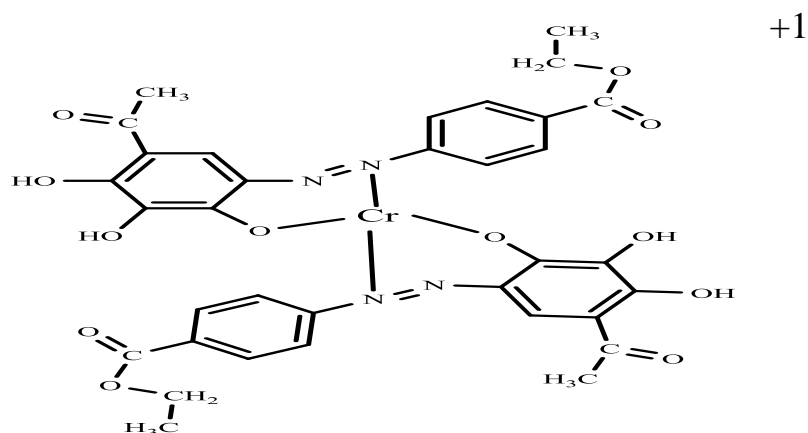
Figure (3.21): the suggested structure of Chrome (III) complex

3.42 Application of Chromium (III) Ion

The concentrations of chromium (III) ions in drug sample samples were determined using the indicated approach. It was based on the percentage of chromium (III) ions specified in the medication, and the actual results were fairly close to what was stated in the medications. table (3-33) summarizes the experiment's findings for chromium (III) ion determination [102].

Table 3-33 Application of the chromium (lll) determination.

Pills	Manufacturer	the present Concentration ($\mu g.mL^{-1}$)	Absorption	The found Concentration ($\mu g.mL^{-1}$)	Recovery percentage %	Error%
Chromium Niacin	Madamar	4.00	0.033	3.95	98.75	1.25
Chromium A/Z Multiway	THORNE	25.0	0.073	24.8	99.23	0.77

When the statistical and actual amount of sample compared it was noticed that the spectrophotometric approach were in good agreement for that The technique can be used to check the quality of cobalt (II)-containing pharmaceutical dosage forms.

3.43 Conclusions

1.Trace amount of Co (II) and Cr (III) ions can be measured using the EATDB spectrophotometric, which has colored complexes.

2. Because the Lambert-Beer rule is followed, a broad range of concentrations can be obtained.

3.The stoichiometry for both Co(II) and Cr (III) complexes were(1:2) (M:L)

4.According to the results of the masking agent effect study, Ascorbic Acid exhibits no influence on the method of determining cobalt ions. Hence, this effectively employed as masking agent in analytical procedures to counteract potential interferences and improve the accuracy of cobalt (II) ion determination.

5. The thermodynamic investigation provided compelling evidence that the reaction between the reagent's complexes and cobalt (II) as well as chromium (III) ions is both exothermic and spontaneous. This conclusion is substantiated by the negative values of ΔG (Gibbs free energy) and ΔH (enthalpy) observed at high temperatures for both complexes. Moreover, at low temperatures, values of ΔH and ΔG that are negative for the Cr (III) in conjunction with reagent further emphasize the exothermic and spontaneous nature of the reaction. These thermodynamic behaviors elucidate the underlying energetic aspects of the complexes' formation and highlight their stability over a broad range of temperatures, providing valuable insights for future applications and theoretical considerations in chemical and analytical studies.

6. The comparison of stability constant values between the Cr (lll) complex and the cobalt (ll) complex with the reagent (EATDB) indicates that the Cr (lll) complex is more stable. The higher stability constant of the Cr (lll) complex suggests that it has a stronger bond and is less prone to dissociation compared to the cobalt (ll) complex with the reagent. This increased stability enhances the feasibility and reliability of using the reagent (EATDB) for spectrophotometric analysis of chromium (III) ions.

7.Through the determination of molar conductivity and charge, it was revealed that both the Co (II) and Cr (III) complexes exhibited a lack of charge. This insightful finding indicates that these complexes do not possess ionic characteristics in their solutions and maintain an overall neutral state without any net charge. The absence of charge suggests a non-ionic behavior, which is crucial in understanding the molecular properties and interactions of these complexes in various solution environments.

The high sensitivity of the spectral method was evident from the low R.S.D% and relative error in percent, showcasing its remarkable precision and accuracy. This straightforward and efficient method eliminates the need for pre-treatment or complicated procedures like separation or ion exchange. Its ability to provide reliable results with minimal error makes it a highly valuable tool for analytical purposes.

3.44 Recommendations.

1. The feasibility of utilizing (EATDB) for calculating concentration for additional ions located at diverse media was investigated. The results showed that the reagent demonstrated good potential for quantifying various metal ions in different solutions. The method was found to be sensitive, accurate, and reliable in determining the concentration of these ions. The reagent's ability to form stable complexes with different metal ions allowed for precise measurements across a wide range of media. Overall, the use of the reagent (EATDB) as a versatile tool for analyzing diverse metal ions holds promise for various analytical applications.

2. The creation of new reagent derivatives to enhance the reagent's characteristics and selectivity, as well as the reagent's application in estimating other components.

3. Since the reagent that is synthesized can be consistent with many other ions, it might be employed to extract various transition elements.

4. It should keep track of how the created reagent affects biological activity since azo compounds, which are a key component of limiting biological activity.

References

[1]   Z. Holzbecher, S. Kotrlý, and R. A. Chalmers, *Handbook of organic reagents in inorganic analysis*. E. Horwood Ltd. and distributed [by] Halsted Press, 1976. [Online]. Available: https://cir.nii.ac.jp/crid/1130000797679084800.bib?lang=en

[2]   H. F. Walton, *Principles and methods of chemical analysis*, 2nd ed. Prentice-Hall, 1964. [Online].

[3]   Q. Li, X. Zhao, K. Jiang, and G. Liu, "Study of spectrophotometric method for determination of trace copper after the separation and enrichment with solid phase extractant-microcrystalline phenolphthalein," *Chinese Sci. Bull.*, vol. 52, no. 1, pp. 65–70, 2007, doi: 10.1007/s11434-007-0018-2.

[4]   A. Kumar, R. Dass, and R. Chaudhary, "Extraction and spectrophotometric determination of molybdenum(V) as its thiocyanate complex in industrial, environmental and soil samples," *J. Indian Chem. Soc.*, vol. 86, pp. 275–280, Mar. 2009.

[5]   Felicia Dragan, Lucian Hîncu, and Ioan Bratu, "Determination of cobalt in human biological liquids from electrothermal atomic absorption spectrometry," *J. Phys. Conf. Ser.*, vol. 182, no. 1, p. 12006, 2009,

[6]   S. Babu, K. Reddy, and Y. Lingappa, "Spectrophotometric determination of cobalt in biological samples using 2-acetylpyridine semicarbazone," *J. Indian Chem. Soc.*, vol. 86, pp. 312–315, Mar. 2009.

[7]   M. Hiraoka, "Chapter 1 - Introductory Remarks," in *Crown Ethers and Analogous Compounds*, M. B. T.-S. in O. C. Hiraoka, Ed., Elsevier, pp. 1–16. 1992.

[8]   T. A Geissman, *Principles of organic chemistry*, 4th ed. W. H. Freeman, 1977.

[9]   C. R. Noller, *Chemistry of organic compounds*, 3d ed. Saunders, 1965. [Online]. Available: https://cir.nii.ac.jp/crid/1130282270442666624.bib?lang=en

[10] J.M. Coxon and R.O.C. Norman, *Principles of Organic Synthesis*, 3rd ed. Blackie Academic & Pro., 1993.

[11] F. Z. Dörwald, *Side Reactions in Organic Synthesis: A Guide to Successful Synthesis Design*. 2006. [Online]. Available: https://books.google.com/books/about/Side_Reactions_in_Organic_Synthesis.html?id=1rYCEcbECW4C&pgis=1

[12] Louis F. Fieser and Kenneth L Williamson, *Organic Experiments*, 7th ed. 1992.

[13] H. D. K. Drew and F. H. Pearman, "5. Chemiluminescent organic compounds. Part II. The effect of substituents on the closure of phthalhydrazides to 5- and 6-membered rings," *J. Chem. Soc.*, no. 0,

[14] G. Goldstein, D. L. Manning, O. Menis, and J. A. dean, "Spectrophotometric methods for the determination of osmium-III: Reaction of osmium tetroxide with 1:5-diphenylcarbo- hydrazide in aqueous solutions followed by extraction of the complex," *Talanta*, vol. 7, no. 3, pp. 307–315, 1961, doi: https://doi.org/10.1016/0039-9140(61)80025-8.

[15] L. Feng Li, Ke-An, C. Wen, W. Yan-Sheng, Y. Tuan-Li, and T. Shen-Yang, "Preconcentration and separation of trace Pd(II) and Pt(IV) with silica, gel bonded by aminopropyl-benzoylazo-4-(2-pyridylazo)-resorcinol," *Chinese J. Chem.*, vol. 18, no. 4, pp. 537–541, Jul. 2000,

[16] M. Akhond and M. Bagheri, "Highly Copper(II) Ion-selective Transport through Liquid Membrane Containing 1-(2-Pyridylazo)-2-naphthol," *Anal. Sci.*, vol. 18, no. 9, pp. 1051–1054, 2002, doi: 10.2116/analsci.18.1051.

[17] V. H. Pavlidis, "Organic Chemistry (4th edition). R J Fessenden and J S Fessenden, Brooks/Cole, California, 1990. Pp 1137. £19.95. ISBN 0 534 98175 5," *Appl. Organomet. Chem.*, vol. 5, no. 2, p. 139, Mar. 1991,

[18] I. V Ledenyova, V. V Didenko, and K. S. Shikhaliev, "Chemistry of Pyrazole-3(5)-Diazonium Salts (Review)*," *Chem. Heterocycl. Compd.*, vol. 50, no. 9, pp. 1214–1243, 2014, doi: 10.1007/s10593-014-1585-1.

[19] Charles Owens Wilson and Ole Gisvold, *Wilson and Gisvold's Textbook of Organic Medicinal and Pharmaceutical Chemistry*, Illustrate. Lippincott Williams & Wilkins, 2004.

[20] F. Alihosseini and G. Sun, "17 - Antibacterial colorants for textiles," in *Woodhead Publishing Series in Textiles*, N. Pan and G. B. T.-F. T. for I. P. Sun Protection and Health, Eds., Woodhead Publishing, pp. 376–403. 2011.

[21] I. Szele and H. Zollinger, "Azo coupling reactions structures and mechanisms BT - Preparative Organic Chemistry," Berlin, Heidelberg: Springer Berlin Heidelberg, pp. 1–66.1983

[22] H. Yousefi, A. Yahyazadeh, E. O. M. Rufchahi, and M. Rassa, "Synthesis, spectral properties, biological activity and application of new 4-(benzyloxy)phenol derived azo dyes for polyester fiber dyeing," *J. Mol. Liq.*, vol. 180, pp. 51–58, 2013,

[23] N. M. Aljamali, "Review in (NMR and UV-Vis) Spectra," *Int. J. Med. Res. Pharm. Sci.*, vol. 2, no. 1, pp. 28–36, 2015.

[24] A. Sureka and S. Murugesan, "Review in Cyclic Compounds with HeteroatomReview in Cyclic Compounds with Heteroatom," *Int. J. Curr. Res. Biol. Med.*, vol. 4, no. 11, pp. 1–10, 2017,

[25] Aljamali Nagham Mahmood, "Review in Cyclic Compounds with Heteroatom," *Asian J. Res. Chem.*, vol. 7, no. 11, pp. 975–1006, 2014.

[26] Y. Ju, D. Kumar, and R. S. Varma, "Revisiting Nucleophilic Substitution Reactions: Microwave-Assisted Synthesis of Azides, Thiocyanates, and Sulfones in an Aqueous Medium," *J. Org. Chem.*, vol. 71, no. 17, pp. 6697–6700,. 2006, doi: 10.1021/jo061114h.

[27] N. Iranpoor, H. Firouzabadi, B. Akhlaghinia, and R. Azadi, "Conversion of Alcohols, Thiols, Carboxylic Acids, Trimethylsilyl Ethers, and Carboxylates to Thiocyanates with Triphenylphosphine/ Diethylazodicarboxylate/NH4SCN," *Synthesis (Stuttg).*, no. 1, pp. 92–96, 2004, doi: 10.1055/s-2003-44369.

[28] M. Iinuma, K. Moriyama, and H. Togo, "Simple and practical method for preparation of [(diacetoxy)iodo]arenes with iodoarenes and m-chloroperoxybenzoic acid," *Synlett*, vol. 23, no. 18, pp. 2663–2666, 2012, doi: 10.1055/s-0032-1317345.

[29] D. S. Bhalerao and K. G. Akamanchi, "Efficient and novel method for thiocyanation of aromatic and heteroaromatic compounds using bromodimethylsulfonium bromide and ammonium thiocyanate," *Synlett*, no. 19, pp. 2952–2956, 2007, doi: 10.1055/s-2007-992367.

[30] H. S. Freeman, "Aromatic amines: Use in azo dye chemistry," *Front. Biosci.*, vol. 18, no. 1, pp. 145–164, 2013, doi: 10.2741/4093.

[31] B. W. Gung and R. T. Taylor, "Parallel Combinatorial Synthesis of Azo Dyes: A Combinatorial Experiment Suitable for Undergraduate Laboratories," *J. Chem. Educ.*, vol. 81, no. 11, p. 1630, Nov. 2004,

[32] C. Decelles, "The story of dyes and dyeing.," *J. Chem. Educ.*, vol. 26, no. 11, p. 583, 1949,

[33] U. P. Azad, V. Ganesan, and M. Pal, "Catalytic reduction of organic dyes at gold nanoparticles impregnated silica materials: influence of functional groups and surfactants," *J. Nanoparticle Res.*, vol. 13, no. 9, pp. 3951–3959, 2011, doi: 10.1007/s11051-011-0317-z.

[34] R. Sharma, M. Singla, and K. C. Kalia, "Synthesis and characterization of some tris (2-arylazophenolato)rhodium(III) chelates," *Indian J. Chem. - Sect. A Inorganic, Phys. Theor. Anal. Chem.*, vol. 35, no. 7, pp. 611–613, 1996.

[35] E. J. Parker and A. J. Pratt, "Amino Acid Biosynthesis," in *Amino Acids, Peptides and Proteins in Organic Chemistry*, pp. 1–82. 2010

[36] H. R. Maradiya and V. S. Patel, "Synthesis and Dyeing Performance of Some Novel Heterocyclic Azo Disperse Dyes," *Journal of the Brazilian Chemical Society*, vol. 12. scielo , 2001.

[37] R. J. Chudgar, "Azo Dyes," in *Kirk-Othmer Encyclopedia of Chemical Technology*, 2000.

[38] K. A. H. Al-ali, "Study the Electrical Conductivity for a New Azo Compound," vol. 34, pp. 51–57, 2008.

[39] R. Morrin Acheson, *An Introduction To The Chemistry Of Heterocyclic Compounds*, 3rd ed. Wiley India, 2008.

[40] A. Vázquez-Salazar, A. Becerra, and A. Lazcano, "Evolutionary convergence in the biosyntheses of the imidazole moieties of histidine and purines.," *PLoS One*, vol. 13, no. 4, p. e0196349, 2018,

[41] A. Hussain, *Anew Study of preparation and characterization of new one azo compounds and study the possibility of using in spectral determination of Cu(II) ion* 2019.

[42] S. Shibata, M. Furukawa, and R. Nakashima, "Syntheses of azo dyes containing 4,5-diphenylimidazole and their evaluation as analytical reagents," *Anal. Chim. Acta*, vol. 81, no. 1, pp. 131–141, 1976,

[43] P. Byabartta, S. Jasimuddin, B. K. Ghosh, C. Sinha, A. M. Z. Slawin, and J. D. Woollins, "Nitro–ruthenium(ii)–arylazoimidazoles: synthesis, spectra, crystal structure and electrochemistry of dinitro-bis{1-alkyl-2-(arylazo)imidazole}ruthenium(ii). Nitro–nitroso derivatives and reactivity of the electrophilic {Ru-NO}6 system," *New J. Chem.*, vol. 26, no. 10, pp. 1415–1424, 2002, doi: 10.1039/B204442K.

[44] H.-B. Zhang, X.-F. Zhang, L.-Q. Chai, L.-J. Tang, and H.-S. Zhang, "Zinc(II) and Cadmium(II) complexes containing imidazole ring:

Structural, spectroscopic, antibacterial, DFT calculations and Hirshfeld surface analysis," *Inorganica Chim. Acta*, vol. 507, p. 119610, 2020,

[45] U. Ray, D. Banerjee, G. Mostafa, T.-H. Lu, and C. Sinha, "Copper coordination compounds of chelating imidazole-azo-aryl ligand. The molecular structures of bis[1-ethyl-2-(p-tolylazo)imidazole]-bis-(azido)copper(ii) and bis[1-methyl-2-(phenylazo)imidazole]-bis(thiocyanato)copper(ii)," *New J. Chem.*, vol. 28, no. 12, pp. 1437–1442, 2004,

[46] S. A. Naman, A. H. Jassim, and M. F. Alias, "Photodecomposition of molybdenum(II) and tungsten(II) carbonyl complexes with triazole, benzimidazole, and oxadiazole acetylinic derivatives," *J. Photochem. Photobiol. A Chem.*, vol. 150, no. 1–3, pp. 41–48, 2002, doi: 10.1016/S1010-6030(02)00033-3.

[47] J. A. Mondal, G. Saha, C. Sinha, and D. K. Palit, "Photoisomerization dynamics of N-1-methyl-2-(tolylazo) imidazole and the effect of complexation with Cu(II).," *Phys. Chem. Chem. Phys.*, vol. 14, no. 37, pp. 13027–13034, Oct. 2012,.

[48] K. K. Sarker, D. Sardar, K. Suwa, J. Otsuki, and C. Sinha, "Cadmium(II) Complexes of (Arylazo)imidazoles: Synthesis, Structure, Photochromism, and Density Functional Theory Calculation," *Inorg. Chem.*, vol. 46, no. 20, pp. 8291–8301, Oct. 2007,

[49] J. Sk and C. Sinha, "Synthesis and spectral characterization of palladium(II) and silver(I) complexes of antipyrine-azo-imidazoles," *Indian J. Chem. Sect. a*, vol. 45A, p. 5, May 2006.

[50] E. Bobrowska-Grzesik and A. Grossman, "Derivative spectrophotometry in the determination of metal ions with 4-(pyridyl-2-azo)resorcinol (PAR)," *Fresenius. J. Anal. Chem.*, vol. 354, no. 4, pp. 498–502, 1996,

[51] M. Kurahashi, "The Crystal and Molecular Structure of 1-(2-Thiazolylazo)-2-naphthol," *Bull. Chem. Soc. Jpn.*, vol. 49, no. 11, pp. 2927–2933, Nov. 1976,

[52] W. Fu-Sheng, Q. Pei-Hua, S. Nai-Kui, and Y. Fang, "Sensitive spectrophotometric determination of nickel(II) with 2-(5-bromo-2-pyridylazo)-5-diethylaminophenol," *Talanta*, vol. 28, no. 3, pp. 189–191, 1981,

[53] P. J. T. Morris and A. S. Travis, "A history of the international dyestuff industry," *Am. Dyest. Report.*, vol. 81, no. 11, 1992.

[54] M. K. Beklemishev, T. A. Stoyan, and I. F. Dolmanova, "Sorption-catalytic determination of cadmium using bromobenzothiazo noncovalently bound to silica and paper," *Fresenius. J. Anal. Chem.*, vol. 367, no. 1, pp. 17–23, 2000,

[55] W. H. Mills and J. G. Breckenridge, "309. Molecular dissymmetry dependent on restriction of rotation about a single bond. Part II. Optically active 8-benzenesulphonylethylamino-1-ethylquinolinium salts," *J. Chem. Soc.*, no. 0, pp. 2209–2216, 1932,

[56] D. J. Paustenbach, B. E. Tvermoes, K. M. Unice, B. L. Finley, and B. D. Kerger, "A review of the health hazards posed by cobalt.," *Crit. Rev. Toxicol.*, vol. 43, no. 4, pp. 316–362, Apr. 2013,

[57] S. Strachan, "Trace elements," *Curr. Anaesth. Crit. Care*, vol. 21, no. 1, pp. 44–48, 2010,

[58] J. A. Jenkins, M. Musgrove, and S. J. O. White, "Outlining Potential Biomarkers of Exposure and Effect to Critical Minerals: Nutritionally Essential Trace Elements and the Rare Earth Elements," *Toxics*, vol. 11, no. 2. 2023.

[59] "Cobalt in hard metals and cobalt sulfate, gallium arsenide, indium phosphide and vanadium pentoxide.," *IARC Monogr. Eval. Carcinog. risks to humans*, vol. 86, pp. 1–294, 2006.

[60] S. Catalani, M. C. Rizzetti, A. Padovani, and P. Apostoli, "Neurotoxicity of cobalt.," *Hum. Exp. Toxicol.*, vol. 31, no. 5, pp. 421–437, May 2012,

[61] A. C. Cheung *et al.*, "Systemic cobalt toxicity from total hip arthroplasties: review of a rare condition Part 1 - history, mechanism, measurements, and pathophysiology.," *Bone Joint J.*, vol. 98–B, no. 1, pp. 6–13, Jan. 2016,

[62] M. Hosseini, N. Dalali, and S. Moghaddasifar, "Ionic liquid for homogeneous liquid-liquid microextraction separation/preconcentration and determination of cobalt in saline samples," *J. Anal. Chem.*, vol. 69, no. 12, pp. 1141–1146, 2014,

[63] X. Kong, Q. Jia, and W. Zhou, "Coupling on-line preconcentration by ion-exchange with microwave plasma torch-atomic emission spectrometry for the determination of cobalt and nickel," *Microchem. J.*, vol. 87, no. 2, pp. 132–138, 2007,

[64] M. M. Berger and A. Shenkin, "Vitamins and trace elements: practical aspects of supplementation.," *Nutrition*, vol. 22, no. 9, pp. 952–955, Sep.

2006,

[65] M. Ghaedi, F. Ahmadi, and M. Soylak, "Preconcentration and separation of nickel, copper and cobalt using solid phase extraction and their determination in some real samples," *J. Hazard. Mater.*, vol. 147, no. 1, pp. 226–231, 2007,

[66] A. Amin, "Study on the solid phase extraction and spectrophotometric determination of cobalt with 5-(2-benzothiazolylazo)-8-hydroxyquinolene," *Arab. J. Chem.*, vol. 7, Nov. 2014,

[67] F. Shemirani and N. Shokoufi, "Laser induced thermal lens spectrometry for cobalt determination after cloud point extraction.," *Anal. Chim. Acta*, vol. 577, no. 2, pp. 238–243, Sep. 2006,

[68] P. Berton and R. G. Wuilloud, "Highly selective ionic liquid-based microextraction method for sensitive trace cobalt determination in environmental and biological samples.," *Anal. Chim. Acta*, vol. 662, no. 2, pp. 155–162, Mar. 2010,

[69] S. Cadore, R. D. Goi, and N. Baccan, "Flame atomic absorption

morpholinedithiocarbamate complex," *Journal of the Brazilian Chemical Society*, vol. 16. scielo , 2005.

[70] N. Baghban, A. M. H. Shabani, S. Dadfarnia, and A. A. Jafari, "Flame atomic absorption spectrometric determination of trace amounts of cobalt after cloud point extraction as 2-[(2-Mercaptophenylimino)methyl]phenol complex," *Journal of the Brazilian Chemical Society*, vol. 20. scielo , 2009.

[71] R. J. Cassella, V. A. Salim, L. S. Jesuíno, R. E. Santelli, S. L. Ferreira, and M. S. de Carvalho, "Flow injection determination of cobalt after its sorption onto polyurethane foam loaded with 2-(2-thiazolylazo)-p-cresol (TAC).," *Talanta*, vol. 54, no. 1, pp. 61–67, Mar. 2001, [72]   S. Chen, Y. Liu, J. Yan, C. Wang, and D. Lu, "Dispersive Micro-solid Phase Extraction with Fibrous TiO 2 @ g- C 3 N 4 Nanocomposites Coupled with ICP-MS for the Determination of Cobalt and Nickel in Environmental and Biological Samples," vol. 41, no. 4, pp. 169–174, 2020, doi: 10.46770/AS.2020.04.005.

[73] M. A. Akl and W. S. A. Alharawi, "A Green and Simple Technique for Flotation and Spectrophotometric Determination of Cobalt(II) in Pharmaceutical and Water Samples," *Egypt. J. Chem.*, vol. 61, no. 4, pp. 639–650, 2018,

[74] H. Abdolmohammad-Zadeh and E. Ebrahimzadeh, "Determination of cobalt in water samples by atomic absorption spectrometry after pre-concentration with a simple ionic liquid-based dispersive liquid-liquid micro-extraction methodology," vol. 8, no. 3, pp. 617–625, 2010,

[75] R. E. Taljaard and J. F. va. Staden, "Simultaneous determination of cobalt(II) and Ni(II) in water and soil samples with sequential injection analysis," *Anal. Chim. Acta*, vol. 366, no. 1, pp. 177–186, 1998,

[76] N. K. Temel, K. Sertakan, and R. Gürkan, "Preconcentration and Determination of Trace Nickel and Cobalt in Milk-Based Samples by Ultrasound-Assisted Cloud Point Extraction Coupled with Flame Atomic Absorption Spectrometry.," *Biol. Trace Elem. Res.*, vol. 186, no. 2, pp. 597–607, Dec. 2018,

[77] M. S. Centre, "Modified method for the determination of cobalt (II) and copper (II) ions by adopting schiff base complexes in water of Shatt Al-Arab river," *Mesopot. J. Mar. Sci.*, vol. 26, no. 2, pp. 170–181, 2011,

[78] M. Arain, E. Yilmaz, and M. Soylak, "Deep eutectic solvent based ultrasonic assisted liquid phase microextraction for the FAAS determination of cobalt," *J. Mol. Liq.*, vol. 224, Oct. 2016,

[79] M. R. Jamali, B. Soleimani, R. Rahnama, and S. H. A. Rahimi, "Development of an in situ solvent formation microextraction and preconcentration method based on ionic liquids for the determination of trace cobalt (II) in water samples by flame atomic absorption spectrometry," *Arab. J. Chem.*, vol. 10, pp. S321–S327, 2017,

[80] R. F. Hertel, "Sources of exposure and biological effects of chromium.," *IARC Sci. Publ.*, no. 71, pp. 63–77, 1986.

[81] R. A. Anderson, "Chromium in the prevention and control of diabetes.," *Diabetes Metab.*, vol. 26, no. 1, pp. 22–27, Feb. 2000.

[82] Z. Khammas, S. Jawad, and I. Ali, "A New Spectrophotometric Determination of Chromium (VI) as Cr2O7 2- After Cloud-Point Extraction Using a Laboratory- Made Organic Reagent," *Glob. J. Sci. Front. Res. Chem.*, vol. 13, pp. 9–19, Jan. 2013.

[83] K. M. Diniz and C. R. T. Tarley, "Speciation analysis of chromium in water samples through sequential combination of dispersive magnetic solid phase extraction using mesoporous amino-functionalized Fe3O4/SiO2 nanoparticles and cloud point extraction," *Microchem. J.*, vol. 123, pp. 185–195, 2015,

[84] W. Ahmad, A. S. Bashammakh, A. A. Al-Sibaai, H. Alwael, and M. S. El-Shahawi, "Trace determination of Cr(III) and Cr(VI) species in water samples via dispersive liquid-liquid microextraction and microvolume UV–Vis spectrometry. Thermodynamics, speciation study," *J. Mol. Liq.*, vol. 224, Oct. 2016.

[85] N. H. Shekho and H. A. Mahmoud, "Spectrophotometric Determination of Chromium Using Indigo Carmine -Application in Various Samples," *Baghdad Sci. J.*, vol. 13, no. 3, p. 0556, 2016,

[86] K. J. Al-Adilee, S. M. Eassa, and H. K. Dakhil, "Spectrophotometric determination of chromium(III) and iron(III)by used of 2-((E)-(1H-benzo[d]imidazol2-yl)   diazenyl)-5-((E)-benzylideneimino)phenol;(BIADPI)as organic reagent," *Orient. J. Chem.*, vol. 32, no. 5, pp. 2481–2491, 2016,

[87] S. M. Eassa, "Spectrophotometric determination for Chromium (III) and Cobalt (II) with 4-(nitro phenyl azo imidazole)(NPAI) as organic reagent.," *J. Chem. Pharm. Res.*, vol. 8, no. 8, pp. 85–92, 2016.

[88] A. S. Amin and M. A. Kassem, "Chromium speciation in environmental samples using a solid phase spectrophotometric method," *Spectrochim. Acta Part A Mol. Biomol. Spectrosc.*, vol. 96, pp. 541–547, 2012,

[89] A. R. Chakraborty and R. K. Mishra, "Speciation and determination of chromium in waters+," *Chem. Speciat. Bioavailab.*, vol. 4, no. 4, pp. 131–134, Dec. 1992,

[90] J. Tóth and Y. Bazeľ, "Development of a New Kinetic Spectrophotometric Method for the Determination of Chromium with an Optical Probe," *Appl. Spectrosc.*, vol. 73, no. 5, pp. 492–502, 2019,

[91] B. W.A and O. N.S, "Spectrophotometric Determination of Benzocaine by Azo-Dye Formation Reaction with N-(1-naphthyl)ethylenediamine as Coupling Agent," *J. Educ. Sci.*, vol. 17, no. 3, pp. 48–60, 2005.

[92] N. S. Suhaimi, J. Mountstephens, and J. Teo, "EEG-Based Emotion Recognition: A State-of-the-Art Review of Current Trends and Opportunities," *Comput. Intell. Neurosci.*, vol. 2020, 2020,

[93] M. H. Atiyah and A. F. Hussain, "Spectrophotometric determination of micro amount of copper (II) using a new of (AZO) derivative, study of thermodynamic functions and their analytical application," *Syst. Rev. Pharm.*, vol. 11, no. 10, pp. 171–181, 2020,

[94] S. A. Tirmizi, F. H. Wattoo, M. H. S. Wattoo, S. Sarwar, A. N. Memon,

and A. B. Ghangro, "Spectrophotometric study of stability constants of cimetidine-Ni(II) complex at different temperatures," *Arab. J. Chem.*, vol. 5, no. 3, pp. 309–314, 2012,

[95] S. Jeon, J. Chien, C. Song, and J. Hong, "A Preliminary Study on Precision Image Guidance for Electrode Placement in an EEG Study.," *Brain Topogr.*, vol. 31, no. 2, pp. 174–185, Mar. 2018,

[96] B. Hellenkamp *et al.*, "Precision and accuracy of single-molecule FRET measurements—a multi-laboratory benchmark study," *Nat. Methods*, vol. 15, no. 9, pp. 669–676, 2018,:

[97] L. Orola, M. Veidis, I. Mutikainen, and I. Sarcevica, "Neutral and Ionic Supramolecular Complexes of Phenanthridine and Some Common Dicarboxylic Acids: Hydrogen Bond and Melting Point Considerations," *Cryst. Growth Des.*, vol. 11, Aug. 2011,.

[98] C. Concentrations and S. K. Inhabitants, "Archive of SID Manganese and Cobalt Concentrations in Hair and Nail Archive of SID," *Distribution*, vol. 4, no. 2, pp. 333–340, 2010.

[99] A. J. Jarad, "Synthesis and Characterization of New Azo Dye Complexes with Selected Metal Ions," *J. Al-Nahrain Univ. Sci.*, vol. 15, no. 4, pp. 74–81, 2012,

[100] M. B. Ibrahim and A. Moyosore, "Spectrophotometric Study of Stability Constants of Co (II), Ni (II) and Cu (II) Complexes of 2 , 2 – Bipyridine at Different Temperatures," *ChemSearch J.*, vol. 5, no. 1, pp. 51–55, 2014.

[101] A. T. Syed, M. H. S. Wattoo, S. Sarwar, and W. Anwar, "SPECTROPHOTOMETRIC STUDY OF STABILITY CONSTANTS OF FAMOTIDINE-Cu(II) COMPLEX AT DIFFERENT TEMPERATURES," *Arab. J. Sci. Eng.* ·, vol. 34, no. 2A, pp. 44–47, 2009.

[102] S. Khalil, A. E. El-Beltagy, M. E. A. El-Sayed, A. A. A. Fattah, Y. F. M. Kishk, and S. S. Alharthi, "Chitosan based nano-membrane for Chromium(III) Determination in Pharmaceutical and Foodstuff Samples," *Int. J. Electrochem. Sci.*, vol. 16, pp. 1–12, 2021,

الخلاصة

تضمنت الدراسة تحضيرو تشخيص لكاشف جديد لاحد مركبات مشتقات الازو، وهو الإيثيل 4-(5-أسيتيل-4،3،2-تريهيدروكسيفينيل) ديازينيل بنزوات (.EATDB) تم تحضير الكاشف عن طريق اقتران الآزو بين مشتق الإميدازول مع ملح الديازونيوم لإيثيل 4-أمينو بنزوات (بنزوكائين). وتم تعريض المركب الناتج لتحليل مكثف، باستخدام أساليب متطورة مثل كروماتوغرافيا الغاز- كتلة (جي.سي. ماس)، وتحليل الأشعة فوق البنفسجية والمرئية، ورنين البروتونات النووي (HNMR[1])، و(CNMR[13])، وطيفية الأشعة تحت الحمراء FT.IR. ومن الملاحظ أن الظروف المثلى للتفاعل الأيونين مع العامل تم استكشافها بدقة. وشمل ذلك دراسة تأثير الدالة الحامضية، وتسلسل الإضافة، ومدة استقرار المركبات المعقدة، وتركيز الليكاند وتأثير درجة الحرارة، وتأثير القوة الأيونية.

تم إعداد منحنيات المعايرة لأيوني الكوبالت (II) والكروم (III) مع نطاق تركيز من (100-1 μg.ml^{-1}) لكلا الأيونين. البارامترات التحليلية المحصل عليها هي معامل الخطية (R[2]) 0.9980 و 0.9939 ، والامتصاصية المولارية $0.212 \times 10^{2}0$ L.mol^{-1}.cm^{-1} و 0.935×10^{3} L.mol[-0] .cm^{-1} ، وحساسية ساندل (μg.cm^{-2}) 0.278 μg.cm^{-2} و 0.554 لأيوني الكوبالت (II) والكروم (III) على التوالي. للتحقق من تكافؤ المعقدات، تم استخدام طرق متعددة بما في ذلك طريقة نسبة المول، وطريقة جوب، وطريقة مولارد. تبين أن ثوابت الاستقرار (Ksta) لمعقدات الكوبالت(II) والكروم (III) هي $.967 \times 10^{8}$ و $1.125. \times 10^{14}$ على التوالي.

علاوة على ذلك، أشارت الدوال الثرموداينميكية (ΔS,ΔH,ΔG) للمعقدات لكل من الكوبالت (II) والكروم (III) إلى أن تفاعلات معقدات (II) Co و (III) Cr كانت تفاعلات باعثة للحرارة. ومع ذلك، لوحظ في الدراسة وجود تداخل من عدة أيونات موجبه وسالبه أثناء تقدير أيوني الكوبالت (II) والكروم (III).

وبناءً على ذلك، تم دراسة عوامل حجب مناسبة، مع مراعاة درجات التفاعل المتباينة اعتمادًا على طبيعة وتركيز الأيونات المتداخلة. ، أشار تحليل المعقدات المذابة إلى أن معقدي الكوبالت (II) والكروم (III)كانا غير مشحونين حسب قياس التوصيلية.

تم تقييم دقة الطريقة التحليلية بعناية فائقة من خلال حساب لثلاث تراكيز مختلفة من الأيونات، ومن ثم حساب الانحراف المعياري النسبي (RSD%) كمقياس للتباين. أظهرت البيانات المحصل عليها دقة ممتازة، حيث تراوحت نسبة RSD% من (0.874. – 0.479.)لأيون الكوبالت (II) ومن

APPENDIX

(0.742% - .0.896%) لأيون الكروم (III). بالاضافة الى دلك ، تراوحت نسبة الاسترداد النسبي من 98.43% - 101.764% لأيون الكوبالت (II) ومن 99.41% - 101.47% لأيون الكروم (III).

كان حد الكشف الكمي L.O.Q مهمًا لتحديد حساسية الطريقة جنبًا إلى جنب مع حد الكشف .L.O.D بالنسبة لأيون الكوبالت(II) ، تبين أن الحد الكشف الكمي وحد الكشف L.O.D و L.O.Q هما 0.749 و 2.471مايكوكرام لكل مل⁻¹ على التوالي. و تبين أن الحد الكمي وحد الكشف L.O.D و L.O.Qهما (0.864 و 2.851 مايكوكرام لكل مل⁻¹) بالنسبة لايون الكروم (III) بالإضافة إلى ذلك، تمت دراسة الكاشف والمعقدين لخصائص الاستقرار والخصائص الفيزيائية، بما في ذلك نقطة الانصهار والتوصيلية المولارية. أثبتت هذه الطريقة التحليلية فعاليتها في تحديد كميات ضئيلة من أيوني الكوبالت (II) والكروم (III) الموجودين في عينة دوائية، مما يسلط الضوء على فائدتها في تحليل الأيونات بدقة وحساسية.

جامعة كربلاء

كلية العلوم

قسم الكيمياء

التقدير الطيفي لايوني الكوبلت (II) والكروم (III) باستخدام مركب الازو الجديد وتطبيقاتها

رسالة مقدمة الى كلية العلوم / جامعة كربلاء

وهي جزء من متطلبات نيل درجة الماجستير في علوم الكيمياء

من قبل

عبد الحر راضي عودة

باشراف

أ.م.د. احسان مهدي شهيد

APPENDIX

Appendixes

1- Statistical treatment.

Calculation of the R.S.D %

Statistical treatment and calculated of RSD% values for Co (ll) ion.

Table (1) calculated of the RSD% of the Co (ll) ion at concentration 1.74×10^{-4}M.

Absorbance(Xi)	MeanX	(xi-$\bar{x}$)	Σ(xi-$\bar{x}$) ^{2}	S.D = $\sqrt{\frac{\Sigma(Xi-\bar{X})2}{N-1}}$	$R.S.D\% = \frac{S.D}{\bar{X}} * 100$
0.360		-0.001			
0.362	0.361	0.001	1.2×10^{-5}	1.732×10^{-3}	0.479 %
0.364		0.003			
0.361		0.000			
0.360		-0.001			

Table (2) calculated of the RSD% of cobalt (ll) ion at concentration 3.4×10^{-4}M

Abs (Xi)	Mean ($\bar{X}$)	(xi-$\bar{x}$)	Σ(xi-$\bar{x}$) ^{2}	S.D = $\sqrt{\frac{\Sigma(Xi-\bar{X})2}{N-1}}$	$R.S.D\% = \frac{S.D}{\bar{X}} * 100$
0.415		-0.005			
0.418	0.420	0.002	5.4×10^{-5}	3.674×10^{-3}	0.874 %
0.420		0.00			
0.422		0.005			
0.425					

Table (3) calculated of the RSD% of the Cobalt (ll) ion at concentration 5.1×10^{-4}M

Abs (Xi)	mean ($\bar{X}$)	(xi-$\bar{x}$)	Σ(xi-$\bar{x}$) ^{2}	S.D = $\sqrt{\frac{\Sigma(Xi-\bar{X})2}{N-1}}$	$R.S.D\% = \frac{S.D}{\bar{X}} * 100$
0.427		-0.001			
0.430	0.428	0.002	1.4×10^{-5}	1.87×10^{-3}	0.437 %
0.429		0.001			
0.428		0.002			
0.430		0.002			

APPENDIX

2- Statistical treatment and calculation of %RSD values for chromium (III) ion.

Table (4) calculated of the RSD% of the Cr (lll) ion at concentration 1.7×10^{-4}M

Abs Xi	Mean ($\bar{X}$)	(xi-$\bar{x}$)	Σ(xi-$\bar{x}$)^2	S.D = $\sqrt{\frac{\Sigma(Xi-\bar{X})2}{N-1}}$	$R.S.D\% = \frac{S.D}{\bar{X}} * 100$
0.164		-0.001			
0.167	0.165	-0.002	6×10^{-6}	1.22×10^{-3}	0.742 %
0.165		0.000			
0.165		0.001			
0,165		0.000			

Table (5) calculated of the RSD% of the Cr (lll) ion at concentration 3.4×10^{-4}M

Abs Xi	mean ($\bar{X}$)	(xi-$\bar{x}$)	Σ(xi-$\bar{x}$)^2	S.D = $\sqrt{\frac{\Sigma(Xi-\bar{X})2}{N-1}}$	$R.S.D\% = \frac{S.D}{\bar{X}} * 100$
0.184		-0.001			
0.185	0.185	0.000	1.1×10^{-5}	1.658×10^{-3}	0.896 %
0.185		0.000			
0.184		0.001			
0.188		0.003			

Table (6) calculated of the RSD% of the Cr (lll) ion at concentration 5.1×10^{-4}M

Abs Xi	mean ($\bar{X}$)	(xi-$\bar{x}$)	Σ(xi-$\bar{x}$)^2	S.D = $\sqrt{\frac{\Sigma(Xi-\bar{X})2}{N-1}}$	$R.S.D\% = \frac{S.D}{\bar{X}} * 100$
0.199		0.000			
0.198	0.199	-0.001	1.1×10^{-5}	1.658×10^{-3}	0.833 %
0.200		0.001			
0.199		0.000			
0.201		0.003			

APPENDIX

1- Statistical treatment and calculation of L.O.D values for Co (ll) ion.

Table (7) calculation of the D.L of Co (ll) ion at concentration 0.5 µg.mL^{-1} equal to (8.62x10^{-6} M).

no	Abs Xi	mean (x')	(xi-x')	Σ(xi-x')^2	S.D = $\sqrt{\frac{\Sigma(Xi-\bar{X})2}{N-1}}$	$D.L = \frac{S.D}{slope} * 3.3$
1	0.028		0.000			
2	0.029		0.001			
3	0.028		0.000			
4	0.027		-0.001			
5	0.028		0.000			
6	0.029	0.028	0.001	6x10^{-6}	8.165x10^{-4}	0.748
7	0.027		-0.001			
8	0.029		0.001			
9	0.028		0.000			
10	0.027		-0.001			

2- Statistical treatment and calculation of L.O.D values for Cr (lll) ion

Table (8) calculation of the D.L of Cr (lll) ion at concentration 0.7 µg.mL^{-1} equal to 1.34x10^{-5} M

no	Abs Xi	mean (x')	(xi-x')	Σ(xi-x')^2	S.D = $\sqrt{\frac{\Sigma(Xi-\bar{X})2}{N-1}}$	$D.L = \frac{S.D}{Slope} * 3.3$
1	0.024		0.000			
2	0.023		-0.001			
3	0.024		0.000			
4	0.024		0.000			
5	0.024		0.000			
6	0.025	0.024	0.001	2x10^{-6}	4.714x10^{-4}	0.864
7	0.024		0.000			
8	0.024		0.000			
9	0.024		0.000			
10	0.024		0.000			